COLD FIBER SOLID PHASE MICROEXTRACTION

by

Shokouh Hosseinzadeh Haddadi

A thesis

presented to the University of Waterloo

in fulfillment of the

thesis requirement for the degree of

Doctor of Philosophy

in

Chemistry

Waterloo, Ontario, Canada, 2008

Declaration

I hereby declare that I am the sole author of this thesis. This is a true copy of the thesis, including any required final revisions, as accepted by my examiners.

I understand that my thesis may be made electronically available to the public.

ABSTRACT

A cold fiber solid phase microextraction device was designed and constructed based on the use of a thermoelectric cooler (TEC). A three-stage thermoelectric cooler was used for cooling a copper rod coated with a polydimethylsiloxane (PDMS) hollow fiber, which served as the SPME fiber. The copper rod was mounted on a commercial SPME plunger and exposed to the cold surface of the TEC, which was enclosed in a small aluminum box. A heat sink and a fan dissipated the generated heat at the hot side of the TEC. By applying an appropriate DC voltage to the TEC, the upper part of the copper rod, which was in contact to the cold side of the TEC, was cooled and the hollow fiber reached a lower temperature through heat transfer. A thermocouple was embedded in the cold side of the TEC for indirect measurement of the fiber temperature. A portable cold fiber SPME device was made by using a car battery as the power supply.

The cold fiber SPME device with thermoelectric cooling was applied in quantitative analysis of off-flavors in rice. Hexanal, nonanal, and undecanal were chosen as three test analytes in rice. These analytes were identified according to their retention times and analyzed with a GC/FID instrument. Headspace extraction conditions (i.e. extraction temperature and extraction time) were optimized. Standard addition calibration graphs were obtained at the optimized conditions and the concentrations of the three analytes were calculated. The developed method was compared to a conventional solvent extraction method.

The applicability of the portable cold fiber SPME with TEC for field sampling was tested. The effect of cooling on extraction recovery and the reproducibility of extraction were examined for extractions from an n-alkane flow through system. It was found that the extraction recoveries were significantly higher when the fiber was cooled. To further investigate the effect of cooling on the sensitivity of SPME in field sampling, the portable cold fiber SPME was used for extraction of volatile components from living wisteria flowers. Both the number of identified compounds and the related peak areas increased for extractions with cold PDMS fiber relative to without cooling and commercial PDMS and PA fibers. The portable cold fiber SPME device was also used for field sampling of volatile components of living lily-of-the-valley flowers and the extracted compounds were analyzed with GC/MS.

The desorption kinetics of hydrophobic organic compounds (HOCs) from environmental solid matrices was investigated using cold fiber SPME with CO_2 cooling. Polycyclic aromatic hydrocarbons (PAHs) and selected volatile organic compounds (i.e. toluene, ethylbenzene, *o*-xylene) were used as test analytes. Sand, silica gel, and clay were used as laboratory model solid matrices and were contaminated by the test analytes. Certified sediments were used as naturally contaminated samples. In this approach, the organic compounds, released from contaminated solid samples at different elevated temperatures, were exhaustively extracted with cold fiber SPME over different extraction times. The extraction data were used to obtain desorption and Arrhenius plots. The rate constants of desorption and activation energies of desorption were measured for each contaminant using these plots. The results were comparable to those reported in the literature.

ACKNOWLEDGMENTS

I would like to record my gratitude to Dr. Pawliszyn for his supervision, advice, and guidance from the very early stage of this research as well as giving me advice through out the work.

I gratefully acknowledge Dr. Chong, Dr. Kleinke, And Dr. Lipcowski, for their constructive comments on this research work during the committee meetings and on writing the thesis.

I am grateful to Dr. Clement and Dr. Barker for accepting to be the examiners of this thesis in the midst of all their activity.

I would like to thank the staff of student technical services (STS) for their collaboration in providing the devices used in this study. They were always helpful and kindly addressed my problems in the shortest possible time.

Many thanks to the staff of the chemistry department, especially to Cathy van Esch for their kind assistance.

Collective and individual acknowledgments are also owed to all my colleagues. My thanks go in particular to Dr. Yong Chen, Dr. Heather Lord, Dr. Gangfeng Ouyang, Dr. Anca Tugulea, and Leslie Bragg.

I would like to thank my family who have always supported me in achieving my goals. Words fail me to express my appreciation to my husband Vadoud, whose dedication, love and persistent confidence in me, has taken the load off my shoulder. I owe him for his intelligence, passions, and ambitions. He has been an intimate friend, a loving husband, a knowledgeable colleague and a responsible, caring father for our daughter, Eileen.

I would also like to thank my friends, Mahkameh Maddadi, Azadeh Samadi, Mahboubeh Abdollahi, Azar Ghaffari, Ziba Parsi, Saharnaz Saffari, Siranoush Shahrzad, Zinat Goudarzi, Masoumeh Foroutan and Ashraf Nankali, who encouraged and supported me through my studies.

Finally, I would like to thank everybody who was important to the success of this thesis, as well as expressing my apology that I could not mention their names individually.

DEDICATION

In memory of my mother,

I dedicate this thesis to my father.

TABLE OF CONTENTS

LIST OF TABLES

LIST OF FIGURES

LIST OF ABBREVIATIONS

CAR	Carboxen
CIS	Cooled injection system
CW	Carbowax
DDT	Dichloro diphenyl trichloroethane
DVB	Divinylbenzene
FID	Flame ionization detector
GC	Gas chromatography
GC/MS	Gas chromatography/Mass spectrometry
HETP	Hight Equivalent to a Theoretical Plate
HOCs	Hydrophobic organic compounds
HPLC	High performance liquid chromatography
LTPRI	Linear temperature program retention index
NAPL	Non-aqueous phase liquids
NIST	National Institute of Standards and Technology
PA	Polyacrylate
PAHs	Polycyclic aromatic hydrocarbons
PDMS	Polydimethyl siloxane
POP	Persistant organic pollutants
PTFE	Polytetrafluoroethylene
SFE	Supercritical fluid extraction
SOM	Sorbent organic matter
SPE	Solid phase extraction
SPME	Solid phase microextraction
TEC	Thermoelectric cooler
TFRC	Two-compartment first order rate constant
TPR	Templated resin
UST	Underground storage tanks

Chapter 1

Introduction

The analytical process typically consists of several steps: sampling, sample preparation, separation, identification and/or quantification, and statistical evaluation.[1] Each step is important in obtaining precise and accurate results; however, efficient sample preparation is the key to a successful analysis.[2,3] Although some samples are naturally ready for analysis, it is not practically possible to directly introduce the sample to most analytical instruments and some form of sample pre-treatment is required to both extract and concentrate the analytes from the matrix before the final analysis.[2] Solid and semi-solid samples, in particular, typically require complex, multi-step sample preparation procedures.[4] Compared to the effort invested in the development of separation techniques, particularly chromatography, there has been little scientific interest in sample preparation.[2] Since sampling and sample preparation steps typically account for over 80% of the whole analysis time, and the quality of these steps significantly affects the success of the overall analytical procedure, the improvement of sample preparation is a critical issue.[2] Current trends in sample preparation are toward developing automated methods and miniaturised systems, which increase the precision, throughput, reproducibility, and cost-effectiveness.[2]

Miniaturisation of the sample preparation devices is significant both for automation and on-site sampling/sample preparation. Portable extraction devices are required to make sample preparation possible directly on the site, as a part of an on-site analyses approach to obtain real-time measurement and minimize loss of analytes and appearance of artifacts during sample transportation and storage.[4] On the other hand, the growing public concern over protecting the environment encourages analytical chemists to develop methods that are environmentally friendly.[3] Ironically, traditional sample preparation procedures used in analytical methods for the study of environmental pollution may themselves be a source of contamination. Therefore, another important consideration in the development of sample preparation techniques is to develop approaches that use none or a small amount of organic solvent. A general classification of solvent-free sample preparation methods, based on the extraction phase (gas, membrane, and sorbent), is shown in Figure 1-1.[4]

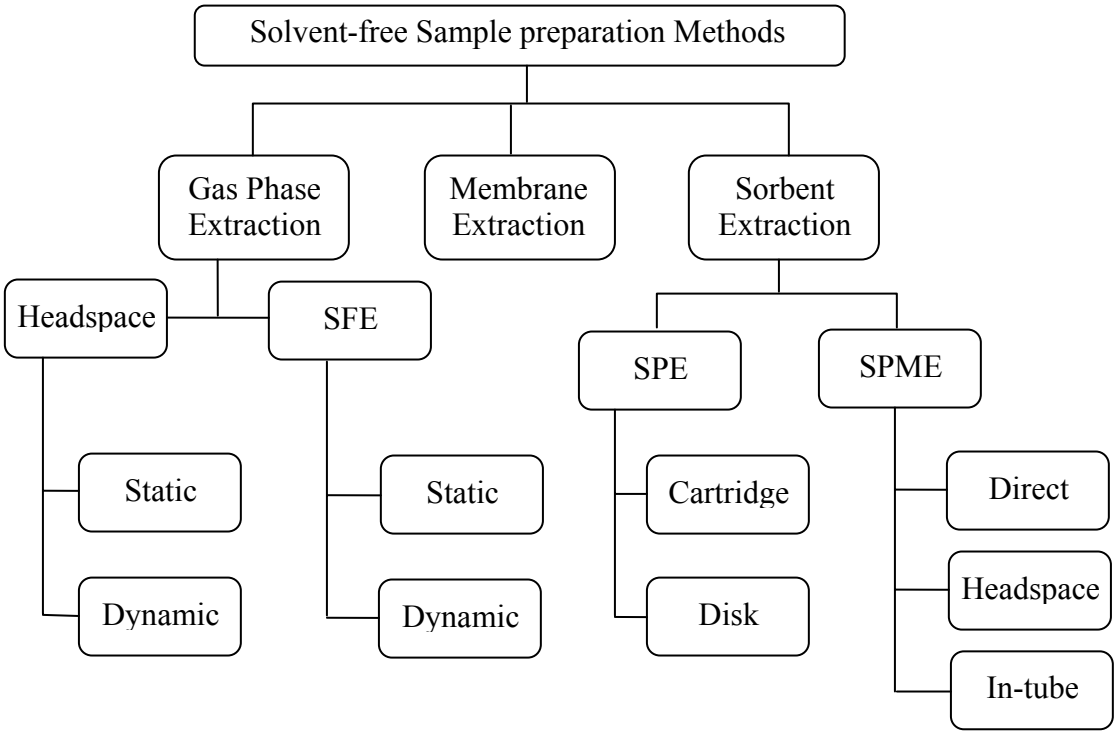

Figure1.1 *Classification of solvent-free sample preparation techniques.*[4]

The most competent solvent-free techniques are headspace, membrane and sorbent approaches.[3] Among the sorbent extraction methods, solid phase microextraction (SPME) has been evolving very quickly during the past two decades, appearing in almost every field of analytical chemistry, from water analysis to in-vivo analysis of biological samples.[5,6,7,8,9,10,11,12] SPME is fast, reproducible and accurate, automated for many applications, and is truly a solvent-free method when used with gas chromatography. Supported by industrial companies namely Sigma-Aldrich[13] and CTC Analytics[14], SPME has been commercialized and automated.

While SPME, together with GC, has been applied to the extraction and pre-concentration of analytes from gas, liquid, and solid samples, it has been more successful for the quantitative analysis of volatile and semi-volatile organic compounds from water samples. Commercial SPME has been shown to be appropriate for qualitative analysis (e.g. comparison of volatile compounds in the headspace of food or natural products); however, it still lacks enough sensitivity to be used as a standard and routine method for quantitative analysis of solid samples, more particularly environmental solid samples e.g. soil, sediment and sludge.

Internally cooled SPME, recently termed as internally cooled coated fiber or cold fiber SPME, that utilizes liquid carbon dioxide (CO_2) for cooling the SPME fiber, was introduced to improve the sensitivity of SPME.[15] Although the first cold fiber SPME system was successfully applied for exhaustive extraction of BTEX (benzene, toluene, ethylbenzene, o-xylene) compounds from soil matrices[15], it was not popular among analytical chemists, due to the fragility of the device, difficulty of operation, and lack of support from industry. To eliminate these shortcomings, this approach was further modified and automated by Chen and Pawliszyn.[16] The modified cold fiber SPME system was applied in the quantitative extraction of flavor compounds from shampoo[17], the quantitative analysis of polycyclic aromatic hydrocarbons (PAHs) in soil matrices[18], the determination of chloroanisoles in cork[19], and the screening of tropical fruit volatile compounds.[20] Cold fiber SPME with CO_2 cooling was shown to be an efficient approach for laboratory analysis; however, due to heavy and high voltage consuming parts, the system was still not appropriate for field analysis. Therefore,

integration of the cooling source and the SPME fiber in a single low-voltage device is feasible for miniaturization of the device, required for automation and field sampling.

The present study focuses on the design and application of an alternative system for cooling the SPME fiber, based on the use of thermoelectric coolers. The possibility of utilizing the cold fiber SPME in the study of temperature dependence of kinetics of desorption of organic compounds from environmental solid matrices has also been investigated.

The first chapter of this dissertation highlights the theory of solid phase microextraction, cold fiber SPME, and the theoretical aspects associated with extraction from solid samples. The second chapter addresses the design and calibration of the cold fiber SPME based on thermoelectric cooling of metal fibers. The applications of this cooling system in extraction of off-flavors in the headspace of rice (laboratory application), and aroma compounds from living flowers (field sampling) are described in Chapter 3. Chapter 4 describes the theory and significance of studying the kinetics of desorption of organic compounds from environmental solid samples (e.g. sediments), and continues with the application of cold fiber SPME with CO_2 cooling in this area of environmental science. The thesis ends with a summary in Chapter 5.

1.1 Solid phase microextraction (SPME)

In this section, the principles of solid phase microextraction n (SPME) technique, necessary for understanding the theory and practice of cold fiber SPME, are briefly discussed.

1.1.1 Construction and operating principles of SPME

Solid phase microextraction was developed with the purpose of rapid sample preparation both in the laboratory and on-site.[21] This technique uses a fused silica or metal fiber coated with a suitable stationary phase attached to a plunger in a syringe-like device (Figure 1-2).

SPME is basically a two step process. In the first step, analytes are partitioned between the sample matrix and the fiber coating. In the second step, the concentrated extract is

desorbed from the fiber into the analytical instrument, usually a gas chromatograph (GC), where the extracted components are thermally desorbed.[22]

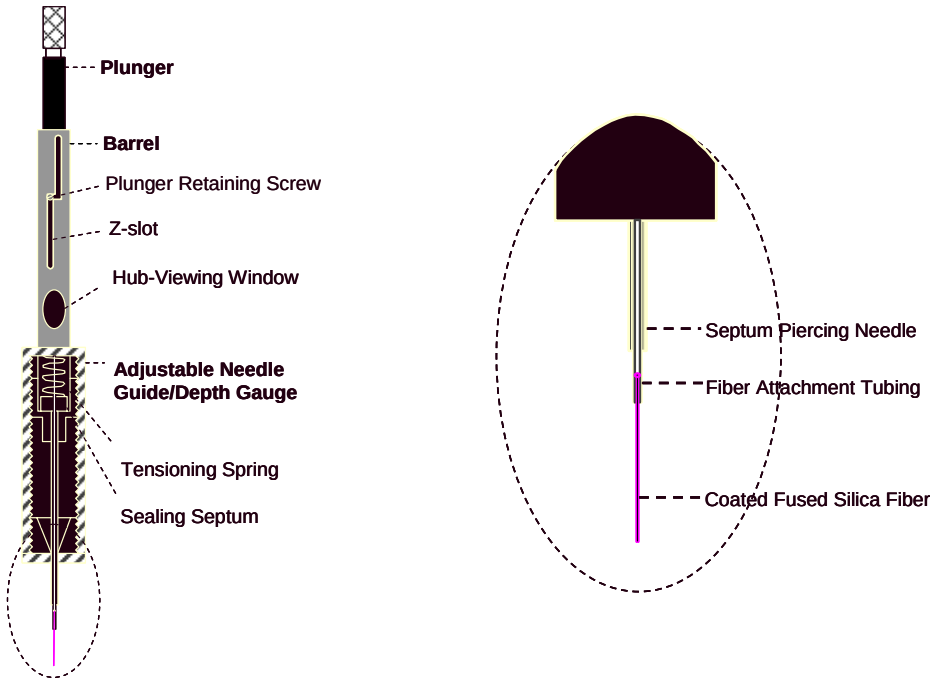

Figure 1.2 *Design of the first commercial SPME device made by Sigma-Aldrich.*[21]

The sensitivity of SPME is mostly affected by the value of the partition coefficient of the analyte between the sample matrix and the stationary phase coated on the fiber.[3] Selecting the appropriate coating is the first step in SPME method development.[3] The coating type is selected based on chemical properties of the analytes.[1] The rule of "like dissolves likes" applies, meaning that the polar compounds are more efficiently extracted on polar coatings and non-polar compounds on non-polar coatings.[3] Several different coatings are commercially available. The most widely used coating is poly(dimethylsiloxane) (PDMS). Although PDMS is considered non-polar and is particularly suitable for the extraction of non-polar compounds, it is often used for wide range screening applications in environmental analysis.[3] Poly(acrylate) (PA) is a highly polar coating for general use and is ideal for the extraction of phenols.[3] The other available coatings are: Carboxen/poly(dimethylsiloxane) (CAR/PDMS), Carbowax/divinylbenzene (CW/DVB), Carbowax/templated resin (CW/TPR) and

divinylbenzene/Carboxen/poly(dimethylsiloxane) (DVB/CAR/PDMS). CAR/PDMS is ideal for gaseous/volatile analytes , CW/DVB is suitable for the extraction of polar analytes, especially for alcohols, CW/TPR is developed for high-performance liquid chromatography (HPLC) applications and finally DVB/CAR/PDMS is the most recent coating, which is ideal for a broad range of analyte polarities (suitable for C_2-C_{20} range).[3]

Extraction is carried out via adsorption or absorption mechanisms, based on the structure of the coating. Among the commercially available fibers, PDMS and PA coatings are non-porous and amorphous polymeric phases that extract analytes via absorption, i.e. the diffusion of organic molecules in these coatings are relatively fast (close to those in organic solvents).[23] The CAR/PDMS, CW/DVB, and CW/TPR, are mixed coatings, in which the primary extracting phase is a porous solid that extracts analytes through adsorption, i.e. diffusion coefficients of organic molecules in the bulk of DVB and Carboxen are small and all the molecules basically remain on the surface of the coating within the time frame of SPME analysis.[23]

Another important factor in selecting the fiber is the thickness of the stationary phase. The best choice is a thin coating that also provides a relatively high partition coefficient of the analytes.[1] However, if the partition coefficient of the analyte is relatively low, for example in case of volatile compounds, thicker coatings allow the extraction of larger amounts of the analytes, enabling their transport to the chromatographic injector without significant loss.[1,3] Thin coatings are recommended for the extraction of high boiling point compounds (with high partition coefficients), to achieve the extraction and desorption steps in a relatively short time.[3]

Using an SPME device does not require high laboratory skills. For a typical laboratory application, the needle is passed through the vial septum and the plunger is depressed. By depressing the plunger, the fiber is extended outside the needle and exposed to the sample matrix (direct SPME)[24], or the headspace of the matrix (headspace SPME). After a well-defined extraction time, the fiber is withdrawn into the needle by pulling the plunger, and the needle is then injected into the hot inlet of a GC[24], similar to injection of a GC syringe.

However, unlike the syringe injection, the fiber is not removed immediately after injection and is left in the injector for a few minutes to allow complete thermal desorption of the analytes. The length of desorption time (i.e. the time duration over which the fiber is exposed to the injector hot zone) depends on the thickness of the coating, the properties of the analytes, the temperature of the injector, and the flow rate of the carrier gas. Longer desorption times are required for thicker coatings and compounds with higher molecular weights which have lower diffusion coefficients in the liquid polymer phase. Upon completion of desorption of analytes, the fiber is once more withdrawn into the needle and removed from the injector. SPME has been also combined with HPLC and electrophoresis separation techniques.[25,26,27,28]

Although the SPME device has been mainly used in laboratory applications, it is also an appropriate device for field sampling. The operating principles of SPME field sampler devices are similar to the SPME device described above, but some modifications are made to protect fibers during sampling, storage, and transportation.[29,30]

1.1.2 Theory

The theoretical aspects of SPME have been investigated parallel to its application from both thermodynamic and kinetic points of view. In this section, the thermodynamics and kinetics of direct and headspace SPME are discussed with more emphasis on the kinetics of headspace SPME.

1.1.2.1 Thermodynamics

1.1.2.1.1 Direct Extraction

In direct SPME, a small amount of the extracting phase coated on a solid support is placed directly in contact with the sample matrix for a pre-determined time (Figure 1-3).

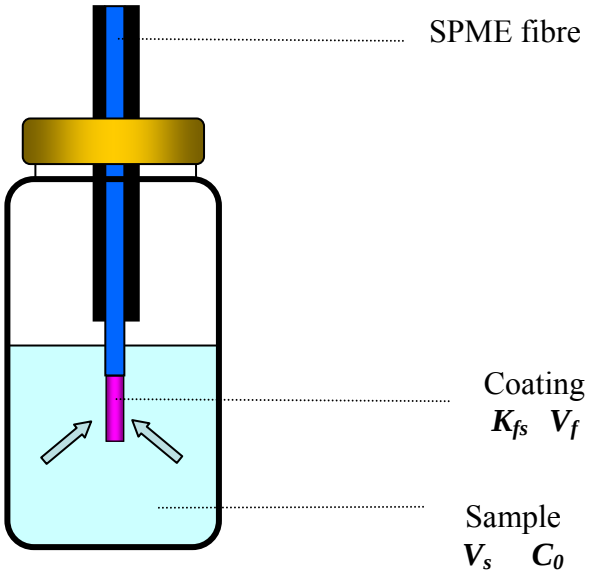

Figure 1.3 *Direct SPME; V_f, volume of fiber coating; K_{fs}, fiber/sample distribution coefficient; V_s, volume of sample; C_0, initial concentration of analyte in the sample.*

As soon as the fiber is exposed to the sample, the analytes transport from the matrix into the coating.[4] The extraction is considered to be complete when the analyte concentration has reached distribution equilibrium between the sample matrix and the fiber coating.[4] This means that after equilibrium is reached, the extracted amount is constant within the limits of experimental error and does not increase with further increase in the extraction time.[4] The equilibrium conditions may be described with equation 1.1[4]:

$$n = \frac{K_{fs} V_f V_s C_0}{K_{fs} V_f + V_s} \qquad \text{Equation 1.1}$$

where n is the amount of the analyte extracted (in moles), K_{fs} is the fiber coating/sample matrix distribution constant, V_f is the volume of the fiber coating, V_s is the volume of the sample, and C_0 is the initial concentration of the analyte in the sample.[4] This equation shows that a linearly proportional relationship exists between the amount of analyte extracted by the fiber coating (n), and the initial concentration of the analyte in the sample matrix (C_0), which

is required for a quantitative analysis. The time needed to reach equilibrium during the SPME sampling depends on the analyte and the matrix properties and can range from a few minutes to several hours.[31]

Although SPME is an equilibrium technique, it may also be utilized for exhaustive extraction of analytes from sample matrices under some conditions, i.e. when the sample volume is very small and/or the distribution coefficient is very large, such as extraction of semi-volatile organic compounds from small volumes of a sample matrix. In such cases, V_s in equation 1.1 is greatly smaller than the product of K_{fs} and V_f, and equation 1.1 can be simplified to:

$$n = V_s C_0 \qquad \text{Equation 1.2}$$

This implies that all analytes are extracted from the sample matrix onto the fiber coating.[24]

1.1.2.1.2 Headspace extraction

Equation 1.1 assumes that the sample matrix is a single homogeneous phase and no headspace is present in the system.[4] However, SPME is also used in headspace mode and equation 1.1 can be modified for a multi-phase system by considering the volumes of the individual phases and the appropriate distribution constants (equation 1.4).[4]

$$n = \frac{K_{fh} K_{hs} V_f V_s}{K_{fh} K_{hs} V_f + K_{hs} V_{hs} + V_s} C_0 \qquad \text{Equation 1.4}$$

where n is the mass of the analyte absorbed on the fiber after equilibrium is reached between the three phases: the sample, the headspace, and the fiber, C_0, is the initial concentration of the analyte in the sample matrix, K_{fh} is the partition coefficient of the analyte between the headspace and the fiber, K_{hs} is the partition coefficient of the analyte between the headspace and the sample, and V_{hs} is the volume of the headspace. The other parameters are the same as in equation 1.1.

1.1.2.2 Kinetics

The speed of SPME extractions is determined by the kinetics of the extraction process. The theory of the dynamic process of SPME has been discussed based on Fick's second law of diffusion in one dimension:[32,33]

$$\frac{\partial C}{\partial t} = D\frac{\partial^2 C}{\partial x^2} \qquad \text{Equation 1.5}$$

where C is the concentration and D is the diffusion coefficient of the analyte. For the cylindrical geometry and sampling system in a three-dimensional space, the above equation is converted to:

$$\frac{\partial C}{\partial t} = D\frac{1}{r}\left[\frac{\partial}{\partial r}\left(r\frac{\partial C}{\partial r}\right)\right] \qquad \text{Equation 1.6}$$

where r is the radius of the cylinder. Examining the kinetics of SPME based on this equation required the determination of the values of the diffusion coefficients and distribution constants, assuming boundary conditions and solving differential equations.[1] These theoretical models could be used to describe extraction time profiles of SPME processes; however, the direct analytical expression that related the amount of the analyte extracted by the fiber to its initial concentration in the matrix was described later.[31]

1.1.2.2.1 Kinetics of direct extraction

The equilibration time, t_e, i.e. the time when 95% of the equilibrium amount of an analyte is extracted from the sample, in perfectly agitated water sample is described by the equation:

$$t_e = t_{95\%} = \frac{(b-a)^2}{2D_f} \qquad \text{Equation 1.7}$$

where *(b-a)* is the thickness of the coating, and D_f is the diffusion coefficient of the analyte in the coating. In perfect agitation, the speed of extraction is controlled by the diffusion of the

analyte in the coating. Although such a system does not exist practically, the above equation can be used to estimate the shortest possible equilibration time.

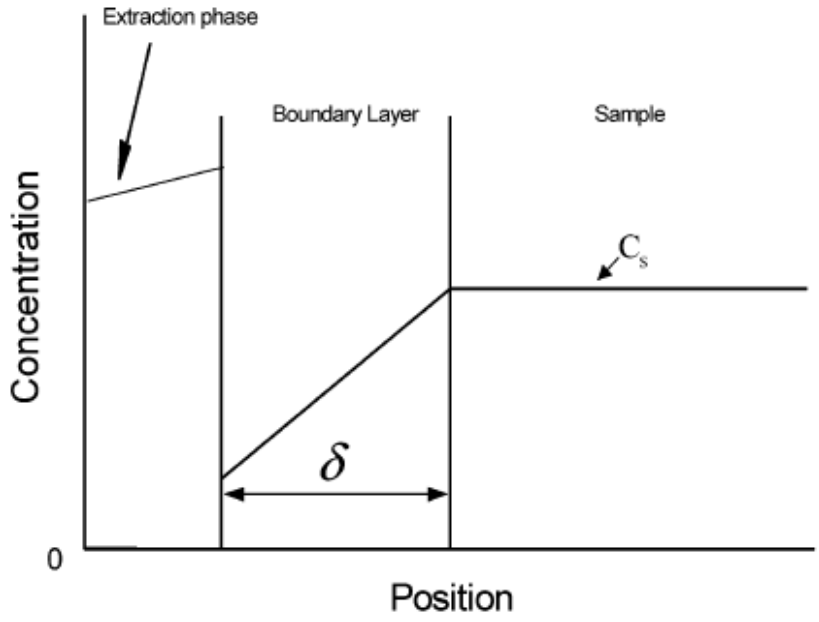

Figure 1.4 *Boundary layer model.*[1]

For practical agitation the boundary layer model is presented: independent from the agitation speed, the part of the fluid contacting the surface of the fiber is always stationary, and as the distance from the fiber surface increases, the fluid movement gradually increases until it reaches the bulk flow in the sample (Figure 1-4).[1] This static layer is called a boundary layer. In this case, the speed of extraction is controlled by the diffusion of the analyte in the boundary layer and the time required to reach equilibration can be estimated by:

$$t_e = t_{95\%} = 3\frac{\delta K_{fs}(b-a)^2}{D_s} \qquad \text{Equation 1.8}$$

where *(b-a)* is the coating thickness, δ is the thickness of the boundary layer, K_{fs} is the partition coefficient of the analyte between the coating and the sample, and D_s is the diffusion coefficient of the analyte in the sample phase.[1]

The boundary layer approach may also be used for the estimation of the equilibration time in a perfectly static system, where the thickness of the boundary layer is the radius of the sampling vial.[1]

1.1.2.2.2 Kinetics of headspace extraction

The geometry of headspace SPME is shown in Figure 1-5.[1]

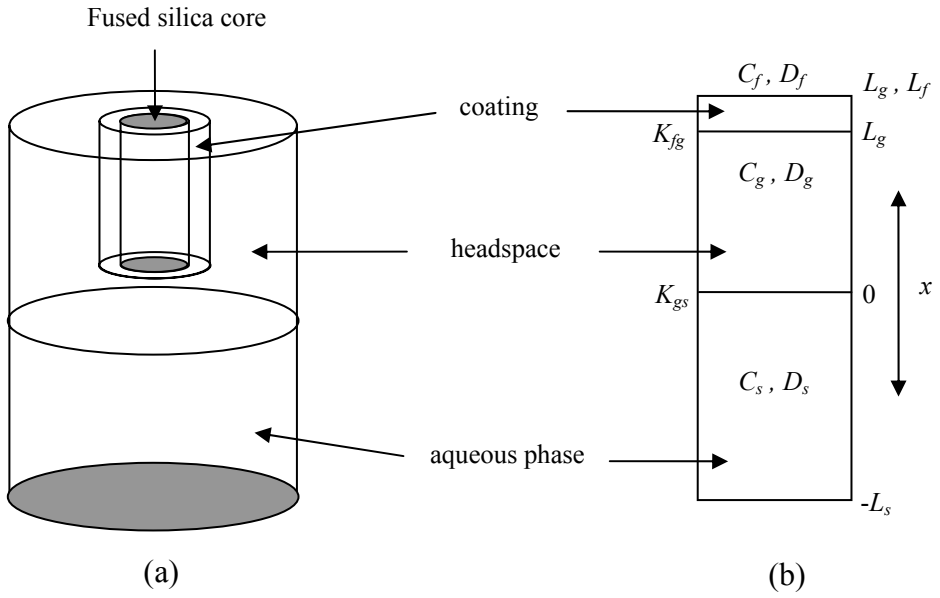

Figure 1.5 *(a) Geometry of SPME headspace sampling; (b) one-dimensional model of the three-phase system; K_{fg} and K_{gs} are the coating/headspace and headspace/water partition coefficients, respectively; D_f, D_g and D_s are the diffusion coefficients of the analyte in the coating, headspace, and water, respectively; L_f, L_g and L_s are the thicknesses of the coating, headspace, and aqueous phase, respectively.*[1]

The mass of the analyte extracted by the coating at any given moment, *M(t),* can be calculated by:[1]

$$M(t) = \int_{L_g}^{L_g + L_f} C(x,t)\,dx \qquad \text{Equation 1.9}$$

Assuming that an aqueous solution with an initial concentration of C_0 is loaded into a vessel and the equilibrium is reached between the headspace and the sample before the headspace SPME is started, the concentration of the analyte in the headspace, C_g^0, and in the sample, C_s^0, before the extraction can be calculated by[1]:

$$C_0 L_s = C_g^0 L_g + C_s^0 L_s \quad with \quad C_g^0 = K_{gs} C_s^0 \qquad \text{Equation 1.10}$$

The concentrations of the analyte in any position, *x*, at any given time can be obtained by solving these equations. The time profile of the mass absorbed by the coating can also be calculated through equation 1.9.[1]

Equilibrium in the three phases during headspace SPME is reached when the concentration of the analyte is uniform within each of the three phases, and the concentration ratios between two adjacent phases satisfy the distribution coefficients between the two phases.[1] The time required to reach equilibrium depends on the thickness of the coating, L_f, the distribution coefficient of the analyte between the fiber and the headspace, K_{fg}, distribution coefficient of the analyte between the headspace and the sample K_{gs}, and the diffusion coefficients of the analyte in the sample and the headspace phases, D_s and D_g, respectively. Longer equilibrium time is associated with thicker coatings. The thicker the coating the more amount of analyte is extracted by the coating and therefore more time is required to reach equilibrium.

The effect of K_{fg} and K_{gs} in equilibration time in the static headspace SPME can be theoretically described. Assuming that K_{gs} is constant, increasing the value of $K_{fg,}$ results in longer equilibration time. The reason is that when the value of K_{fg} is small (e.g. less than 100), only the portion of the analyte present in the headspace is extracted on the coating during

extraction and therefore the equilibration time is short. For larger K_{fg} values, the equilibrium time increases further since a large portion of the extracted analytes originate from the sample and the diffusion of the analyte molecules in the aqueous phase is very slow.[1] For volatile compounds, which have relatively small K_{fg} values and relatively large K_{gs} values, the amount of the analyte extracted by the coating is usually insignificant compared to the amount of the analyte available in the headspace. Therefore, the extraction rate is determined by diffusion in the headspace phase and the equilibrium time is quite short since diffusion coefficients of the analytes are larger in the gas phase.[1]

Assuming that K_{fg} is constant, increasing the value of K_{gs}, results in shorter equilibration time. For less volatile compounds, with small K_{gs} values, the concentration of the analyte in the headspace phase is low. Therefore, extraction of the analytes from the headspace affects the concentration of the analytes in the sample. The equilibrium time is long, because the rate of the extraction is controlled by the slow diffusion of the analytes in the sample.

The above discussion can be generalized in the following equation for estimating the equilibrium time for static headspace SPME[1]:

$$t_e = t_{95\%} = 1.8\left(\frac{L_g}{K_{gs}D_g} + \frac{L_s}{1.6D_s}\right)K_{fs}L_f \qquad \text{Equation 1.11}$$

This equation is valid when the extracted amount by the SPME fiber is a small portion of the amount of the analyte present in the sample.[1] The first term in the parenthesis is associated with the mass transfer in the headspace, whereas the second term is related to the mass transfer in the sample.[1] The mass transfer in the sample is controlled by the diffusion coefficient in the sample, D_s, and the length of the sample through which the analytes diffuse, L_s.[1] On the other hand, the rate of the mass transfer in the headspace is associated with the

headspace/ sample distribution coefficient, K_{gs}, the diffusion coefficient of the analyte in the headspace, D_g, and the length of the headspace phase, L_g.[1] The equilibrium time also increases with the increase of the fiber capacity, which is defined by the product of the coating/sample distribution coefficient, K_{fs}, and the thickness of the coating, L_f.[1]

1.1.2.2.3 Pre-equilibrium extraction

Although equations 1.7, 1.8 and 1.11, can be used to describe the extraction time profiles obtained by SPME, they cannot relate the amount of the analyte extracted by the coating at any given moment to its initial concentration in the matrix. A simple dynamic model was presented by Ai[31], which describes the kinetics of absorption of analytes onto a liquid fiber coating before equilibrium for an effectively agitated matrix.[31] In this model, mass diffusion from the sample matrix to the SPME coating is considered the rate-determining step in reaching equilibrium[31] and the amount extracted by the coating at a given time, n, is related to the initial amount of the analyte in the sample, n_0, by the following equation:

$$n = \left[1 - \exp(-at)\right]\frac{K_{fs}V_fV_s}{K_{fs}V_f + V_s}C_0 \qquad \text{Equation 1.12}$$

In this equation, t, is the extraction time, and a, is a time constant, representing how fast an equilibrium is reached.[31] For long extraction times, equation 1.12 becomes equation 1.1, characterizing equilibrium extraction. Equation 1.12 shows that even before the equilibrium time, a linear relationship exists between the amount of analyte extracted onto the fiber, n, and the initial analyte amount in the sample matrix, n_0, if the agitation, the extraction time, and the extraction temperature are kept constant.[31]

1.2. Cold fiber SPME

In order for HS-SPME to be considered an exhaustive extraction method, more than 90 percent of the initial mass of the analyte in the sample should be transferred to the extraction phase, i.e. the ratio of the mass absorbed on the fiber at equilibrium to the initial mass of the analyte in the sample, n/n_0, should have a value between 0.9 and 1. Equation 1.4 can be written as:

$$\frac{n}{n_0} = \frac{K_{fh} K_{hs} V_f}{K_{fh} K_{hs} V_f + K_{hs} V_{hs} + V_s}$$

where n_0 is the initial amount of the analyte in the matrix. One practical approach for increasing the value of n/n_0 is to increase the value of K_{fh}, which may be achieved by fabricating different types of coatings of different polarities: non-polar, semi polar, and polar.[3] Another means of increasing the n/n_0 ratio is to increase the value of K_{hs}. One possible way to increase this value is to heat the solid sample (thermal desorption). However, the absorption of analytes by the fiber coating is an exothermic process, which means that while the high-temperature enhances the release of analytes from the matrix, it can adversely affect the absorption of analytes by the coating due to the decrease in the value of the partition coefficients.[15]

The effect of temperature on distribution coefficient of the analyte between the sample/headspace above the sample and the fiber may be described by equation 1.13: [1]

$$K = K_0 \exp \frac{-\Delta H}{R}\left(\frac{1}{T} - \frac{1}{T_0}\right) \qquad \text{Equation 1.13}$$

where K_0 and K are the distribution coefficients when both the fiber and the sample/headspace above the sample are at temperatures T_0 and T, respectively; ΔH is the molar change in enthalpy of the analyte, when it transfers from the sample to the fiber coating, and R is the gas constant.[1] ΔH is considered constant over the temperature ranges of SPME experiments.[1] The partitioning of the analyte into the fiber is an exothermic process,

which means $\Delta H<0$. Therefore, equation 1.5 shows that increasing the temperature will result in decrease in K.

As a result, there is usually an optimum temperature for headspace SPME sampling. However, this optimum temperature is often quite low, providing insignificant improvement in the extraction recovery of volatile compounds.[15] To solve this problem, the cold fiber SPME device was introduced to maintain the extraction phase at a relatively low temperature while heating the sample to elevated temperatures.

1.2.1 Construction and operating principles of cold Fiber SPME

Cold fiber SPME devices that have been constructed so far are based on using liquid carbon dioxide as the cooling source for the SPME fiber. Figure 1-3 shows the first design of the cold fiber SPME with liquid CO_2 cooling introduced by Pawliszyn and Zhang.[15]

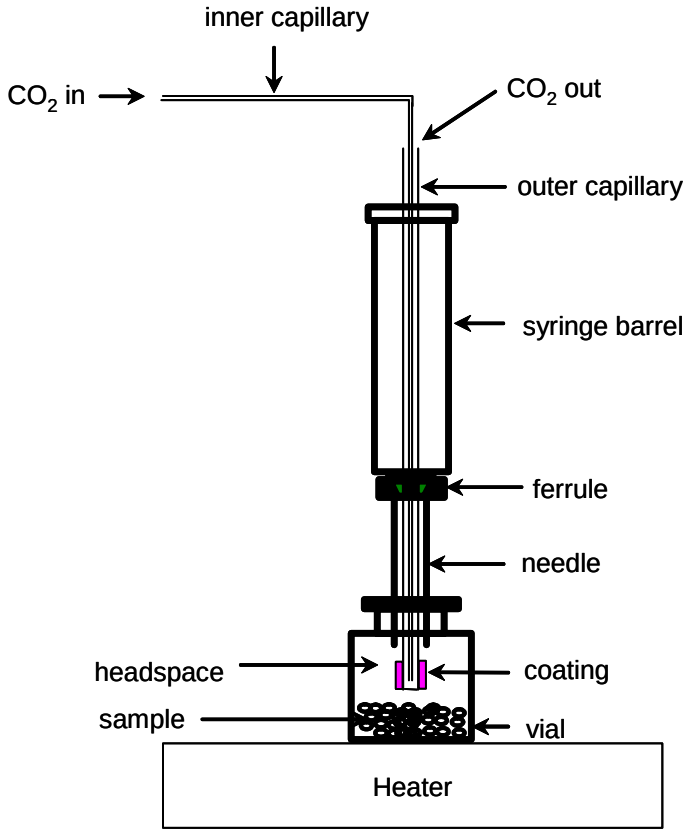

Figure 1.6 *Design of cold fiber SPME device with CO_2 cooling.* [15]

In this device, the outer tubing (made of fused silica) was sealed at one end and coated with a piece of poly(dimethylsiloxane) hollow fiber, which served as the extraction phase. Liquid carbon dioxide was delivered to the coated end of the outer capillary through the inner capillary (fused silica tubing). Evaporation of liquid carbon dioxide resulted in coating temperatures significantly lower than that of the sample. The outer capillary also served as the plunger of the SPME device. The two capillaries were mounted on a 100 μL Hamilton syringe. The needle of the Hamilton syringe was replaced by a 17-gauge needle, which protected the capillary tubing during septum piercing. The temperature of the coating depended on the amount of liquid CO_2 that was delivered and evaporated at the tip of the fiber. The flow of the liquid CO_2 and therefore the temperature of the coating were controlled by the size of the inner capillary tubing, which was connected to a liquid CO_2 tank. The operation of the device was similar to a commercial SPME device; however, it required higher levels of operational skills as the device was made of fragile parts (fused silica tubings). Moreover, this device could only be manually operated. The temperature of the coating was only roughly controlled and it was challenging to introduce a 17-gauge needle into a GC injector.[16]

The described cold fiber SPME device was further miniaturized and automated to allow practical use of this technique.[16] The major modifications are: changing the capillary tubing material from fused silica to a more robust material (stainless steel); embedding a small size thermocouple at the tip of the fiber to enable temperature readings during extraction time (Figure 1-7); controlling the temperature of the fiber via a loop consisted of the described thermocouple, a temperature controller and a solenoid valve (Figure 1-8); using a smaller size (18-gauge) needle to improve injections to the GC injector; and full automation of the extraction and sample introduction steps using a Combi Pal autosampler. The construction and the details of modifications can be found in references 16 and 18.

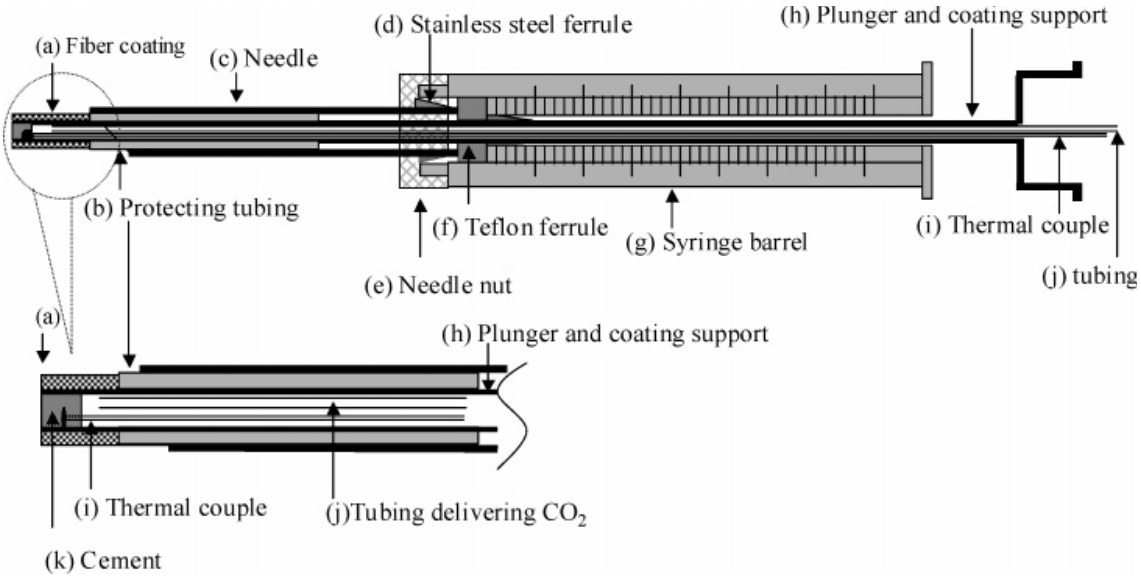

Figures 1.7 *Schematics of the modified cold fiber SPME device.*[16]

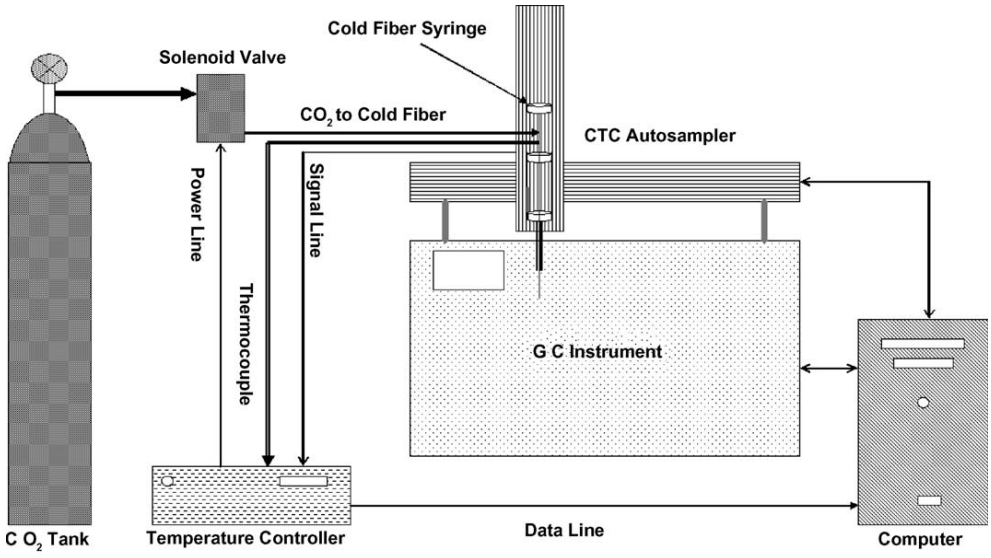

Figure 1.8 *Schematics of the automated cold fiber SPME system.*[18]

1.2.2 Theory

The thermodynamic processes involved in headspace sampling with cold fiber SPME are described by Zhang and Pawliszyn.[15] A simplified headspace SPME system consisting of the headspace and the fiber is considered. It is assumed that most analyte molecules are released to the headspace during the extraction process, and that only one analyte is extracted at a constant pressure.[15] Before the extraction, the gas sample (headspace) containing n_0 mol of the analyte and n_H mol air is in a container of V_s volumem, at temperature T_s, and pressure P_s and the SPME coating (n_c mol) is at temperature T_f and pressure P_s and the two systems are isolated from each other.[15] As soon as the extraction begins, the two systems are connected and only the analyte can partition between the gas phase and the coating.[15] The temperature and the pressure of the coating and the gas phase are kept at their initial values during the extraction.[15] Eventually, a dynamic equilibrium is reached between the coating and the gas phase (with n_f mol of the analyte in the coating and n_s mol in the gas phase; $n_0 = n_f + n_s$), i.e., the rate of desorption of the analyte from the coating equals that of the absorption of the analyte by the coating.[15] Route A in Figure 1.9 illustrates this process.

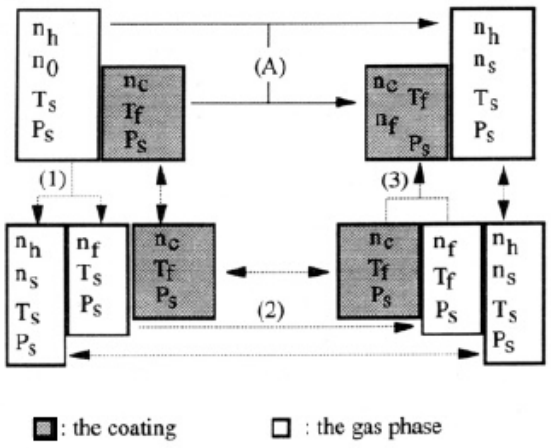

Figure 1.9 *Analyte transferring process (A) during internally cooled SPME sampling and its thermodynamic alternative route, steps 1, 2, and 3. n_h, n_c, and n_0 are molar numbers of air, coating materials, and the analyte, respectively; n_s and n_f ($n_s + n_f = n_0$) are molar numbers of the analyte in the gas phase and the coating, respectively; T_s and T_f are the gas phase and coating temperatures, respectively; P_s is the pressure of the gas phase; and the two-headed arrow indicates that no changes occur for that phase.*[15]

The transfer of the analyte from the gas phase to the coating is forced by the increase in thermodynamic entropy.[15] Equilibrium is reached when the transfer of an extremely small amount of the analyte between the gas phase and the coating will not result in any changes in the entropy of the system.[15] To calculate the entropy of the extraction process, an alternative route with three simple steps can be designed to make the calculation of the entropy easier (steps 1, 2 and 3 in Figure 1.9).[15] It is assumed that in step 1, the fraction of the analyte molecules that is supposed to be extracted on the fiber (n_f) is separated from the rest of the analyte molecules that remain in the headspace (n_s). In the second step, the analyte molecules to be extracted are cooled from the sample temperature (T_s) to the temperature of the fiber (T_f), and finally in the third step, the analyte molecules that are separated and cooled to the temperature of the fiber are transferred from the headspace to the coating. The detailed steps of the calculation of the entropy changes for each of the three steps are discussed in reference 15. In the present text, only the main equations are discussed.

The entropy change for the first step of the analyte transfer as illustrated in Figure 1.9 can be described as:

$$\Delta S = -n_s R \ln \frac{n_s}{n_H} + n_0 R \ln \frac{n_0}{n_H} \qquad \text{Equation 1.14}$$

where n_0 is the number of moles of the analyte initially present in the headspace; n_s is the number of moles of the analyte in the headspace when the equilibrium is reached; n_H is the number of moles of the background gas (air) in the headspace, which is constant during extraction; and R is the gas constant, which has a value of 8.31 $JK^{-1}mol^{-1}$.[15] Equation 1.14 is written assuming that the gases in the headspace behave ideally and $n_H >> n_0$.[15]

The second step in the alternative route is cooling that fraction of the analyte molecules which will be transferred to the coating, from T_s to T_f. The change of the entropy in this step can be written as:

$$\Delta S_2 = n_f C_p \left(\frac{T_s - T_f}{T_f} + \ln \frac{T_f}{T_s} \right) = n_f C_p \left(\frac{\Delta T}{T_f} + \ln \frac{T_f}{T_s} \right) \qquad \text{Equation 1.15}$$

where n_f is the number of moles of the analyte which is to be transferred from the headspace to the coating; C_p is the constant pressure heat capacity of the analyte; and $\Delta T = T_s - T_f$.[15] It is assumed that the heat capacity of the analyte is constant in the involved temperature range.[15] The last step is the absorption of the analyte (n_f) by the liquid coating at constant temperature (T_f) and pressure (P_s). The entropy change for this step is calculated as:

$$\Delta S_3 = -n_f R \ln \left(\frac{T_f n_f V_s}{T_s V_f K_0 n_H} \right) \qquad \text{Equation 1.16}$$

Therefore, the total entropy of the extraction is:

$$\Delta S = \Delta S_1 + \Delta S_2 + \Delta S_3 \qquad \text{Equation 1.17}$$

As mentioned before, the entropy does not change by an infinitesimal transfer of the analyte between the gas phase and the coating when equilibrium is reached or in mathematical terms, at equilibrium:

$$\frac{\partial \Delta S}{\partial n_f} = 0 \qquad \text{Equation 1.18}$$

Partial differential of equation 1.17, considering the conservation of the analyte $n_0 = n_f + n_s$, results in the following equation:

$$C_p \left(\frac{\Delta T}{T_f} + \ln \frac{T_f}{T_s} \right) - R \ln \left(\frac{T_f n_f V_s}{T_s V_f K_0 n_s} \right) = 0 \qquad \text{Equation 1.19}$$

Defining the partition coefficient of the analyte between cold fiber and the hot headspace as $K_T = C_f / C_s = n_f V_s / n_s V_f$, Equation 1.19 can be rewritten as:

$$K_T = K_0 \frac{T_s}{T_f} Exp\left[\frac{C_p}{R}\left(\frac{\Delta T}{T_f} + \ln\frac{T_f}{T_s}\right)\right] \qquad \text{Equation 1.20}$$

where $\Delta T = T_s - T_f$, K_0 is the coating/headspace partition coefficient of the analyte when the coating and the headspace are both at temperature T_f.[15]

Equation 1.20 indicates that three main parameters affect the partition coefficient of a particular analyte: K_0, the partition coefficient of the analyte at temperature T_f, which is determined by the coating temperature (T_f) and the interaction between the analyte and the coating; T_f, the coating temperature, and T_s, the headspace temperature.[15] As the lower the value of T_f, the larger the K_0 (Equation 1.13), maintaining the fiber coating at a low temperature and creating a large temperature gap between the fiber and the headspace can significantly increase the partition coefficient.[15]

1.3 Kinetics of extraction from solid matrices

To understand the kinetics of extraction of analytes from a solid matrix, a general model is presented that involves several fundamental processes occurring during the extraction procedure.[31] In this model, it is assumed that a matrix particle consists of an organic layer on an impermeable but porous core with the analyte adsorbed on the pore surface.[32] The extraction process is modeled by considering several basic steps, as shown in Figure 1.8. To remove the analyte from the extraction vessel, the compound must first be desorbed from the inner surface of the pore (A(M,S), (Figure 1.10); diffuse through the organic part of the matrix (A(M,L)) and reach the matrix/fluid interface (A(M,I)). The analyte must then be solvated by the extraction phase (A(EP,P)) and diffuse through the static phase present inside the pore to reach the portion of the extraction phase that is affected by convection. The analyte is then transported through the interstitial pores of the matrix, eventually reaching the bulk of the extraction phase (A(EP,B)).[32]

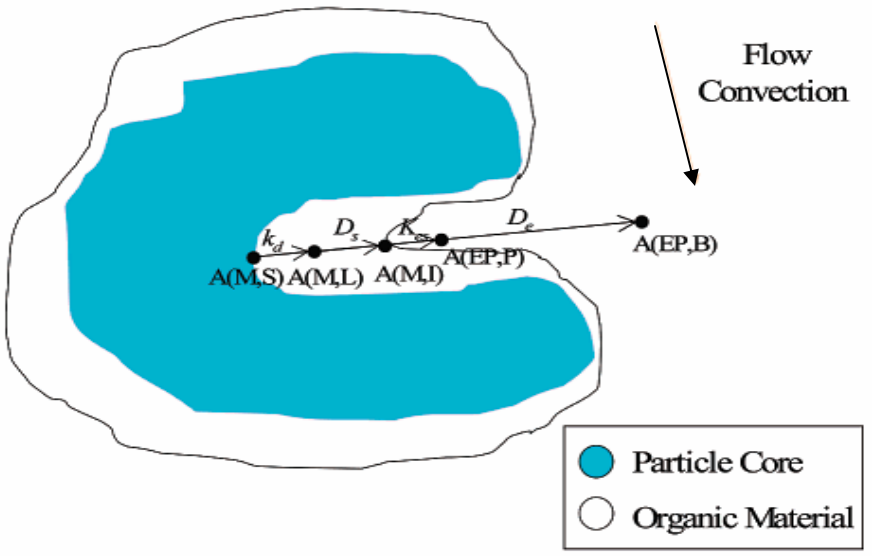

Figure 1.10 Processes involved in the extraction of heterogeneous samples containing porous solid particles.[32]

Extraction can be performed directly in a vessel (e.g. soxhlet, sonication, or microwave extraction) or can be combined with elution from the packed tube (Supercritical Fluid Extraction, Pressurized Fluid Extraction).[33] In the latter case, which is the most efficient and common approach for the extraction of volatile and semi-volatile organic compounds from solid matrices, the sample is typically placed inside the tubing and a linear-flow restrictor is attached to maintain the pressure at the end of the vessel.[33] During the extraction process, the extraction phase continuously removes analytes from the matrix, similar to chromatographic elution with packed columns.[33] Therefore, chromatographic frontal analysis and the corresponding equations have been used to mathematically describe the relationship between the various matrix parameters and flow conditions (e.g. desorption, diffusion, tortuosity, eddy diffusion, longitudinal diffusion) and the elution profiles.[32] This relationship is described as contributions from each of the mass transfer steps to the height equivalent to a theoretical plate (HETP).[4] The analyte concentration profile generated during the extraction as a function of time *C(x, t)* can be presented using the equation that describes the dispersion of a plug of finite width, and consists of terms related to the HETP. The mass of analyte eluted from the vessel during a given extraction time *t* can be calculated from the following equation: [4]

$$\frac{m(t)}{m_0} = \frac{\int_{-\infty}^{-\frac{1}{2}L} C(x,t)}{C_0 L} \qquad \text{Equation 1.21}$$

where $m(t)$ is the extracted amount of the analyte and m_0 is the total amount of the analyte in the vessel at the beginning of the experiment, L is the length of the vessel and C_0 is the initial concentration of the analyte in the matrix.[4] This function is called the "time elution profile", emphasizing the similarity of the extraction process to chromatographic elution.[4]

The above discussion, however, applies only when the analytes are initially present in a fluid phase, e.g. in elution of uniform spikes from the extraction vessel or removing weakly adsorbed native analytes from an organic-poor matrix such as sand.[4] The frontal chromatography approach is appropriate for systems in which the partitioning equilibrium between the matrix and extraction fluid is reached rapidly compared to the rate of the fluid (extraction phase) flow.[4] In most practical circumstances, however, dynamic extraction is performed, from the beginning of extraction, and the system is not expected to reach the initial equilibrium conditions, due to the slow mass transport between the matrix and the fluid (e.g. slow desorption kinetics or slow diffusion in the matrix).[4] In this case, the relationship between the amount of analyte removed from the vessel and the elution time can be obtained by convoluting the function describing the rate of mass transfer between the phases, $F(t)$, with the elution time profile, $m/m_0(t)$:[4]

$$\int_0^{\tau=t} \frac{m(t-\tau)}{m_0} F(\tau)\, d\tau \qquad \text{Equation 1.22}$$

The resulting function describes the process in which elution and mass transfer between the phases occur concurrently and is called the "extraction time profile" to underline that for most extractions these two processes are expected to be combined.[4]

The above conclusion may be stated more generally: convolution among functions describing individual processes occurring during extraction describes the overall extraction process and is a integrated way of describing the kinetics of these complex processes.[4]

Although the exact mathematical solution of the convolution integral is frequently difficult to obtain, it is possible to represent the solution graphically by using Fourier transform or numerical approaches.[4]

1.4. Objectives

The first objective of the present study was to design and construct a new cold fiber SPME device, using thermoelectric coolers as the cooling source for the SPME fiber, with the aim of improving the simplicity, robustness and portability of cold fiber SPME. Application of the new cold fiber SPME in laboratory and field analysis was the next purpose of the present study. Another goal of the present work was to utilize cold fiber SPME for studying the kinetics of desorption of hydrophobic organic compounds (HOCs) from solid matrices (e.g. sediment).

References

1 Pawliszyn, J., *Solid Phase Microextraction – Theory and Practice*; Wiley – VCH; New York, 1997.

2 Hyotylainen, T., *J. Chromatogr. A*, **1153** (2007) 14-28.

3 Wardencki, W.; Curyło, J.; Namieśnik, J., *J. Biochem. Biophys. Methods,* **70** (2007) 275-288.

4 Pawliszyn, J., Ed., *Sampling and Sample Preparation for Field and Laboratory*. Elsevier, Amsterdam, 2002.

5 Júnior, J.L.R.; Ré-Poppi, N., *Talanta*, **72** (2007)1833-1841.

6 Demeestere, K.; Dewulf, J.; De Witte, B.; Van Langenhove, H., *J. Chromatogr. A,* **1153** (2007)130-144.

7 Pragst, F., *Anal. Bioanal. Chem.,* **388** (2007) 1393–1414.

8 Jeleń, H.H., *J. Chromatogr. Sci.*, **44** (2006) 399-415.

9 Aulakh, J.S.; Malik, A.K.; Kaur, V.; Schmitt-Kopplin, P., *Crit. Rev. Anal. Chem.,* **35 (**2005) 71-85.

10 Elena, E.; Stashenko, E.E.; Martínez, J. R., *J. Biochem. Biophys. Methods,* **70** (2007) 235–242.

11 Halasz, A.; Hawari, J., *J. Chromatogr. Sci.*, **44** (2006) 379-386.

12 Musteata, F.M.; Pawliszyn, J., *J. Biochem. Bioph. Methods,* **70** (2007) 181-193.

13 http://www.sigmaaldrich.com/Brands/Supelco_Home/Spotlights/SPME_central.html, 2008.

14 http://www.ctc.ch/misc/documents/CombiBasic.pdf, 2008.

15 Zhang, Z.; Pawliszyn, J., *Anal. Chem*., **67** (1995) 34-43.

16 Chen, Y.; Pawliszyn, J., *Anal. Chem.,* **78** (2006) 5222-5226.

17 Chen, Y.; Frédéric, B.; Chaintreau, A.; Pawliszyn, J., *Flavour Fragr. J.,* **21** (2006) 822–832.

18 Ghiasvand, A.; Hosseinzadeh, S.; Pawlisyn J., *J. Chromatogr. A,* **1124** (2006) 35-42.

19 Carasek, E.; Cudjoe, E.; Pawliszyn, J., *J. Chromatogr. A,* **1138** (2007) 10-17.

20 Carasek, E.; Pawliszyn, J., *J. Agric. Food. Chem.,* **54** (2006)8688-8696.

21 Lord, H.; Pawliszyn, J., *J. Chromatogr. A*, **885** (2000) 153-193.

22 Ridgway, K.; Lalljie, S. P. D.; Smith, R. M., *J. Chromatogr. A,* **1153** (2007) 36–53.

23 Górecki, T.; Yu, X.; Pawliszyn, J., *Analyst*, **124** (1999) 643-649.

24 Chen., Y., *New calibration approaches in solid phase microextraction for on-site analysis*, thesis for the degree of Doctor of Philosophy in Chemistry, Department of Chemistry, University of Waterloo, 2004.

25 Lord, H.L. *J. Chromatogr. A*, **1152** (2007) 2-13.

26 Liu, Z.; Pawliszyn, J., *J. Chromatogr. Sci.*, **44** (2006) 366-374.

27 Zhou, X.; Li, X.; Zeng, Z., *J. Chromatogr. A,* **1104** (2006) 359-365.

28 Fang, H.; Liu, M.; Zeng, Z., *Talanta*, **68** (2006) 979-986.

29 Müller, L.; Górecki, T.; Pawliszyn, J., *Fresenius J. Anal. Chem.*, **364** (1999) 610-616.

30 Chen, Y.; Pawliszyn, J., *Anal.Chem.*, **76** (2004) 6823-6828.

31 Ai, J., *Anal. Chem.*, **69** (1997)1230-1236.

32 Pawliszyn, J., *J. Chromatogr. Sci.*, **31** (1993) 31-37.

33 Pawliszyn, J., *Anal. Chem.*, **75** (2003) 2543-2558.

Chapter 2

Development of cold fiber SPME

2.1 Introduction

Miniaturisation of the sample preparation devices is significant both for automation and on-site sampling/sample preparation. Portable extraction devices are required to make sample preparation possible directly on the site, as a part of an on-site analyses approach to obtain real-time measurement and minimize loss of analytes and appearance of artifacts during sample transportation and storage.[1] In the case of cold fiber SPME devices, the major heavy part of the primary[2] and the modified system[3] is the cooling source, i.e. the liquid CO_2 cylinder. Moreover, because of the nature of cooling with liquid CO_2, it is still not possible even with the improved CO_2 cooling system, to maintain a stable temperature at the tip of the fiber. In other words, cooling occurs upon evaporation of liquid CO_2 at the outlet of the inner capillary tubing (see Figure 1.6) and the temperature of the fiber fluctuates as each portion of the liquid CO_2 is released. The heaviness of the CO_2 tank and instability of the temperature

of the fiber were the motivations to replace this cooling system with a smaller and more reliable cooling source.

One of the most popular cooling sources commonly used in miniaturized analytical devices is the thermoelectric cooler (TEC).[4,5,6,7,8] In a typical thermoelectric device, a junction is formed from two different conducting materials, one containing positive charge carriers (holes) and the other containing negative charge carriers (electrons). When an electric current is passed in the appropriate direction through the junction, both types of charge carriers move away from the junction and convey heat away, thus cooling the junction. Similarly, a heat source at the junction causes carriers to flow away from the junction, making an electrical generator. Such devices have the advantages of containing no moving parts, low cost, small size, low weight, environmental safety and precise temperature control, but low efficiencies have limited their use to specialty applications, such as cooling laser diodes.[9]

In this chapter, the principles of thermoelectric devices and the theoretical considerations in utilizing TEC as the cooling source for SPME fiber are reviewed, the initial tests are briefly discussed, and the construction of the prototypes of cold fiber SPME with thermoelectric cooling, as well as the temperature calibrations are presented.

2.1.1 Principles of thermoelectric coolers (TEC)

Thermoelectric coolers function according to the Peltier Effect discovered in 1834.[10] Based on the Peltier effect, when a direct current (DC) is applied across two dissimilar materials a temperature differential is produced. A typical thermoelectric module is manufactured using a series of P and N doped bismuth-telluride semiconductor material sandwiched between two thin ceramic plates.[10] The ceramic material provides rigidity and electrical insulation while maintaining good heat conductivity.[10] A thermoelectric couple is made by electrically connecting a *p*-type to an *n*-type element, and the thermoelectric module is built by electrically connecting several thermoelectric couples in series. Figure 2.1 illustrates the schematics of a thermoelectric couple composed of two electrically conducting materials: one *n*-type and the other *p*-type, joined at the top by a metal (black bar) to make a junction.[9]

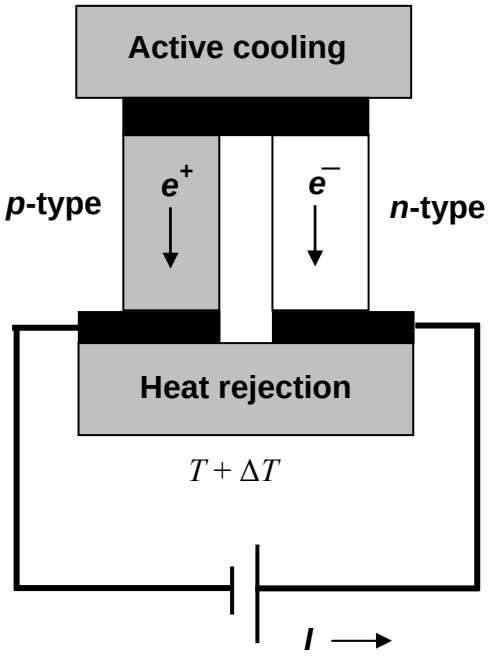

Figure 2.1 *The schematics of a thermoelectric couple.*[9]

When a DC current is applied, both the negatively charged electrons in the *n*-type material and the positively charged holes in the *p*-type material, flow from the junction toward the base, conducting heat away from the junction.[9]

The efficiency of a TEC device, termed as "the coefficient of performance", ϕ, corresponds to the ratio of the cooling rate, Q_c, to the power supplied, W,[11] and is defined as:

$$\phi = \frac{Q_c}{W} = \left(\frac{T}{T_H - T_C} \times \frac{\sqrt{1+ZT}-1}{\sqrt{1+ZT}+1} \right) - \frac{1}{2} \qquad \text{Equation 2.1}$$

where T_H and T_C, are the temperatures of the ambient and the cold part of the cooler, respectively, $T = \frac{T_H + T_C}{2}$, and ZT is the dimensionless figure-of-merit, which can be calculated for a module consisting of *p*-type and *n*-type material using the following equation:[12]

$$ZT = T \times \frac{\left(S_p - S_n\right)^2}{\left[\left(\sqrt{\frac{\kappa_n}{\sigma_n}} + \sqrt{\frac{\kappa_p}{\sigma_p}}\right)\right]^2} \qquad \text{Equation 2.2}$$

where, S_n and S_p, are the Seebeck coefficients, κ_n and κ_p are the total thermal conductivities (sum of the lattice and the electronic contribution), and σ_n and σ_p are the electrical conductivities of the *n*-type and *p*-type semiconductor materials, respectively.[11] According to these equations, materials with high Seebeck coefficients, high electrical conductivities and low thermal conductivities, and therefore high *ZT* values are appropriate for thermoelectric applications. Narrow-gap semiconductors are among these materials[11] and are used in the manufacture of TECs.

TEC modules are made by connecting thermoelectric (TE) couples electrically in series and thermally in parallel, and are available in various sizes, shapes, operating currents, operating voltages and ranges of heat pumping capacity.[10] Figure 2.2, shows a typical single stage TEC module.

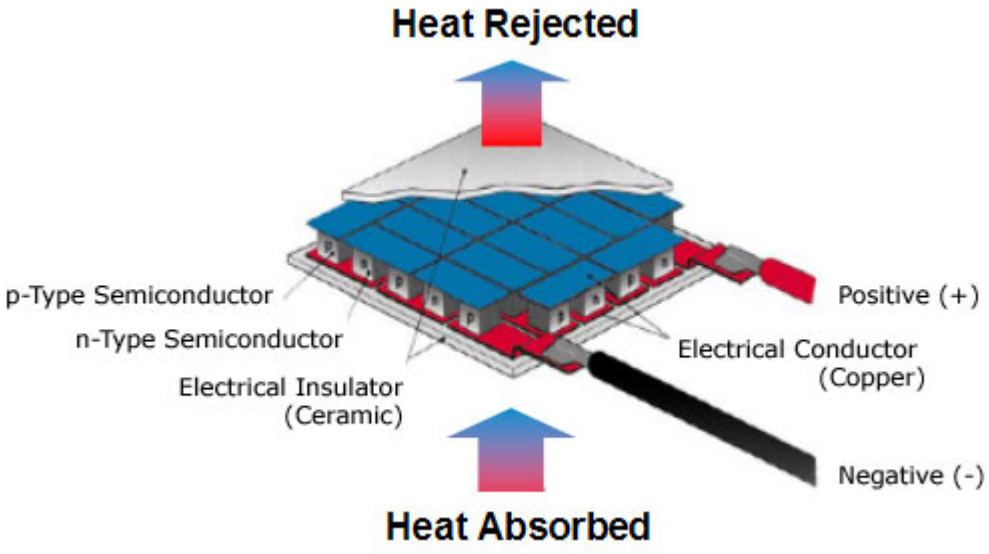

Figure 2.2 *Thermoelectric cooler (TEC) cross-section.*[10]

Selecting the appropriate TEC module for an application depends on at least three parameters, namely: cold surface temperature, hot surface temperature, and the amount of heat to be absorbed at the cold surface of the TEC.[10] In a typical application, the object to be cooled is attached to the cold side of the TEC and a heat sink is attached to the hot side to dissipate the generated heat. The temperature of the hot side is calculated based on the ambient temperature and the efficiency of the heat exchanger that is between the ambient environment and the hot surface of the TEC. If the object to be cooled is attached the cold side of the TEC, the cold side temperature is considered the same as the temperature required for the object. However, in some applications the temperature of the cold side must be much lower than the object to be cooled and should be calculated depending on the situation. The amount of heat load is calculated using applicable heat transfer equations.[10]

2.1.2 Heat transfer modes and rate equations

Understanding the fundamentals and physical mechanisms underlying heat transfer processes is necessary for the design and application of TEC as the cooling source for SPME fiber. In this section the heat transfer modes: conduction, convection, and radiation, as well as the related rate equations, are discussed.

2.1.2.1 Conduction

The term "conduction" is used to describe heat transfer when a temperature gradient exists in a stationary medium that can be solid or liquid.[13] In a liquid medium, heat (thermal energy) is conducted through collision between more energetic molecules (higher temperature) and less energetic ones (lower temperature).[13] In solids, conduction happens due to atomic motions in the form of lattice vibrations.[13] In a non-conductive material the thermal energy is only transferred via lattice vibrations (waves), whereas in a conductive material energy is also transferred through the motion of free electrons.[13]

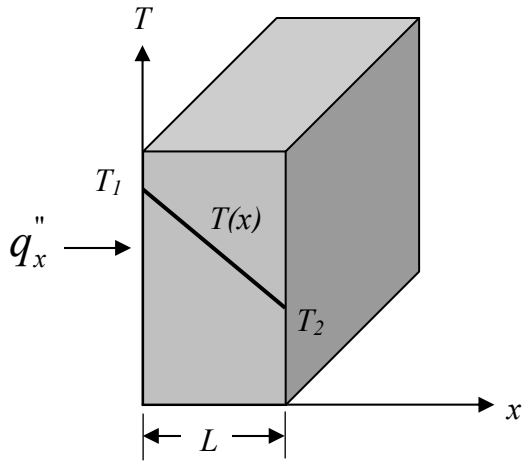

Figure 2.3 *One-dimensional heat transfer by conduction (diffusion of energy).*[13]

Heat transfer processes can be quantified using appropriate rate equations, which allow the calculation of the energy transferred per unit time.[13] For heat conduction, the rate equation is known as Fourier's law.[13] The rate equation for a one-dimensional plane wall, with a temperature distribution of *T(x)*, shown in Figure 2.3, is written as:

$$q'' = -k\frac{dT}{dx} \qquad \text{Equation 2.3}$$

where the heat flux, q'' (W/m^2), is the heat transfer rate in the *x*-direction per unit area perpendicular to this direction, and is proportional to the temperature gradient, *dT/dx*.[13] The proportionality constant, *k*, is thermal conductivity (W/m.K) of the material.[13] The minus sign shows that heat transfers in the direction of decreasing temperature.[13] The temperature gradient for a linear temperature distribution as shown in Figure 2.3 may be written as:

$$\frac{dT}{dx} = \frac{T_2 - T_1}{L}$$

Therefore, the heat flux is

$$q''_x = -k\frac{T_2 - T_1}{L}$$

or

$$q_x'' = k\frac{T_1 - T_2}{L} = k\frac{\Delta T}{L} \qquad \text{Equation 2.4}$$

The product of the heat flux and the area of the plane wall, A, is then the *heat rate* by conduction through the plane wall, $q_x' = q_x''.A$.[13]

2.1.2.2. Convection

In the presence of a temperature gradient, the two mechanisms of random molecular motion (diffusion) and macroscopic motion of the fluid (motion of large numbers of molecules in collections or as aggregates) contributes to heat transfer processes expressed by the term convection.[13]

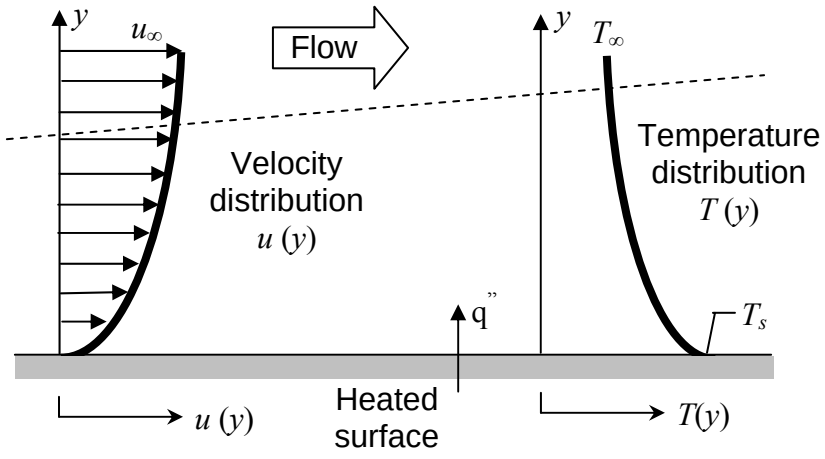

Figure 2.4 *Boundary layer development in convection heat transfer.*[13]

Figure 2.4 shows convection heat transfer between a fluid in motion and a bounding surface when the two are at different temperatures.[13]As a result of the interaction between the surface and the fluid, a velocity boundary layer is developed in the fluid through which the velocity varies from zero at the surface to a finite value u_∞.[13] Moreover, due to the temperature difference between the fluid and the surface, a thermal boundary layer is formed in the fluid through which the temperature varies from T_s at $y=0$, to T_∞ in the bulk.[13] The thermal boundary layer can be smaller, larger, or the same size as the velocity boundary

layer.[13] In any case, if $T_s > T_\infty$, the heat will transfer via convection between the surface and the bulk of the fluid.[13]

Convection heat transfer can be forced convection, in which the flow is caused by an external means, such as a fan, or free (or natural) convection, in which the flow is caused by the density differences due to temperature variations in the fluid.[13] In some conditions, a mixture of both forced and natural convection may happen. There are also convection processes for which there is an additional heat exchange, generally associated with a phase change between the liquid and vapour states of the fluid. Boiling and condensation are two common examples of additional heat exchange that may happen in a convection process.[13]

The appropriate rate equation that describes the convection heat transfer process, also known as Newton's law of cooling, is:

$$q'' = h(T_s - T_\infty) \qquad \text{Equation 2.5}$$

where q'' is the convective heat flux (W/m^2), which is proportional to the difference between the surface and fluid temperatures, T_s and T_∞, respectively.[13] The proportionality constant, h (W/m^2.K), is the convection heat transfer coefficient, and depends on conditions in the boundary layer influenced by surface geometry, the nature of the fluid motion, and the fluid thermodynamics and transport properties.[13] In solving convection heat transfer problems, h is considered known, using typical values presented in table 2.1.

Table 2.1 Typical values of the convection heat transfer coefficient[13]

PROCESS	h (W/m^2.K)
Free convection:	
Gases	2-25
Liquids	50-1000
Forced convection:	
Gases	25-250
Liquids	50-20,000
Convection with phase change	
Boiling or condensation	2500-100,000

The convection heat flux is considered to be positive if the heat is transferred from the surface and negative if heat is transferred to the surface.[13] The convection heat transferred from the surface is therefore:

$$q_{conv} = hA(T_s - T_\infty) \qquad \text{Equation 2.6}$$

2.1.2.3 Radiation

Thermal radiation is the thermal energy of the matter at a finite temperature that is emitted as electromagnetic waves (or photons).[13] The heat flux, *E*, emitted by a surface is expressed as:

$$E = \varepsilon\sigma T_s^4 \qquad \text{Equation 2.7}$$

Where ε is a radiation property of the surface known as emissivity ($0 \le \varepsilon \le 1$), σ is the Stefan-Boltzmann constant (σ = 5.67x10^{-8} W/m^2.K^4), and T_s is the absolute temperature (K) of the surface.[13]

The term irradiation, *G,* on the other hand, is the rate at which thermal energy is incident on a surface by radiation.[13] A portion or all of the irradiation may be absorbed by the surface, thereby increasing the thermal energy of the material. The rate at which radiant energy is absorbed per unit surface area, G_{abs}, is:

$$G_{abs} = \alpha G \qquad \text{Equation 2.8}$$

where α is a surface radiative property named *absorptivity.*

For the case in which radiation exchange happens between a small surface at T_s, and a much larger, isothermal surface that completely surrounds the smaller surface and is at a different temperature T_{sur}, the net rate of radiation heat transfer from the surface, expressed per unit area of the surface is:

$$q''_{rad} = \frac{q}{A} = \varepsilon\sigma\left(T_s^4 - T_{sur}^4\right) \qquad \text{Equation 2.9}$$

assuming that irradiation is approximately equal to the emission from a black body for which $G = \sigma T_{sur}^4$ and that $\alpha = \varepsilon$ for the surface.

Therefore, the net radiation heat exchange is:

$$q_{rad} = \varepsilon A \sigma \left(T_s^4 - T_{sur}^4 \right) \qquad \text{Equation 2.10}$$

The total heat transfer from a surface is therefore the summation of heat transferred via convection and that transferred through radiation from that surface:

$$q = q_{conv} + q_{rad} = hA\left(T_s - T_\infty \right) = \varepsilon A \sigma \left(T_s^4 - T_{sur}^4 \right) \qquad \text{Equation 2.11}$$

The concepts explained above will be used later in this chapter to estimate the amount of heat needed to be removed from the fiber by the TEC module used in the cold fiber device.

2.2 Fabricating the cold fiber SPME with thermoelectric cooling

In order to cool the SPME coating with a TEC, a conductive material was used as the support for the SPME coating. The upper part of the SPME support (a rod made of conductive material) was in contact with the cold surface of the TEC, and the lower part was placed the extraction vessel. Heat was supplied at a steady rate to one end (in the vessel), and drained from the other end (in the TEC). Therefore, a linear temperature gradient was established, which depends on the length and the cross-sectional area of the copper rod. The first step of the design of the device based on thermoelectric cooling was to choose the suitable conductive material and to optimize the dimensions (length and diameter) of the rod.

2.2.1 Selecting SPME support material

The parameters considered in choosing the appropriate material included good thermal conductivity and price. According to the thermal conductivity tables[13], the thermal conductivity of copper is 385 W/m K, which is between those of silver (430 W/m K) and gold (310 W/m K). Since copper is more cost efficient, it was chosen for the SPME fiber support (rod).

2.2.2 Optimizing the SPME fiber support dimensions

The diameter of the fiber support (copper rod) was limited to the dimensions of the needle of the SPME device, which was in turn limited by the GC injector nut. The standard injector nuts are manufactured to be used with 23- and 24-gauge needles; however, considering the possibility of enlarging the hole of the injector nut, the inner diameter of a standard 18-gauge needle (838 micrometer) was considered the maximum allowable diameter for the copper rod. Therefore, copper rods with diameters equal to or less than 800 micrometer were tested. The length of the copper rod was selected according to the distance between the tip of the fiber and the head of the injector nut, after SPME fiber was injected to the GC injector. The shortest distance between the tip of the copper rod and the cold surface of the TEC that could be used with the available GC injector (Optic 2 ATAS programmable high volume injector) was 3 cm. Optimization of the diameter of the copper rod and the distance between the tip of the copper rod and the cold side of the TEC was performed using a simple set-up. In this section, the primary tests together with the initial observations are explained.

2.2.2.1 Materials

Copper and constantan wires of different diameters (0.25, 0.38, 0.80 mm), were purchased from Omega. Two single-stage thermoelectric coolers together with heat sink and fan were purchased from Melcor (Trenton, NJ, USA). Sample vials, 4 mL, were purchased from Supelco (Bellefonte, PA, USA). T-type thermocouple wires were purchased from Omega (Stamford, CT, USA).

2.2.2.2 Experimental set-up

The set-up illustrated in Figure 2.5 was used for optimization experiments. The insulation of the copper wire was removed at different lengths (depending on the test) and the upper part of the bare copper wire was cooled between two single-stage TECs and the other end (outside the cooling source) was placed in a vial. To measure the temperature of the fiber (T_1), a constantan wire was welded to the tip of the copper wire using a Spot Welding device (66V,

limited current) equipped with a graphite anode, to make a T-type thermocouple. In other words, the copper wire, which is going to be used as the fiber support, acted as one of the wires of a T-type thermocouple. This thermocouple was passed through the septum of a screw cap of a 4 mL glass and the cap was fastened on the vial. Another T-type thermocouple was also embedded between the two TECs to allow monitoring the temperature of the cold side of the TECs, referred to as T_2. Both thermocouples were connected to a digital thermometer to monitor the temperatures T_1 and T_2.

Using a DC power supply, the appropriate DC current was applied to TECs. The minimum temperature of the cold side of the TEC was around -10 ºC. The temperatures were read after a stable temperature was reached (10 min after applying the DC current). The tests were performed with the vial at room temperature (22 ºC).

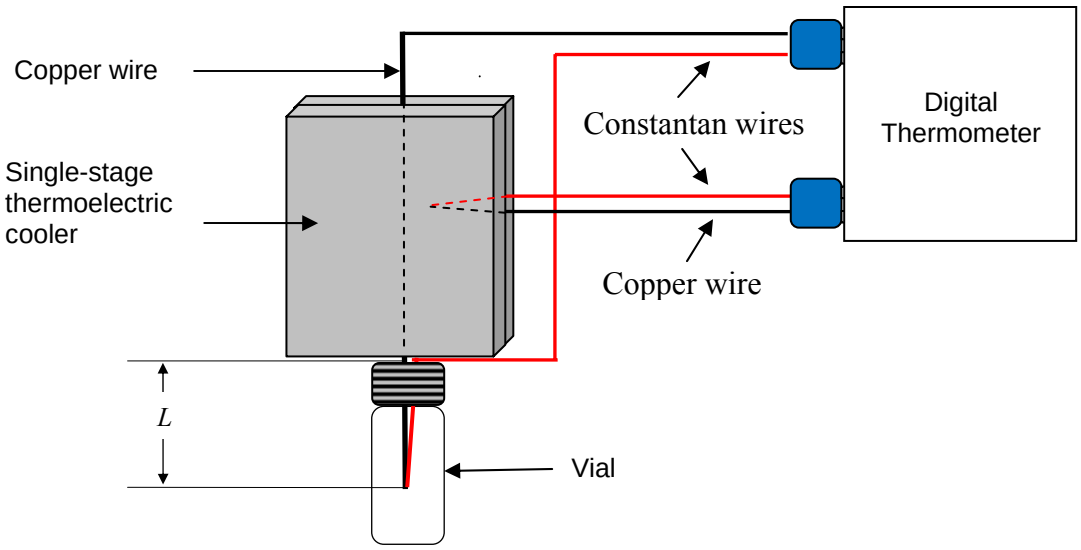

Figure 2.5 *Experimental set up for optimization of copper rod diameter and length.*

Copper wires of different diameters (250, 380, and 800 µm) were made into thermocouples and were placed in the set up explained in the above section. The temperature of the tip of the

fiber, T_1, was monitored for each wire by changing the position of the wire on the cold surface, indicated by L, in Figure 2.5.

2.2.2.3 Temperature measurement results

Figure 2.6 shows the changes in the temperature of the tip of the fiber, T_1, versus the distance from the cooling source, L, for the three different wires. The temperature of the fiber decreased by decreasing L, the distance from the cooling source, and by increasing the cross-sectional area (or diameter) of the copper wire. Since the lowest fiber temperatures were related to the wire with 800 µm diameter, this wire was chosen as the SPME fiber support. Moreover, considering the minimum required length for fiber to be at the hot zone of the GC injector (after injection), a 30 mm distance from the cooling source was chosen as the optimum distance.

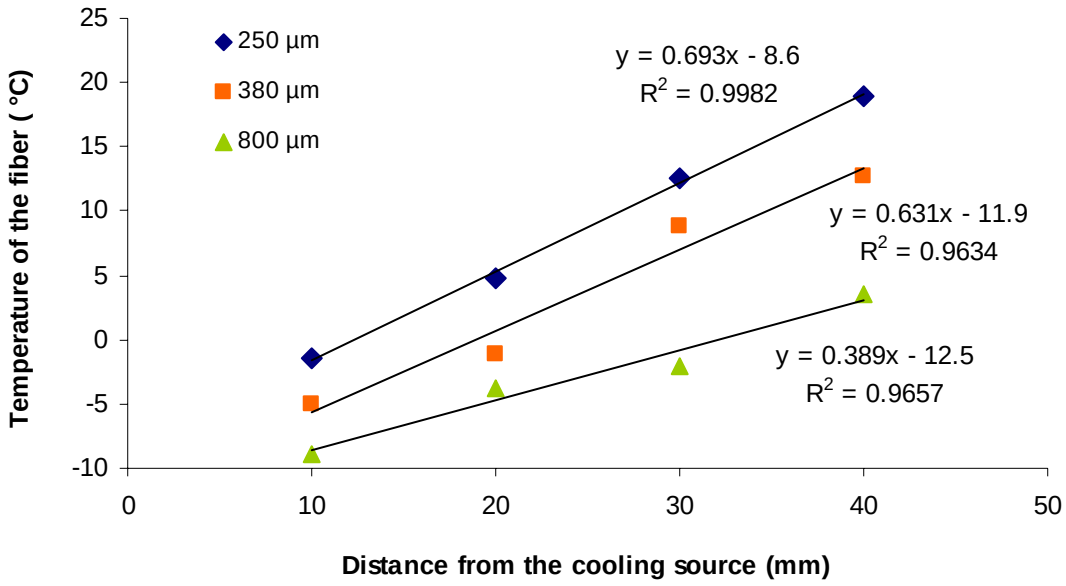

Figure 2.6 *Temperature of the fiber versus distance from the cooling source for different diameters.*

2.2.3 Selecting the appropriate TEC

As explained earlier in the introduction, one of the parameters required for the selection of appropriate TEC for an application is the amount of heat loaded from the object to be cooled. In the present application, the heat loaded from the SPME fiber can be estimated using heat transfer formulae explained in the introduction part of this chapter. The schematics of heat transfer processes occurring during cold fiber headspace extraction are illustrated in Figure 2.7.

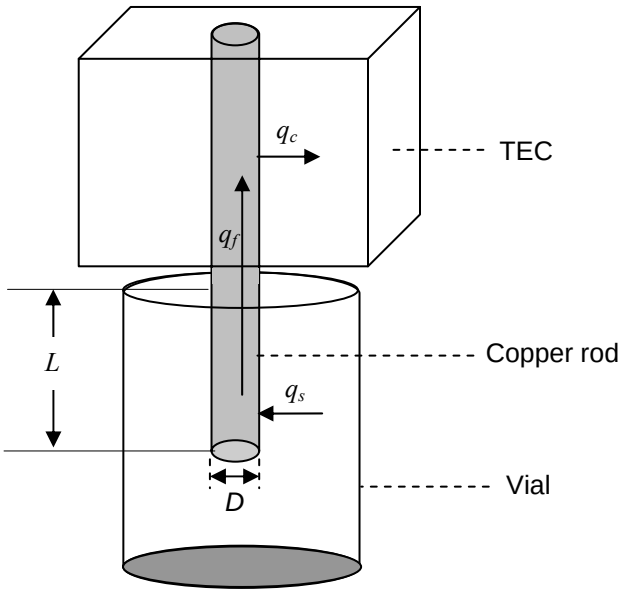

Figure 2.7 *Schematics of the heat transfer during extraction with cold fiber SPME.*

In a typical extraction, SPME fiber with the temperature of T_f, is exposed to a gaseous sample or the headspace of a sample in a vessel, at T_s, while the cold side of the TEC is at T_c. Heat is supplied to the fiber by convection and radiation, q_s, at the surface of the fiber and is transferred via conduction along the copper rod, q_f, to the cold surface of the thermoelectric cooler and is drained into the cooler, q_c. To estimate the heat loaded by TEC, the following assumptions are made:

1. Steady-state conditions exist
2. The temperature is the same along the copper rod outside the TEC
3. Surface emissivity and absorptivity are the same and equal to 1.

For steady-state condition, we may write: $q_s=q_f=q_c=q$, therefore, the amount of heat loaded by the TEC can be calculated by calculating the heat transferred to the fiber through convection and radiation, q_s, by applying equation 2-9. Replacing temperature of the surface, T_s by temperature of the fiber, T_f, and T_{sur} and T_∞ by the temperature of the sample, T_s, gives:

$$q_s = q_{conv} + q_{rad} = hA(T_f - T_s) + \varepsilon A\sigma\left(T_f^4 - T_s^4\right)$$

Considering maximum sample temperature of 200 ºC and minimum fiber temperature of 0 ºC, with A equal to the surface area of the copper rod, $A = \pi DL$, where D is the diameter of the copper rod (0.0008 m), and L is the length of the copper rod that is outside the TEC cold surface during extraction (0.03 m), and with h =30 W/m^2.K:

$$q = h(\pi DL)(T_f - T_s) + \varepsilon(\pi DL)\sigma\left(T_f^4 - T_s^4\right)$$

$$q = 30\ \text{W/m}^2\text{.K}\ (3.14\times0.0008\text{m}\times0.03\text{m})(200)$$

$$+1(3.14\times0.0008\text{m}\times0.03\text{m})\ 5.67\times10^{-8}\ \text{W/m}^2\text{.K}(473^4\text{-}273^4)$$

$$q = 0.452\text{W}+0.190\text{W}=0.642\text{W}$$

However, in real samples that contain water, heat might also be exchanged at the surface of the fiber due to water condensation. In this case, by replacing h with 100,000 (table 2.1), the heat exchanged at the fiber, q, is equal to 1506 W. Therefore, the amount of heat that is loaded to the fiber varies within a wide range, depending on the water content of the sample.

The other specification needed for the selection of TEC is the temperature of the cold side of the TEC, T_c. As according to equation 2.4, the linear heat rate through the copper rod is directly proportional to the temperature difference across the rod, the lower the T_c, the more efficient would be the conductive heat transfer through the copper rod. Since the diameter of the copper rod is relatively small, there is a high resistance through the rod, and a very large temperature difference is required for efficient heat transfer. For example, even by considering the lowest heat gained at the fiber (0.642 W), the temperature difference required for a copper rod with the diameter of 0.0008 m, is 99.5 °C.

Therefore, the ideal TEC for this study should provide a low temperature and a high heat load. However, the thermoelectric coolers are designed to either provide a high temperature

difference between the ambient and the cooler, or a high heat load. Looking through the Melcor catalogue it was found that a TEC module that could provide a high heat load would need a heat sink and fan with sizes that were too large to be used as a part of the SPME device, and also required high voltages, which was not desirable for a portable device. Therefore, the best available TEC module was selected by considering all the above mentioned parameters, i.e. low operating voltage, high heat load, low temperature and reasonable size.

2.2.4 Construction and calibration of the cold fiber SPME with TEC

After selecting the appropriate TEC and deciding about the best dimensions of the copper rod, prototype devices were designed and constructed.

2.2.4.1 Materials

Three-stage thermoelectric cooler (part number: 3 CP 055 065-71-31-17) and related heat sink and fan were purchased from Melcor (Trenton, NJ, USA). Stainless steel tubing, 18-gauge, was purchased from Small Parts. Polydimethylsiloxane liquid polymer tubing (hollow fiber), with a thickness of 178 μm was purchased from New Age Industries (Southampton, PA, USA) and was used as the SPME fiber coating. K-type thermocouples, copper wire (0.8 mm diameter used as the SPME support) and digital thermometer were purchased from Omega (Stamford, CT, USA). Copper plate, aluminium parts, insulating material, DC power supply and voltage regulator were provided by the University of Waterloo Science Technical Services (STS). Car battery was purchased from a local Canadian Tire store.

2.2.4.2 Construction of the cold fiber SPME device prototypes

2.2.4.2.1 First prototype

Figure 2.8 illustrates the picture and the schematics of the first cold fiber SPME prototype. The hot side of the thermoelectric cooler was attached to a heat sink and fan, which were used to dissipate the generated heat. A copper plate was attached to the cold surface of the TEC. A groove of 0.5 mm depth was made in the middle of the copper plate. The groove acted as a

seat for the SPME fiber. A K-type thermocouple (not shown in the picture) was embedded in the copper plate close to the groove, to monitor the temperature of the cold side of the TEC. An aluminum box was built around the TEC module, which was filled with insulating material. The upper and lower sides of the box were machined to serve as the seat for the plunger and the septum, and the needle hub, respectively. A needle, 1.5 cm, was soldered to a hub and was mounted on the lower side of the aluminum box. The SPME fiber was made by removing 9 cm of the insulation of a copper wire, 0.8 mm diameter, and was mounted on the plunger and passed through the device. One centimetre of the PDMS hollow fiber was cut, swollen in hexane, and placed at the tip of the copper wire to serve as the extraction phase.

A direct current (DC) power supply and a custom-made voltage regulator were used to apply the appropriate power both to the TEC and the fan. The total voltage required to run the system was 12 volts. The temperature of the cold side of the TEC was controlled by the direct current passing through the TEC.

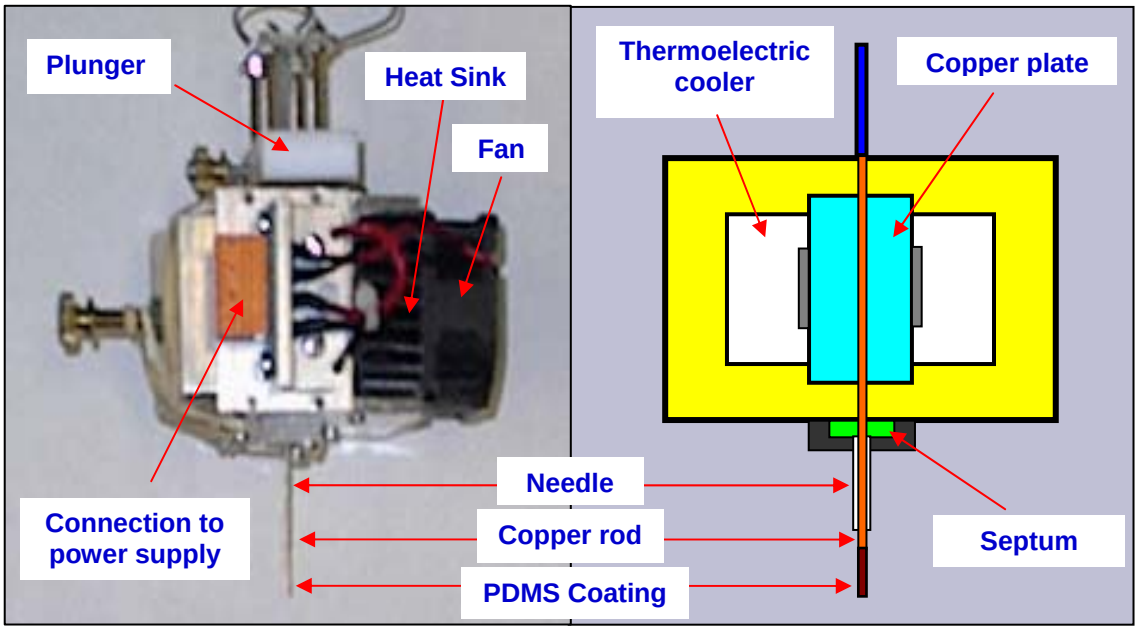

Figure 2.8 *Schematic and picture of first prototype of cold fiber SPME device.*

2.2.4.2.2 Second prototype

A second prototype was constructed with improvements in the plunger and the contact part between the copper rod and the cold side of the thermoelectric cooler (Figure 2.9).

Similar to the first prototype, a copper plate was attached to the cold surface of the TEC. A groove, 0.5 mm, was made in the middle of the copper plate. A K-type thermocouple (not shown in the picture) was embedded at this copper plate close to the groove to monitor the temperature of the cold side of the TEC. Two pieces of aluminum (upper and lower pieces in Figure 2.9) were machined to serve as the seat for the SPME plunger (in the upper piece), and the septum and the needle hub (in the lower piece). Three aluminum plates were also used as the sides of the device. To improve better contact between the copper rod and the copper plate, a plastic part was machined and fixed over the copper plate. A needle, 1.5 cm, was soldered to a hub and was mounted on the lower aluminum piece. The SPME fiber was made with a copper wire of 0.762 mm diameter and 8.5 cm length. The plunger of a commercially available SPME device was removed and used as the plunger for the second prototype. The copper rod was mounted on the plunger by using a plastic screw and was passed through the hole in the upper piece, the space between the copper and plastic plates, the septum, and the needle. After passing the copper rod through the device, the plunger was screwed to the upper aluminium piece. One centimetre of the PDMS hollow fiber was cut, swollen in hexane, and placed at the tip of the copper wire to serve as the extraction phase. In order to achieve better cooling, the empty space between the copper plate and the aluminium parts was filled with glass wool. The copper rod was in a good contact with the copper plate and could be easily moved up and down using the plunger.

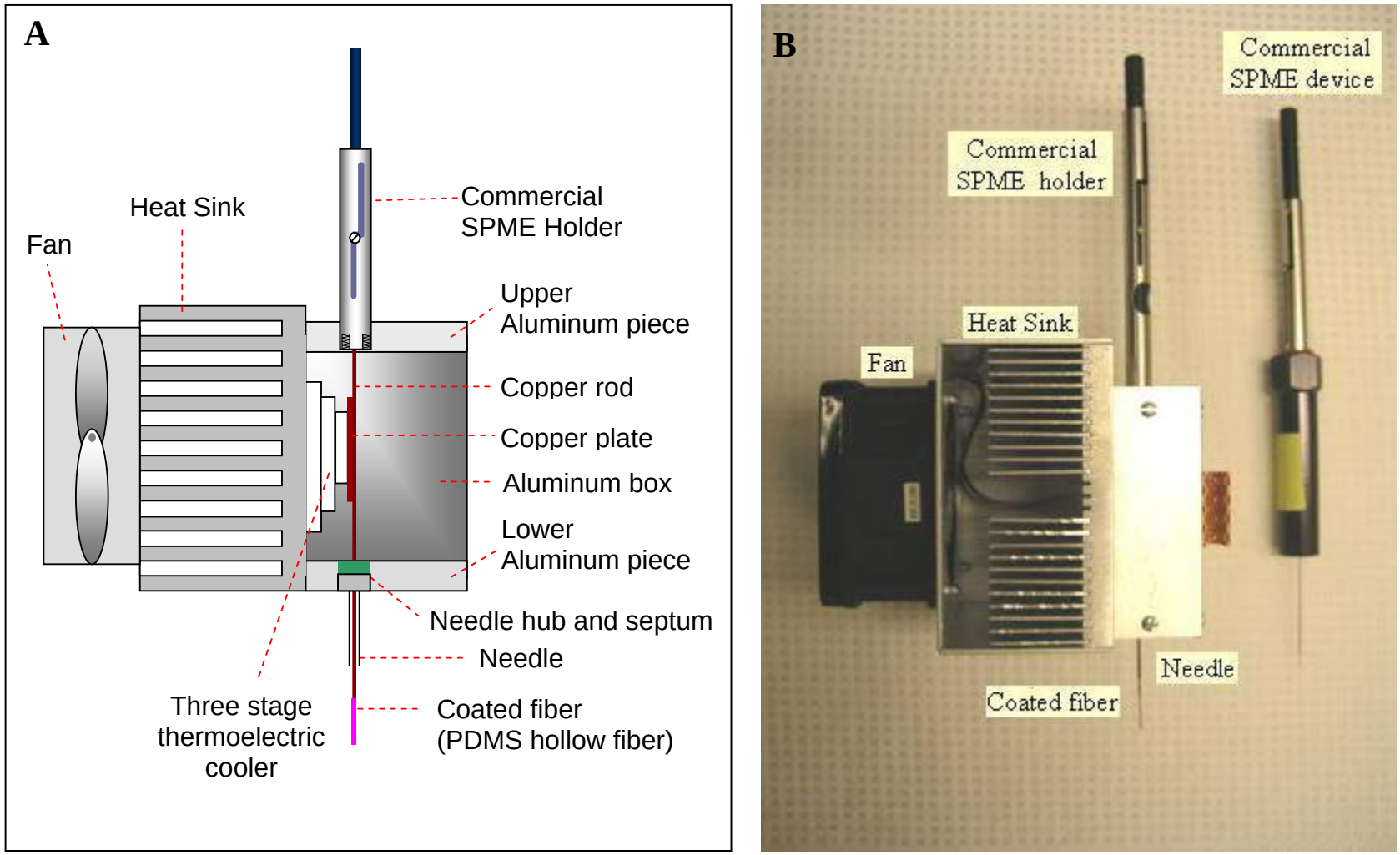

Figure 2.9 *(A) Schematics and (B) picture of the second prototype of cold fiber SPME device*

2.2.4.2.3 Portable cold fiber SPME with TEC

Portable cold fiber SPME with TEC was prepared by replacing the DC power supply by a car battery. Figure 2.10 illustrates the schematics of the portable device. The portable device was applied to the extraction of volatile compounds from live flowers (see Chapter3).

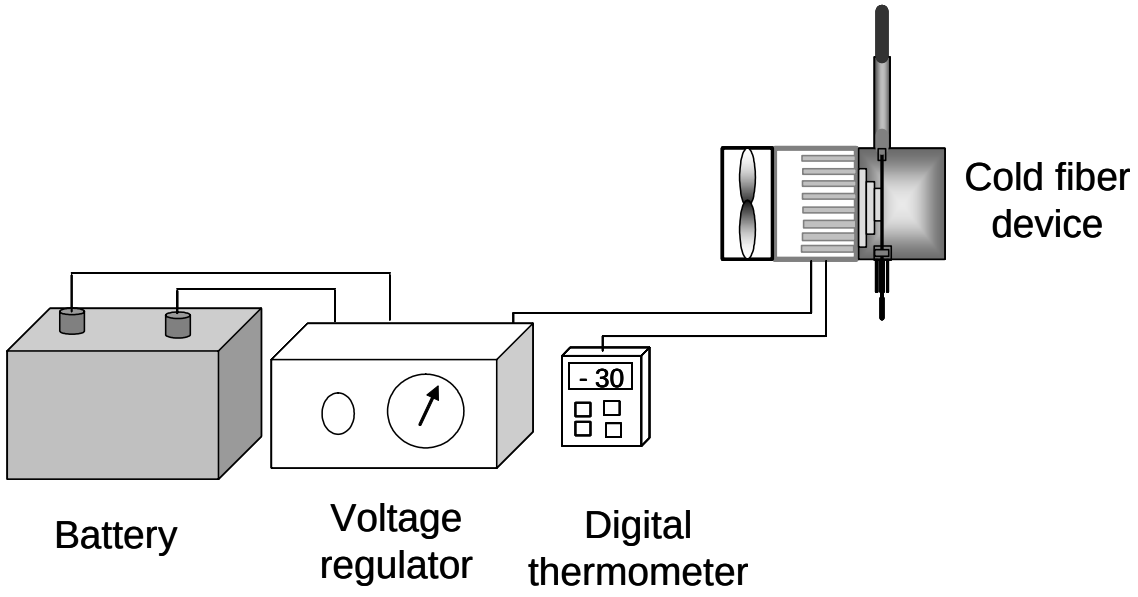

Figure 2.10 *Schematics of portable cold fiber SPME system.*

2.2.4.3 Temperature calibration

The structure of the cold fiber SPME device based on thermoelectric cooling of a metal fiber does not allow the in situ measurement of the temperature of the fiber, i.e. measuring the temperature of the fiber during extraction step; however, it is possible to calibrate the device for different sample temperatures.

As the temperature of the fiber depends on the sample conditions, it is important that the temperature of the fiber is measured at the experimental conditions, before the extraction is

carried out. The temperature calibration was performed by placing a small thermocouple beneath the hollow fiber and placing the fiber in the extraction vial containing the sample. A thermocouple and the needle of the device were passed through the vial septum first and the fiber was pushed out by pushing the plunger in, 2 cm of the hollow fiber were cut and soaked in hexane for a few minutes and after it was swelled, the thermocouple was passed half way through it, and the other half was mounted quickly on the copper fiber in a way that the thermocouple joint touched the fiber at 5 mm from the end of the fiber. In this way, the fiber was coated (similar to extraction step) and the thermocouple was held on the fiber by the use of the hollow fiber. Then, the sample was loaded in the vial and the cap was screwed to the vial. Another thermocouple was placed in the vial to monitor the temperature of the vial. The temperature of the cooler, temperature of the sample and the temperature of the fiber were measured for calibration.

2.2.4.3.1 First prototype

The initial temperature measurements performed for the first prototype at different temperatures of the vial are shown in Figure 2.11. Sample temperatures of 28, 100 and 150 ºC were tested. The temperature of the cooler was -25 ºC.

Before the cooling was started, the temperature of the fiber was lower than the temperature of the sample, because the copper has a high conductivity and removes the heat from the hot zone (in the vial) to the cold side (out side the vial). After the cooling was started, the temperature of the TEC and the fiber decreased and reached a minimum after 5 min, which remained constant during the time that cooling was applied.

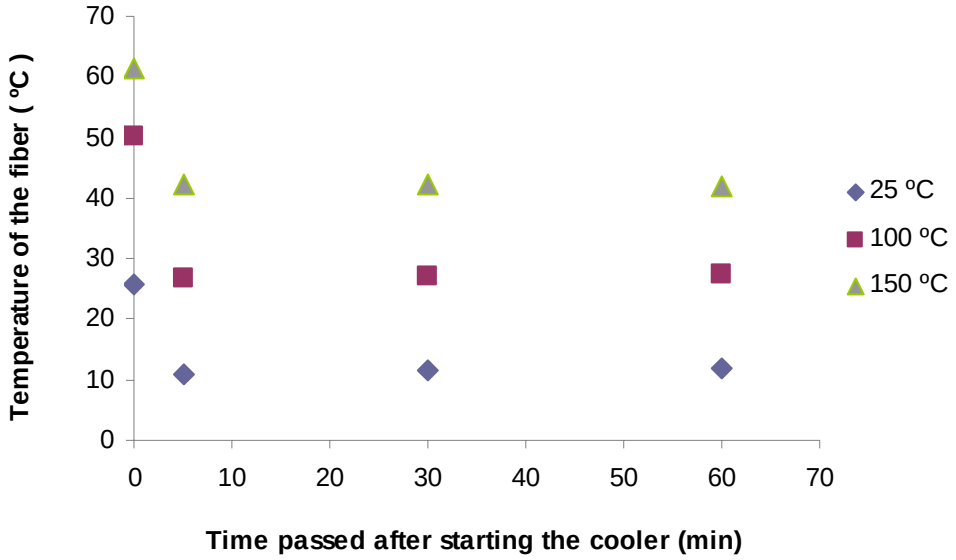

Figure 2.11 *Temperature calibration of the first prototype.*

2.2.4.3.2 Second prototype

Temperature of the fiber was calibrated for the second prototype using the same procedure. The calibrations were performed for four different sample temperatures (40, 50, 80 and 100 °C). The current applied to the TEC was increased from zero to 2 amp, at each temperature, and a plot of the temperature of the fiber versus the temperature of the cooler was obtained. Sand, 2 g, was used as the sample in these temperature measurements. The temperature calibration plots provide an estimation of the fiber temperature at different sample temperatures. The plots are shown in Figure 2.12.

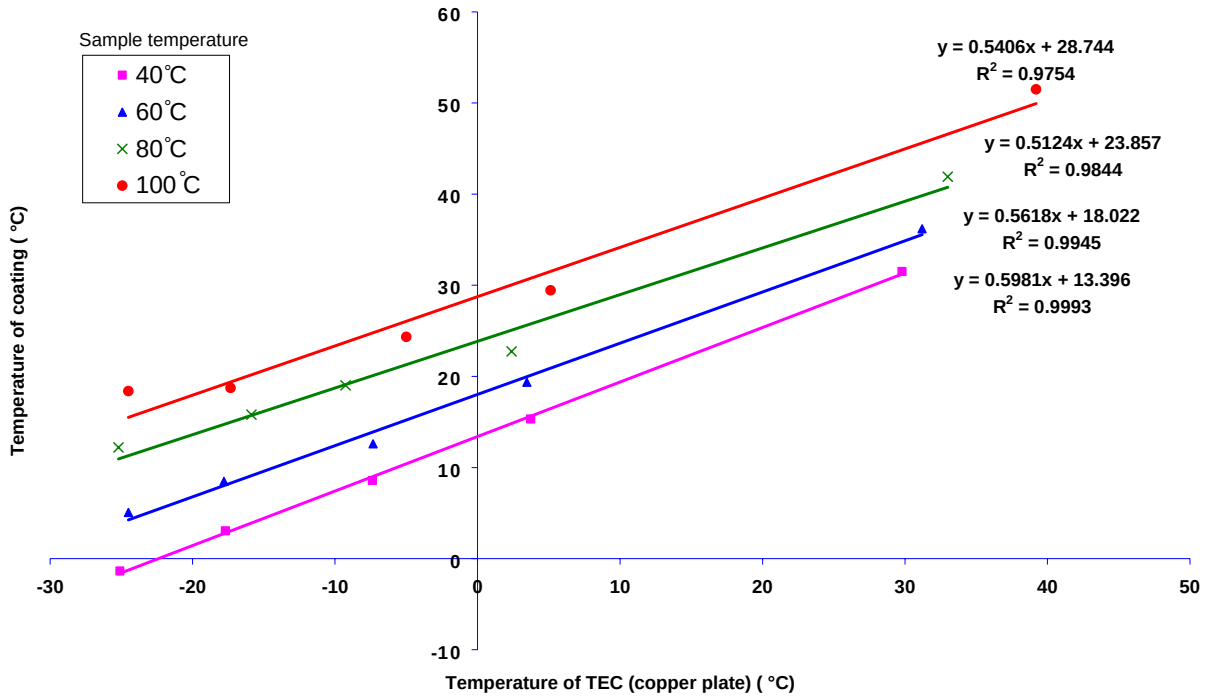

Figure 2.12 *Temperature calibration of the second cold fiber device prototype: temperature of the fiber versus the temperature of the cold side of the TEC measured at different sample temperatures.*

2.2.4.3.3 Effect of sample water content

As water can condense on the cold surface of the fiber and increase the temperature, it is important to experimentally observe the effect of water content on the temperature of the cold fiber.

In order to calibrate the device for different water content levels, different amounts of water (1, 3, 5, and 10 w/w%) were added to two grams of sand in 40 mL vials at room temperature. Each vial was shaken for 15 min and immediately mounted on the device, as explained in the temperature calibration section, and was placed in the heat block (previously set at the desired temperature). After 15 min the TEC was turned on with different currents passing through the circuit, and the temperatures of cooler, coating, headspace and the sample were monitored for 10

min. The temperature measurements were done for sample temperatures of 40, 60, 80, and 100 ºC. Figure 2.13 illustrates the effect of sample water content on the temperature of the fiber at different sample temperatures.

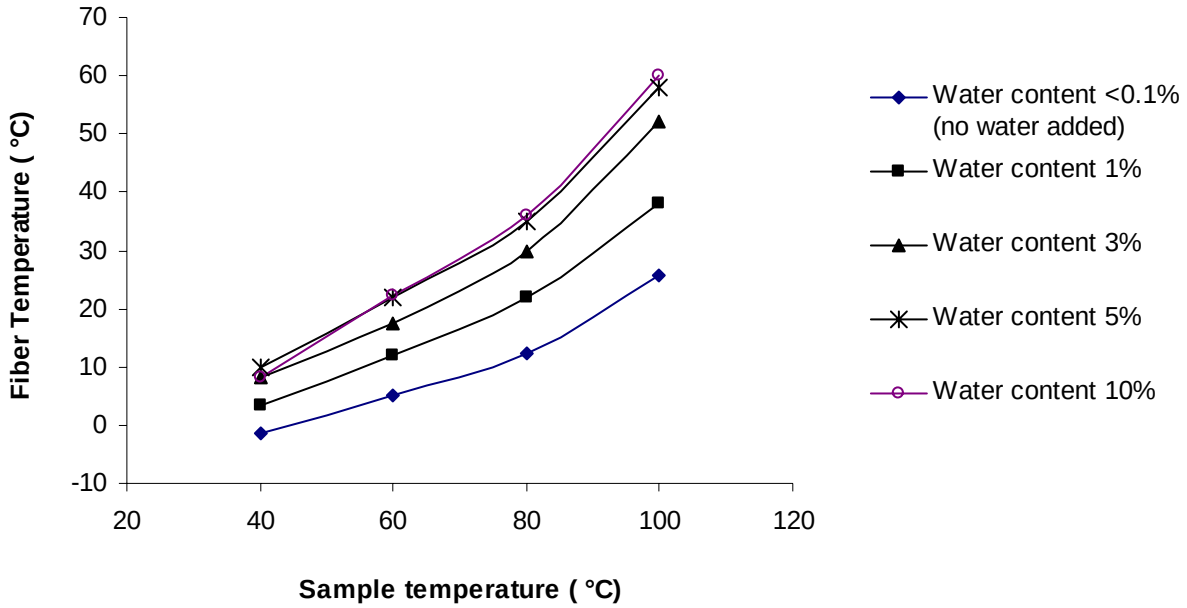

Figure 2.13 *Effect of the sample water content on the temperature of the fiber at different sample temperatures (second prototype). The average RSD% for the cooler and coating temperatures were 5% and 17%, respectively, calculated by running a selected experiment (10% water content and 80 ºC sample temperature) in triplicate.*

It was found that as the water content increased from less than 0.1% to 5%, the temperature of the fiber increased at all sample temperatures; however, increasing the water content from 5 to 10 % did not result in further increase in the fiber temperature. On the other hand, increasing the temperature from 40 to 100 ºC resulted in a gradual increase in the temperature of the fiber with a steeper slope from 80 to 100 ºC. The increase in the temperature of the fiber is related to the number of moles of the water that condense at the coating, at all sample temperatures, increasing the water content results in more water molecules in the headspace; however, it appears that at

5% water content, the surface of the coating is covered with a layer of condensed water, which drops off and is replaced by another layer of water molecules and increasing the sample water content from 5 to 10% does not result in further increase of the fiber temperature. In other words, the number of moles of the water that condense on the fiber remains constant after 5% water content. Moreover, the temperature increased at a higher rate when the temperature of the sample was increased from 80 to 100 ºC. As the temperature of the sample reached the boiling point of water the, vapour pressure of water was increased and more water molecules were present in the headspace. In summary, the presence of water can dramatically increase the temperature of the fiber, especially when the sample temperature is close to the boiling point of water. For example, the fiber temperature increased from 20 ºC, for <0.1% water content, to around 60 ºC for 5% water content (at 100 ºC sample temperature).

The water content of the original sand sample (without adding water) was measured by the following procedure: three 50 mL beakers were weighted and heated in a furnace at 200 ºC overnight. The beakers were cooled down to room temperature in a dessicator and weighted for a second time. Sand, 10 gram, was loaded to each beaker and the weights were measured. The beakers were then placed in the furnace at 200 ºC, and weighted after two hours. To completely dry the sand samples, the loaded beakers were placed in the furnace overnight and weighted the following day. The water content was calculated by calculating the difference between the weights of the loaded beakers before and after heating the sand in the furnace, divided by the initial weight of the sand, and multiplied by 100. The water content of the sand, calculated by this procedure, was less than 0.1 %.

2.3 Conclusion

Application of thermoelectric cooler modules as the cooling source for the SPME fiber requires understanding the fundamentals of thermoelectric coolers and the heat transfer processes involved in extraction using the cold fiber SPME. In this chapter, these fundamentals were explained and the specifications required for selecting a TEC module were calculated by applying proper heat transfer rates and making appropriate assumptions. The dimensions of the copper rod used as the SPME support were also experimentally optimized. The structure and temperature calibration results of the two cold fiber SPME prototypes and the effect of water content were illustrated.

It is concluded that the cold fiber SPME device with thermoelectric cooling of the metal fiber, can provide efficient cooling for lower sample temperatures, due to the low efficiency of the thermoelectric cooler. Therefore, this device is more suitable for applications in which the sample is at a relatively low temperature (below 100 ºC), such as food analysis or volatile compounds emitted by live flowers, where heating the sample to elevated temperature can result in changing/damaging the sample. These two prototypes were used in experiments explained in chapter 3 of this dissertation.

References

1 Pawliszyn, J., Ed. *Sampling and Sample Preparation for Field and Laboratory*, Elsevier, Amsterdam, 2002.

2 Zhang, Z.; Pawliszyn, J., *Anal. Chem*., **67** (1995) 34-43.

3 Chen, Y.; Pawliszyn, J., *Anal. Chem*., **78** (2006) 5222-5226.

4 Sgro, A.E.; Allen, P.B.; Chiu, D.T., *Anal. Chem*., **79** (2007) 4845-4851.

5 El-Ali, J.; Gaudet, S.; Günther, A.; Sorger, P.K.; Jensen, K.F., *Anal. Chem*., **77** (2005) 3629-3636.

6 Liu, J.; Jiang, G.; Zhou, Q.; Liu, J.; Wen, M., *Anal. Sci.*, **19** (2003)1407-1411.

7 Mosier-Boss, P.A.; Lieberman, S.H., *Anal. Chim. Acta*, **488** (2003)15-23.

8 Jiemin, L.; Guibin, J.; Jingfu, L.; Qunfang, Z.; Ziwei, Y., *J. Sep. Sci.*, **26** (2003) 629-634.

9 DiSalvo, F.J., *Science,* **285** (1999) 703-706.

10 *Thermoelectric Handbook,* http://www.melcor.com/handbook.html, 2008.

11 Soheilnia, N., *Thermoelectric properties of new transition metal arsenides and antimonides,* thesis for the degree of Doctor of Philosophy in Chemistry, Department of Chemistry, University of Waterloo, 2007.

12 Nolas, G.S.; Sharp, J.; Goldsmid, H. J., *Thermoelectrics, Basic principles and new materials developments*, Springer, New York, NY, 2001.

13 Incropera, F. P.; Dewitt, P. D., *Fundamentals of Heat and Mass Transfer*, John Wiley & Sons, New York, NY, 1997.

Chapter 3

Applications of cold fiber SPME with thermoelectric cooling

In the second chapter of this dissertation a new approach for cooling the SPME fiber during extractions from headspace of samples - cold fiber SPME with thermoelectric cooling - was introduced. The present chapter describes three different studies conducted by using the new cold fiber device. In the first study the extraction efficiency of cold fiber SPME with thermoelectric cooling approach was investigated by developing a method for the extraction of polycyclic aromatic hydrocarbons (PAHs) from laboratory contaminated sand samples. The second study was focused on method development for quantification of off-flavours in rice samples. Finally, in the third study, the new cold fiber device was used for on-site field sampling followed by GC/MS analysis of volatile compounds from living flowers.

3.1 Extraction of PAHs from laboratory spiked sand

In order to illustrate the efficiency of the cold fiber SPME device with thermoelectric cooling, a method was developed for quantification of PAHs from spiked sand samples. The method development included optimization of extraction temperature and extraction time, as well as establishing the calibration curves at the optimized extraction conditions for these compounds.

3.1.1 Experimental

3.1.1.1 Chemicals and materials

Naphthalene, acenaphthylene, acenaphthene, fluorene, anthracene, fluoranthene and pyrene were purchased from Supelco (Oakville, ON, Canada). Benzene, toluene, ethylbenzene, *o*-xylene were all purchased from Sigma-Aldrich (Mississauga, ON, Canada). Manual SPME holder and 100 μm PDMS fiber were purchased from Suplco (Oakville, ON, Canada). The sand matrix was provided by the Waterloo Center for Groundwater Research. All the gases were supplied by Praxair (Kitchener, ON, Canada).

3.1.1.2 Instruments and supplies

Extractions were carried out by the second prototype of cold fiber SPME with TEC cooling (see Chapter 2). Gas chromatography was performed on a Varian 3400 GC system equipped with a flame ionization detector (FID) and an Optic 2 ATAS programmable high volume injector. Separations were performed using a 30 m × 0.25 mm I.D., 0.25 μm CP-Sil & CB Low Bleed/MS fused silica column from Varian (Mississauga, Canada). Helium was chosen as the carrier gas. The injector was used in a splitless mode with a constant temperature of 270 °C and splitless time of 10 min. The transfer pressure of carrier gas was set at 40 psi. The

initial and final pressures of the carrier gas were set at 35 psi. The split flow rate and the purge flow rate were 100 and 5 mL/min, respectively. For liquid injections the initial temperature of the injector was set at 50 °C, increasing with the maximum ramp of 16 °C/sec to 270 °C. The column temperature was initially set at -20 °C for 2 min, increased to 150 °C at a rate of 15 °C/min and held for 1 min, then ramped at 10 °C/min to 250 °C and held for 1 min and finally ramped at 30 °C/min to 280 °C and held constant for 5 min. The FID system was used at a temperature of 300 °C with gas flows for hydrogen, high-purity air and nitrogen (make-up gas) set at 30, 300 and 30 mL/min, respectively.

3.1.1.3 Extraction of PAHs from spiked sand

In experiments performed for extraction temperature and extraction time profiles, 10 µL of 100 ppm solution of PAHs in methanol were spiked to 2 g sand (0.5 ppm PAHs in sand) in 40 mL vials. The samples were then shaken at 250 rpm for 15 min and left at a heat-block for 10 min to reach to the desired temperature. Extractions were carried out using the cold fiber SPME device with thermoelectric cooling. The temperature of the coating was set at minimum by applying a maximum current to the TEC (see Chapter 2).

3.1.2 Results and discussions

3.1.2.1 Optimization of extraction temperature

In order to obtain the extraction-temperature profiles, the extractions were carried out for 60 min at different temperatures of the sample, i.e., 40, 60, 80, and 100 ºC. The extraction temperature profiles for PAHs are illustrated in Figure 3.1. The extracted amount was obtained by comparing the peak areas with those obtained by direct injection of standard solutions of PAHs under the same instrumental conditions.

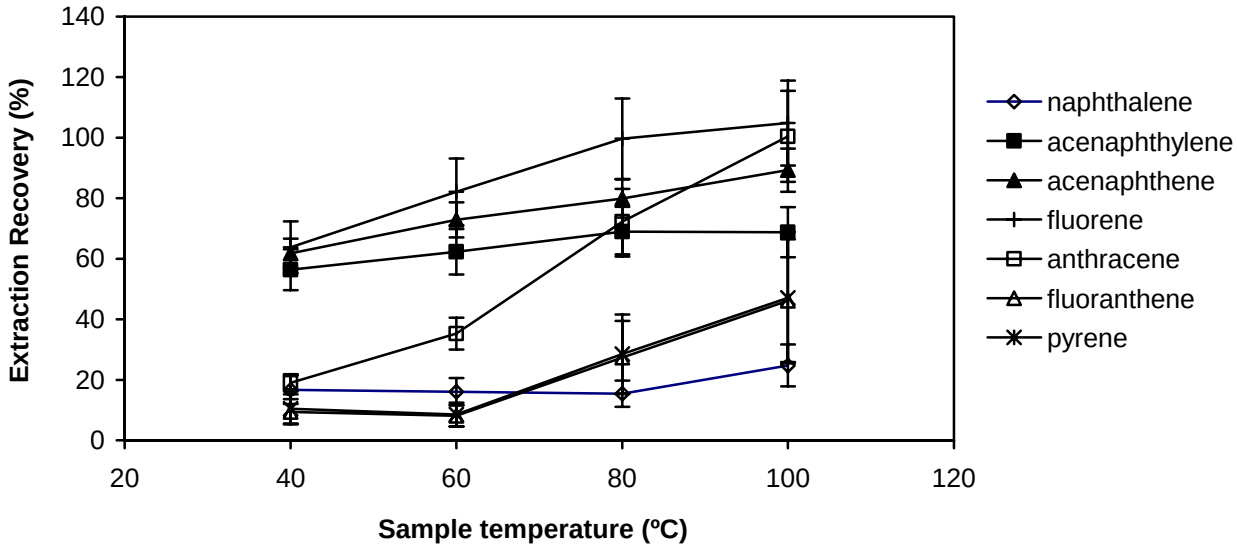

Figure 3.1 *Extraction temperature profiles of 0.5 ppm PAHs from spiked sand matrix – extraction time 60 min.*

The extraction recovery increased with increasing temperature for all compounds except for naphthalene. The recovery for naphthalene was very low, which is because this compound has a smaller partition coefficient on PDMS compared to the other compounds and a larger temperature gap between the sample and the coating or smaller headspace volumes are required to trap this compound completely on the coating. Flourene, on the other hand is completely extracted from the matrix after 60 min extraction at 100°C. The recoveries of acenaphthylene and acenaphthene are above 50%, and lower than the recovery of fluorene. Therefore, the recovery decreases in the order of volatility, which is due to the low partition coefficients of more volatile compounds on the fiber. However, the more volatile compounds, pyrene and fluoranthene, show recoveries less than 50%. Although these compounds have larger partition coefficients on the PDMS coating, both kinetics of desorption from the matrix and kinetics of absorption on the SPME coating is slower for these compounds due to the smaller diffusion coefficients, which means longer extraction times and higher sample temperatures are required to achieve higher recoveries.

3.1.2.2 Optimization of extraction time

The extraction time profiles were obtained within the range of 5 to 90 min at the sample temperature of 100°C (Figure 3.2).

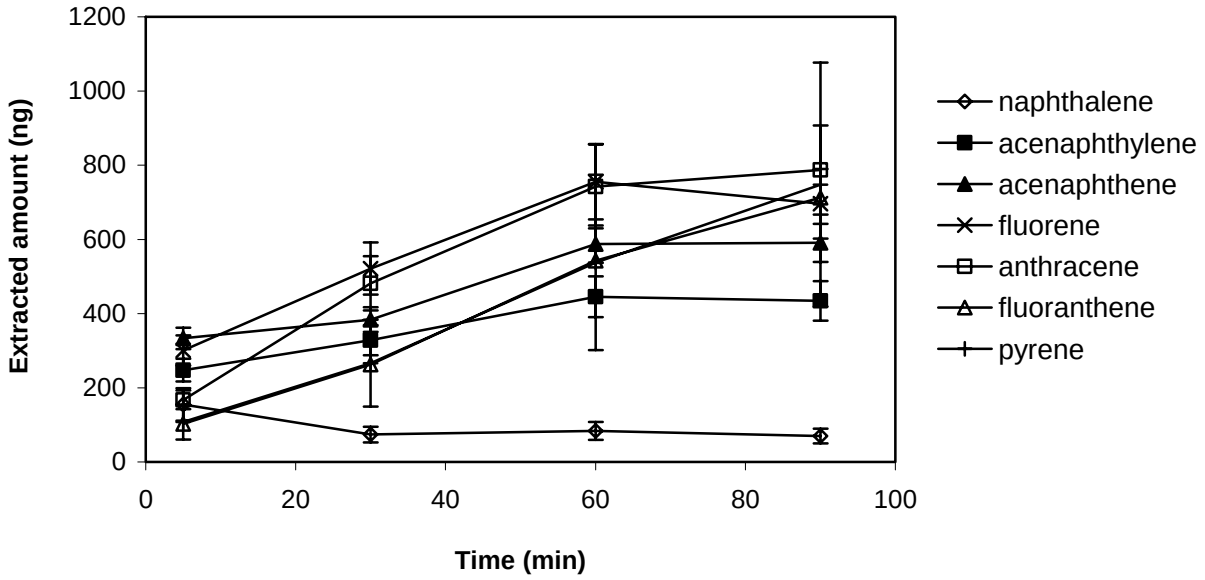

Figure 3.2 *Extraction time profile of 0.5 ppm PAHs from spiked sand matrix – extraction temperature 100 ºC, fiber temperature 14 ºC.*

Acenaphthylene, acenaphthene, fluorene and anthracene reach equilibrium after 60 min. Fluoranthene and pyrene do not reach equilibrium even after 90 min. The results show that the amount of extracted naphthalene does not increase by increasing the extraction time from 5 to 90 min, which means the equilibrium is reached in less than 5 min.

3.1.2.3 Calibration graphs

Calibration graphs were obtained using internal standard methods. Two standard solutions of PAHs with concentrations of 200 and 10 ppm were prepared. Different volumes of either of the two solutions were spiked into 2 g clean sand in 40 mL vials to make a range of concentrations of PAHs. 1 µL of 500 ppm biphenyl solution in methanol was also added as the internal standard. The concentrations ranged from 5 ppb to 500 ppb, which corresponds to 10 to 1000 ng of compounds in the sample. The samples were shaken at 250 rpm for 15 min

and left at the heat block for 10 min to reach to the desired temperature (100 °C) before performing extractions. The equations of calibration graphs, the square of regression coefficients and the limits of detection are summarised in Table 3.1. The general definition given in the literature[1], ($y_B+3\sigma_B$), was used for the estimation of the limit of detection.

Table 3.1 Calibration equations, square of regression coefficients and limits of detection for PAHs from spiked sand.

Analyte	Calibration equation	R^2	LOD (ppb)
naphthalene	y = 1.00E-2 + 4.19E-3 x	0.9927	6.6
acenaphthylene	y = 1.97E-2 + 6.05E-4 x	0.9737	20.9
acenaphthene	y = 1.19E-2 + 2.55E-3 x	0.9986	3.6
fluorene	y = 2.87E-2 + 2.33E-3 x	0.9722	0.8
anthracene	y = 1.06E-2 + 6.91E-4 x	0.9493	8.1
fluoranthene	y = -4.06E-3 + 2.44E-4 x	0.9922	12.2
pyrene	y = -2.46E-3 + 2.09E-4 x	0.9960	15.7

3.2 Analysis of off-flavors in the headspace of rice

Traditionally, quality control of agricultural products has been based on human observation. The existing instrumental methods are time consuming and expensive, often provide insufficient sensitivity, and are generally impractical for large-scale analyses required in monitoring the quality control of agricultural products. Rapid methods are required to help rice breeders make their selections from the large number of lines they evaluate each year. Such methods would also be beneficial in genetic and storage studies, where large numbers of samples are required.

The two significant issues from an industrial perspective are the aroma of aromatic rice and off flavors due to rancidity. The aromatic compound 2-acetyl-1-pyrroline (2-AP) is the primary component known to be responsible for aromatic (scented) rice aroma.[2,3] Other volatiles associated with rice aroma are carbonyl compounds, which give a stale or rancid aroma to many foods.[4] High levels of these compounds are associated with lipid oxidation. Among these compounds, hexanal increases the most during storage, and has therefore been used as an indicator of rancidity.[5,6,7,8,9] Both 2-AP and hexanal have been quantified in rice by

methods based on solvent extraction, which are accurate but relatively time consuming (not suitable for large research projects, breeding programs, or quality control departments).

Solid-phase microextraction has been used for screening volatile compounds in the headspace of rice.[10] However, to our knowledge it has not been applied for quantification of these compounds in rice due to its poor sensitivity. The objective of the present study was to develop and evaluate a method for quantifying important rice volatile compounds that is fast and requires small sample sizes.

3.2.1 Experimental

3.2.1.1 Chemicals and materials

Hexanal, nonanal, and undecanal were purchased from Sigma-Aldrich (Mississauga, ON, Canada). Optima grade methylene chloride and HPLC grade methanol were purchased from EDM Biosciences (Affiliate of Merck, Darmstadt, Germany). All gases were purchased from Praxair (Kitchener, ON, Canada).

Sample vials, 2- and 10 mL, with crimp caps and PTFE coated silicone septa, and DVB/CAR/PDMS fibers were purchased from Supelco (Bellefonte, PA, USA). The second prototype of cold fiber SPME with TEC (see Chapter 2) was prepared at the Science Technical Services (STS) of the University of Waterloo.

Two brands of rice were used in this study: Basmati Khushi rice was used for the study of temperature profiles, and Noname rice was used for extraction time profile experiments and also quantification of off-flavors. Both types of rice were purchased from a local supermarket in Waterloo, ON, Canada. The samples were prepared by grinding rice grains, using a household coffee grinder. The rice sample was kept in the refrigerator (at 5 ºC) and the ground samples were freshly prepared every day before analysis.

3.2.1.2 Instruments

Gas chromatography was performed on a Varian 3800 GC system coupled to a flame ionization detection (FID) system using Star Chromatography Workstation software (version 5.51). The instrument was equipped with a single arm CombiPal auto sampler. The agitation and incubation of the samples were carried out in the heater/agitator of the auto-sampler and the rest of the experiment (extraction and injection) were performed manually. Separations were performed using a 30 m × 0.25 mm I.D., 0.25 μm CP-Sil & CB Low Bleed/MS fused silica column from Varian (Mississauga, Canada). Helium was chosen as the carrier gas. The GC was operated in the splitless mode over a 2 min splitless period. The injector was maintained at 300 °C during desorption splitless time. When performing SPME extractions, the column temperature was initially set at 40 °C for 1 min; increased to 150 °C at a rate of 7 °C/min and held for 1 min; and finally ramped at 30 °C/min to 280 °C and held constant until the end of the 30 min total run time. The FID system was used at 300 ºC with gas flows for hydrogen, high-purity air and nitrogen (make-up gas) set at 30, 300 and 30 mL/min, respectively. The carrier gas flow rate was set at 1 mL/min.

For direct liquid injection the injector temperature was ramped from 60 to 250 ºC (at the rate of 200 ºC/s) and the carrier gas flow rate was increased to 7.2 mL/min. All other parameters were kept the same.

The injector nut and the septum support were drilled to be large enough to host the relatively large needle used in the cold fiber device.

3.2.1.3 Target analytes and standard solutions

Hexanal, nonanal, and undecanal were chosen as target off-flavors in rice. Hexanal is a known indicator of rancidity in food samples, including rice.[11] Nonanal and undecanal, two aldehydes present in the rice sample, were chosen to study the efficiency of the cooling and

heating system in quantitative extraction of three compounds of the same functional group but containing different numbers of carbon atoms and therefore different volatilities. The compounds were identified in the rice sample by comparing their retention times to those of the standards. Standard solutions with increasing concentrations with respect to the target analytes were prepared and used in the standard addition method for quantifying the target analytes in the rice samples.

3.2.1.4 HS-SPME of off-flavors from rice samples

In all experiments, 2 g ground rice samples were loaded in 10 mL crimp cap vials. The vial was then capped, transferred to the heater/agitator, and was shaken for 10 min at the experimental temperature. The SPME fiber was then exposed to the headspace of the rice sample for extraction. After the desired extraction time, the fiber was removed from the vial and transferred to the GC injector. When cold fiber SPME device was used, the TEC was turned on 10 min before exposing the fiber to the sample and was turned off immediately after injection. In commercial SPME, the fiber was removed from the injector at the end of desorption time (1 min), whereas, with cold fiber SPME, the fiber was left in the injector during the GC run time to avoid carry-over (amount of compounds remained on the fiber after desorption in the injector).

3.2.1.5 Conventional solvent extraction

The solvent extraction method proposed by Bergman et al.[12] was used with some modifications to measure the hexanal in the rice samples. A 0.6 g sample of ground rice was loaded into a 2 mL crimp cap vial and 0.5 mL of methylene chloride was added as the extracting solvent. The extraction was performed at 85 ºC in a water bath for 3.5 h. After centrifugation, the extraction liquid was pipetted out and 3 μL of the solution were injected into the GC/FID for analysis.

3.2.2 Results and discussions

3.2.2.1 Optimization of extraction temperature and extraction time

The effects of extraction temperature and time on the extraction recoveries of hexanal, nonanal and undecanal were investigated using the cold fiber SPME. To obtain the extraction temperature profile, the analytical procedure explained in the experimental section was carried out over an extraction time of 20 min. Extraction temperatures of 50, 70, 90, and 110 ºC were investigated. The same experiments were performed using a commercially available DVB/CAR/PDMS fiber, which is recommended for aldehydes and used for extracting aroma compounds from the headspace of rice samples.[10] The temperature profiles obtained by commercial SPME and cold fiber SPME are illustrated in Figure 3.3 for each compound. The temperature profiles for commercial SPME represent the case in which the fiber and the sample are both at the same temperature.

When DVB/CAR/PDMS was used, the profiles reached a maximum at 70 ºC for hexanal (Figure 3.3.a) and for nonanal (Figure 3.3.b) and 90 ºC for undecanal (Figure 3.3.c). Increasing the temperature of the sample helps overcome the energy barriers between the compound and the solid matrix and speeds up the mass transfer processes of the analytes from the matrix to the headspace. It therefore results in higher vapor pressure of the analyte in the headspace and higher extraction recovery. On the other hand, since the partitioning of the analytes between the fiber and the headspace is an exothermic process, the partition coefficient decreases with increasing temperature resulting in a decrease in the amount absorbed on the fiber. Therefore, above a certain temperature the decrease in partition coefficient compensates for the higher vapor pressure, and the amount of analyte absorbed on the fiber at a given extraction time decreases relative to the amount absorbed at a lower temperature. The temperature related to the maximum extraction recovery at a given

extraction time was 70 ºC for the more volatile compound (hexanal), and 90 ºC for the less volatile compound (undecanal); less volatile compounds require higher temperatures for their release from the matrix and their desorption from the fiber.

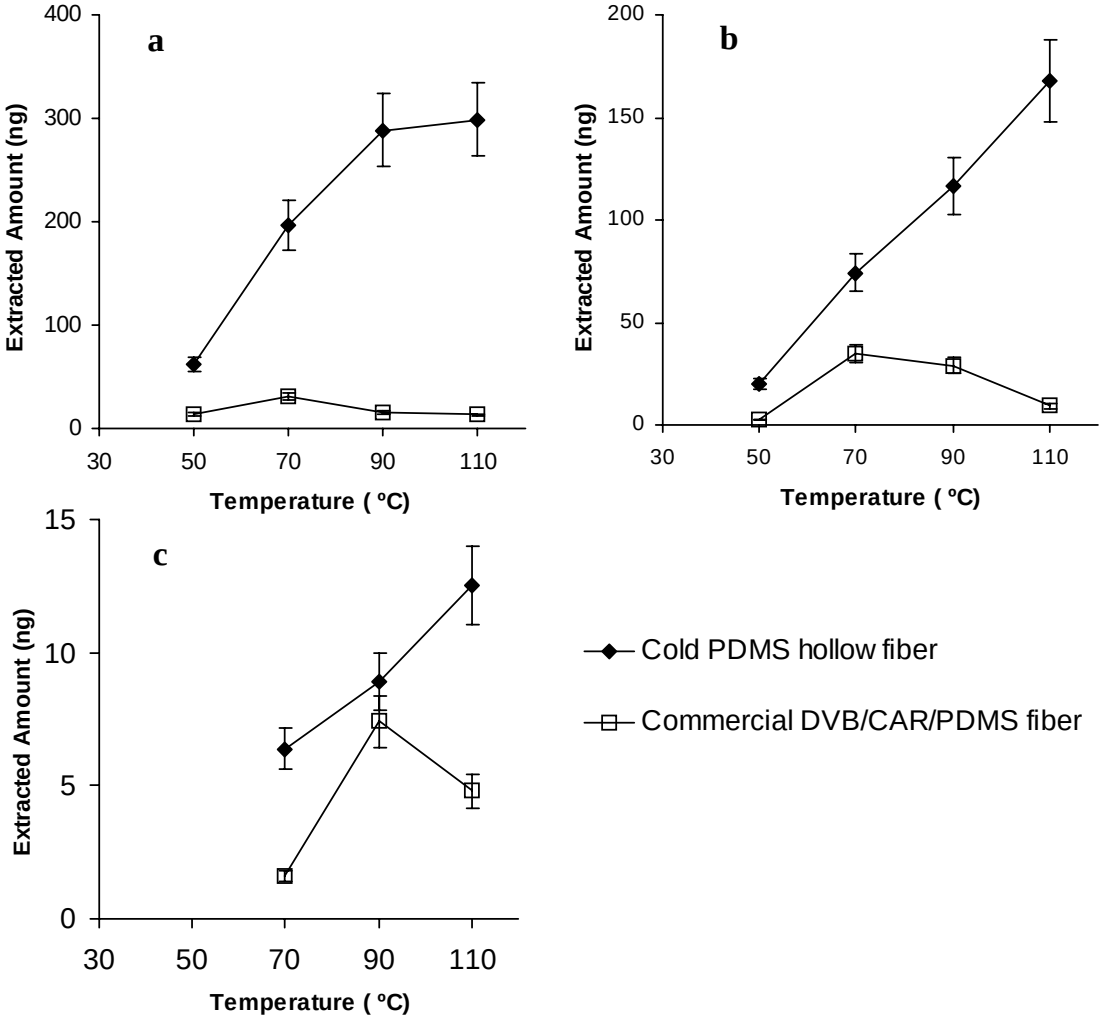

Figure 3.3 *Extraction temperature profiles for (a) hexanal, (b) nonanal, and (c) undecanal from rice.*

When using cold fiber extraction from the headspace of the rice sample, the extraction temperature profiles showed that the recoveries of extraction for all analytes increased when

the temperature of the sample was increased from 50 to 90 ºC (Figure 3.3 a-c). This occurred because the vapor pressure of all analytes in the headspace increased with increasing the sample temperature, due to faster kinetics of desorption from the matrix. On the other hand, the partition coefficient between the fiber and the headspace increased when the fiber was cooled, resulting in the trapping of the compounds in the fiber. When the temperature was increased from 90 to 110 ºC, the amount of hexanal extracted on the fiber did not change significantly, whereas the amounts of extracted nonanal and undecanal increased by a factor of 1.5. This occurred because nonanal and undecanal are less volatile than hexanal, and higher temperatures are required to release them from the matrix to the headspace. Therefore, an extraction temperature of 110 ºC was chosen as the optimum extraction temperature.

Extraction time profiles were obtained at 70 and 110 ºC sample temperature, using the cold fiber SPME. The incubation time was 10 min for all experiments and the extraction time was increased over a range of 5 to 60 min. Extraction time profiles are illustrated in Figure 3.4. The profiles show that increasing the temperature resulted in shorter equilibrium times at the fiber. Both desorption of the analytes from the solid surface (the rate constant of desorption) and the diffusion of the analytes through the solid particles and the headspace (diffusion coefficient) are temperature-dependent. Cooling the fiber while heating the sample, not only resulted in higher extraction recoveries, but also sped up the kinetics of extraction. The optimum extraction time for extraction at 70 ºC was 30 min and as short as 5 min for extraction at 110 ºC.

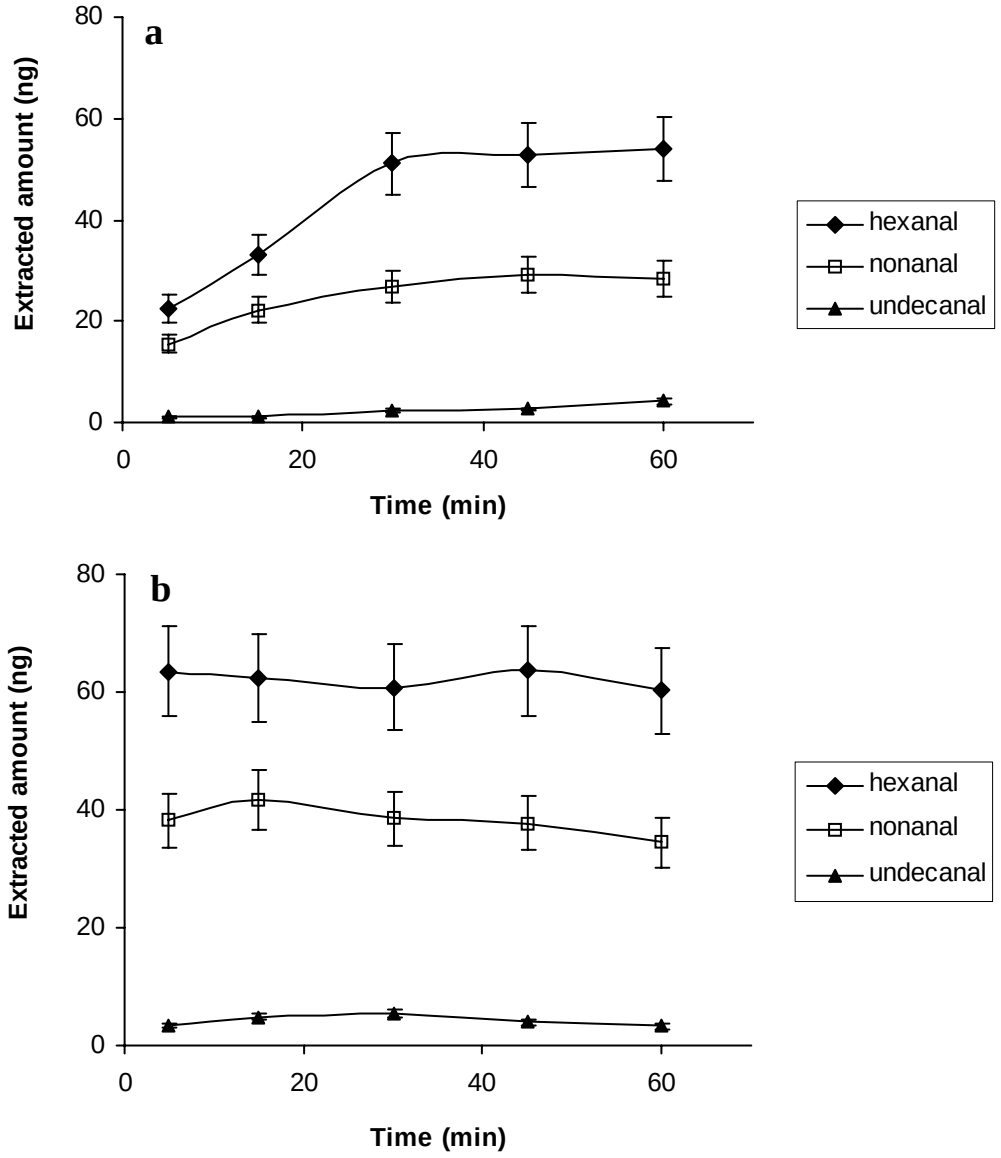

Figure 3.4 *Extraction time profiles at (a) 70 ºC and (b) 110 ºC for hexanal, nonanal and undecanal from rice (n=3).*

3.2.2.2 Quantification of off-flavors in rice

Hexanal, nonanal and undecanal were quantified in the "Noname" rice sample using the method of standard addition. The concentrations of the three target analytes were calculated

using the standard addition calibration graphs, obtained at optimum extraction conditions. Table 3.2 shows the calibration graph equations, the square of regression coefficients and the calculated concentrations for each compound.

Table 3.2 Calibration equations, square of regression coefficients and concentrations of hexanal, nonanal, and undecanal in rice.

Compounds	Equation	R^2	Concentration (ng/g)
hexanal	y = 399 x + 513934	0.998	644 ± 8
nonanal	y = 1401 x + 427919	0.991	153 ± 17
undecanal	y = 2015 x + 37156	0.992	9 ± 1

As hexanal is the most important off-flavor in rice samples, this compound was analyzed in the same rice sample, in triplicate, by a conventional solvent extraction method to compare the experimental results. The concentration of hexanal quantified with the solvent extraction method was 697±143 ng/g, which is comparable to the results obtained with the standard addition method using cold fiber SPME (Table 3.2). The headspace cold fiber SPME method presented in this study provides better precision compared to the solvent extraction method, requires no solvent and is also rapid because it eliminates the intensive manual labor of solvent extraction.

3.3 Extraction of volatile components from living flowers

Identification and quantification of volatiles emitted from fragrant flowers is important in perfumery studies. The requirements for analytical methods used for the determination of floral scents are somewhat different from the usual analytical tasks. Apart from being able to identify the compounds responsible for the scent, and to determine their relative abundance in the air, the methods used have to be able to describe qualitative and quantitative changes in concentrations of individual compounds during the day and during the flowering cycle, which requires the method to be both fast and reproducible. Another important issue is that the used method should evaluate the scent emitting from the flower under natural conditions and the influence of sampling on the investigated plant should be as low as possible.[13] Conventional methods are commonly based on trapping the volatile compounds using an appropriate

sorbent, followed by solvent extraction[14,15,16,17,18] or thermal desorption of the trapped analytes[19,20].These methods require cutting or entrapping the flowers (or plants), which can modify the compounds and their relative abundance in the sampled air compared to their natural composition.

Solid-phase microextraction (SPME) has been widely used as a practical alternative to conventional analytical techniques for monitoring volatile compounds in air and in the headspace of cut plants and flowers, but only a few studies have been reported on direct SPME sampling of volatiles from living flowers.[13,21] Due to the poor sensitivity of SPME compared to conventional methods, the investigators used a chamber trap[21] or performed the extractions for a relatively long time to achieve the required sensitivity for identification purposes. Although the chamber-trapping technique helps to have a higher concentration of the compounds available for SPME extraction, it is known to stress plants, which can result in a change in the relative proportion of compounds detected. Improving the sensitivity of SPME technique by cooling the SPME fiber may eliminate the need for an enclosed chamber and shorten the extraction time for the volatiles from living plants.

The main objective of the present study was to demonstrate that cold fiber SPME has the potential to be used as a more sensitive method compared to conventional SPME (i.e. without cooling) for field sampling of volatile components. Lily-of-the-valley and wisteria flowers were chosen as subjects of this study. Before using cold fiber SPME for extraction of volatile compounds from flowers, the reproducibility and efficiency of the device were tested for extraction of n-alkanes from a flow through system, which simulated extractions from living flowers (i.e. continuous generation of compounds).

3.3.1 Experimental

3.3.1.1 Materials

Lily-of-the-valley and wisteria plants grown in University of Waterloo garden were used as plant subjects. n-alkanes were all purchased from Sigma-Aldrich (Mississauga, ON, Canada).

Portable cold fiber SPME with TEC was used for on-site sampling. SPME holder for manual sampling, 100 μm PDMS fiber, and PA fiber, was purchased from Supelco (Oakville, ON, Canada). The fibers were conditioned in a hot GC injector according to instructions provided by the supplier before using. Round bottom double neck Pyrex flask, 25 mL, was purchased from VWR. Filter flask, 1000 mL, was also purchased from Supelco (Oakville, ON, Canada).

3.3.1.2 Extraction of n-alkanes from a flow-through system

The reproducibility of the cold fiber device was tested by performing triplicate extractions of n-alkanes from a flow through system. Figure 3.5 shows the schematics of the n-alkane flow through system[22]. It consisted of n-alkane permeation tubes placed inside a glass cylinder (Kin-Tek) and swept with constant flow of dilution air. The permeation cylinder is held inside a permeation oven machined from a solid aluminum rod. Two 100 W heating rods are placed inside small holes approximately halfway between the inside and outside diameters of the aluminum cylinder. The temperature of the permeation cylinder is controlled by a K-type thermocouple (Omega, Stamford, CT, USA) and an electronic heat control.[22] The concentration of n-alkanes in air flow is adjusted by temperature of the heater. This system was originally designed for sampling with commercial SPME holders, for which there are side holes on the wall of the chamber. However, since the needle of the cold fiber SPME device is shorter than the commercial SPME holder, the sampling could not be performed through the side holes and a 1000 mL glass bulb was connected to the exit of the chamber, which in turn had a side hole with septum that could be used for sampling. The experiments were started a few days after installing the bulb to make sure that flow of the compounds was stable. The extractions were carried out three times both with and without cooling for 5 min using portable cold fiber SPME. In experiments that were carried out with cooling, the TEC was kept on (at low temperature) during the transfer of the device from the flow through system location to the GC/MS instrument (similar to field sampling experiments).

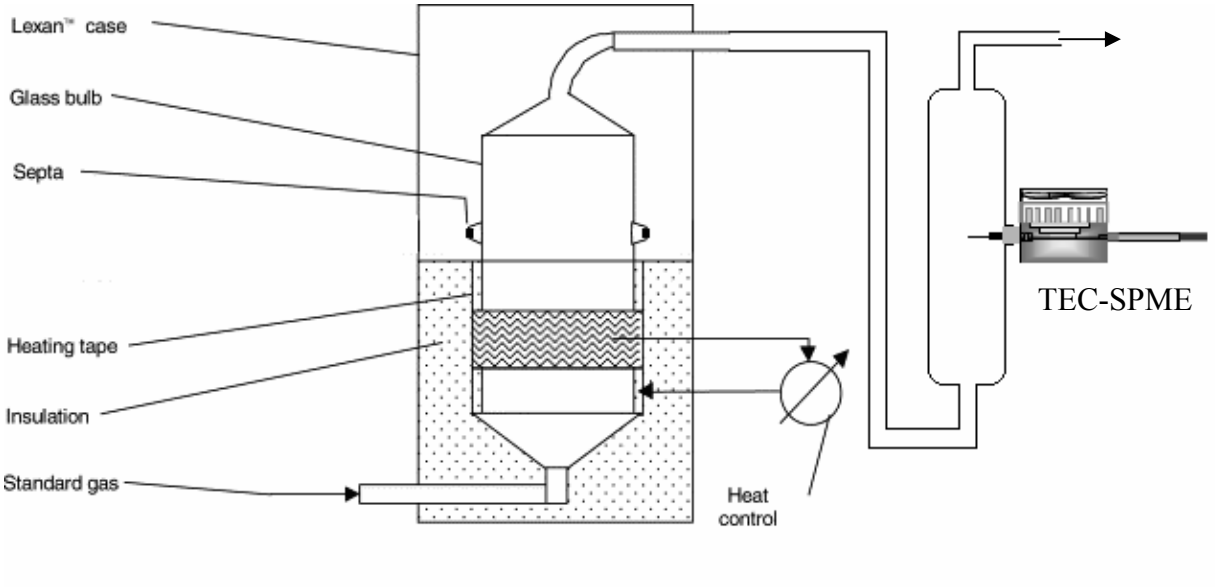

Figure 3.5 *Modified flow through system [22] for sampling by cold fiber SPME with TEC.*

3.3.1.3 Extraction of volatile compounds of living wisteria flowers

For sampling from living wisteria flowers, the head of the same branch of flower was placed into the top opening of a 1000 mL filter flask and the fiber was immediately exposed to the vicinity of the flower buds through the side arm. Since the openings of the flask were not sealed, the flask only acted as a shield and the system worked similar to a flow-through system. After 30 min extraction the fiber was removed, sealed with Teflon plug and was immediately transferred to the lab for analysis (in approximately 5 min). The flower was removed from the flask after the extraction and the flask was not used for one hour before the next extraction to avoid concentrating the fragrance emitted by the flower. The following extractions were carried out:

- Extraction from living flowers using cold fiber SPME device with cooling
- Extraction from living flowers using cold fiber SPME device without cooling
- Extraction from living flowers using commercial PDMS SPME fiber
- Extraction from living flowers using commercial PA SPME fiber

All experiments were carried out during day time (in one day), to avoid the effect of day to day variations of composition of the emitted volatiles.

3.3.1.4 Analysis of volatile components of living lily-of-the-valley flowers

For extraction from living flowers, six living flower heads at the top of a healthy lily-of-the-valley flower plant were surrounded by a clear and empty double-neck round-bottom flask (25 mL) and the fiber was immediately exposed to the vicinity of the flower buds through the side neck. Similar to extractions from wisteria flowers, the openings of the flask were not sealed. After 60 min extraction the fiber was removed, sealed with Teflon seal and was immediately transferred to the lab for analysis. The fiber was kept cold by keeping the TEC on during transportation.

3.3.1.5 Instrumentation and constituents identification

The analyses were performed using an Agilent 6890 GC/MS equipped with a Gerstel septa-free Cooled Injection System (CIS). The CIS was especially built to host the large size (gauge 18) needle of the cold fiber SPME with TEC cooling device. Separations were carried out using a HR-1 (non-polar) column (25 mm × 30 m × 0.25 μm). The column temperature was initially held at 35 ºC for 4 min, increased to 145 ºC with a rate of 3 ºC/min, then increased to 280 ºC with a rate of 35 ºC/min and held at this temperature until the end of the run (total run 50 min). The GC/MS transfer line heater temperature was set at 290 ºC. The MS Quad and the MS source temperatures were set at 150 and 230 ºC, respectively. The mass range was between 40 to 650 m/z. For calculation of Linear Temperature Program Retention Index (LTPRI) for the compounds, a mixture of n-alkanes was injected to the GC/MS using the same column temperature program.

The extracted volatile components were identified by comparing their mass spectra with those in NIST library and comparing the calculated LTPRI with those reported in the literature.

3.3.2 Results and discussion

3.3.2.1 Extraction of n-alkanes from a flow through system

As mentioned earlier in this chapter, one of the requirements for a method to be used for monitoring floral scent is reproducibility. The reproducibility of portable cold fiber SPME device was tested using a flow through system. Figure 3.6 compares the peak areas of representative n-alkanes extracted from a flow through system using the cold fiber SPME device with and without cooling. The differences in the recoveries obtained with and without cooling were significant and the reproducibility of the method was quite acceptable for field sampling.

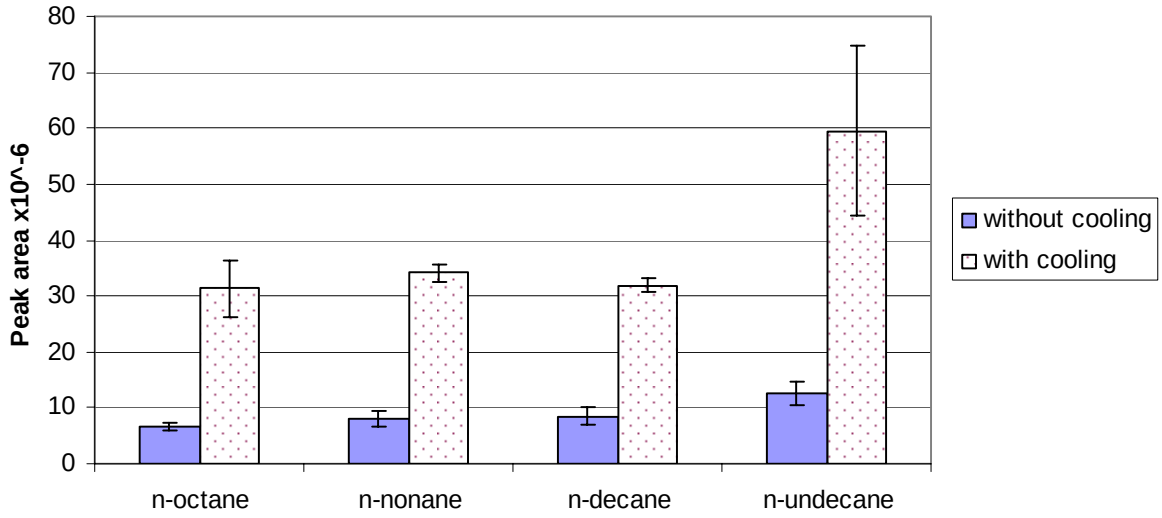

Figure 3.6 *Extraction of n-alkanes from flow through system using cold fiber SPME device with and without cooling.*

3.3.2.2 Extraction of volatile compounds from living wisteria flowers

Figure 3.7 compares the GC/MS chromatograms obtained by cold fiber SPME device (170 µm PDMS) with and without cooling, commercially available 100 µm PDMS fiber and PA fiber.

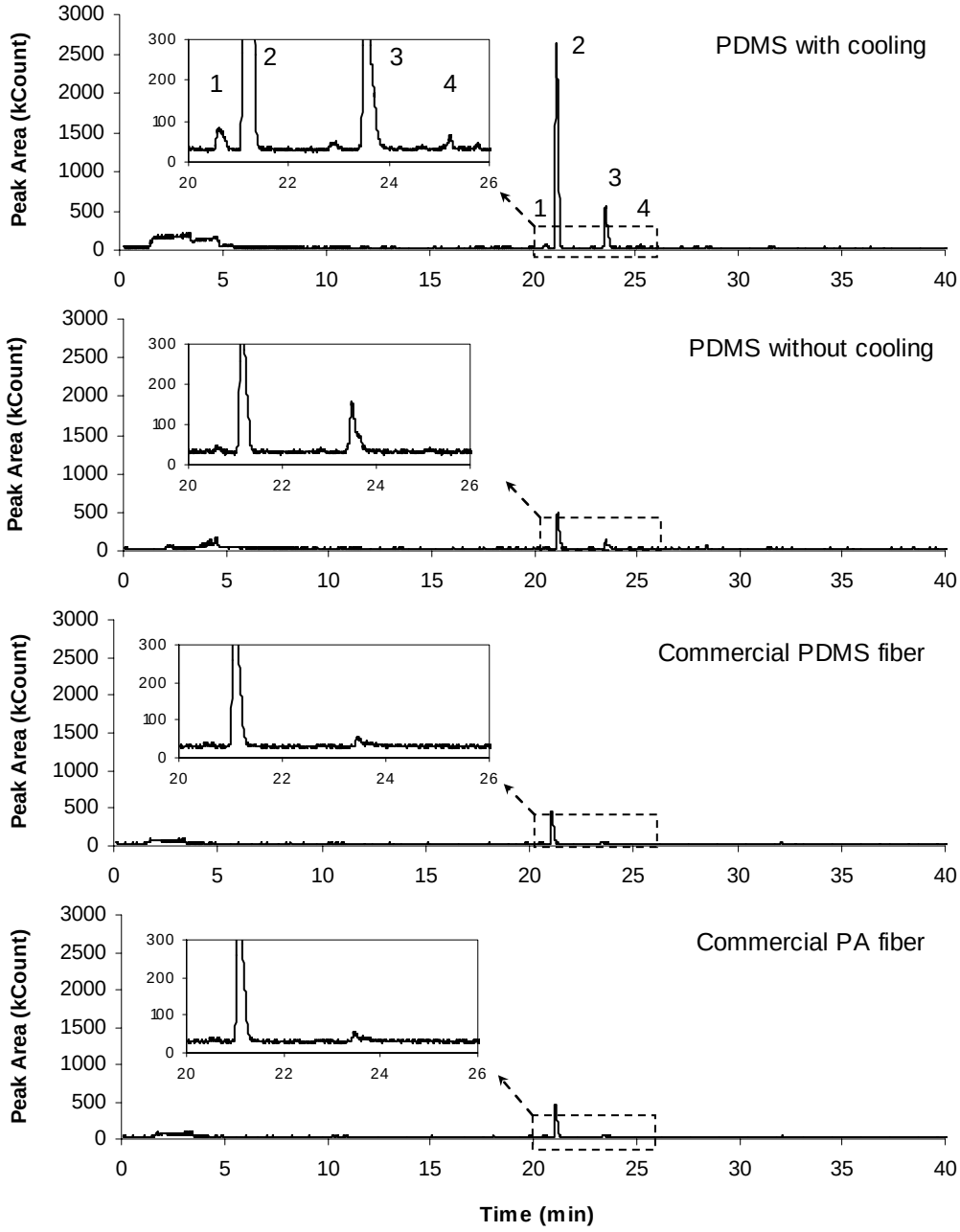

Figure 3.7 *GC/MS chromatograms of field sampling of wisteria fragrance using cold fiber SPME (170 µm PDMS) with and without cooling, commercial 100 µm PDMS and PA fibers. Identified compounds: (1) (E)-beta-ocimene, (2) (Z)-ocimene, (3) linalool, and (4) indole.*

The results showed that (E)-beta-ocimene and indole were only identified using the cold fiber SPME device with cooling. (Z)-ocimene and linalool were identified in all chromatograms; however, the sensitivity of cold fiber SPME was higher for these compounds.

Table 3.3 lists the major identified volatile components of wisteria using cold fiber SPME, together with their calculated LTPRI and the reference LTPRI values.[23]

Table 3.3 Major volatile components of living wisteria flowers

Name	Reference LTPRI#	LTPRI*
(E)-beta-Ocimene	1038	1028
(Z)-Ocimene	1043	1039
Linalool	1100	1085
Indole	1298	1250

* LTPRI: Linear Temperature Program Retention Index
# Reference LTPRI for DB5 column (5% phenyl / 95% dimethylpolysiloxane)[23]

Figure 3.8 compares the peak areas of the detected peaks. The sensitivity of the cold fiber extraction was 7 times better with respect to without cooling, and the commercial PDMS fiber, and showed 36 times better sensitivity compared to PA fibers considering peak area of (Z)-ocimene. The structures of the identified compounds are illustrated in Appendix 3.

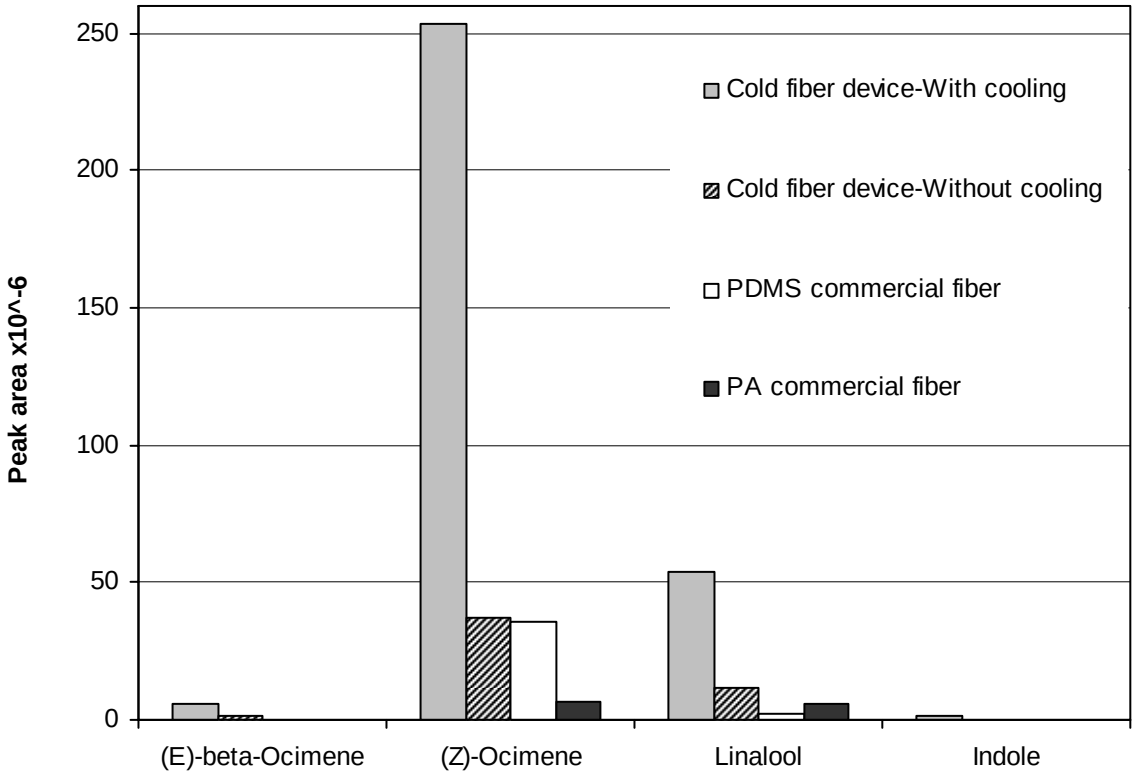

Figure 3.8 *Comparison of the peak areas of major compounds extracted from wisteria flowers obtained by commercial PDMS (100 µm) and PA fiber with those obtained using the cold fiber SPME device with and without cooling (PDMS hollow fiber with 170 µm thickness).*

3.3.2.3 Extraction of volatile compounds from living lily-of-the-valley

Convallaria majalis, commonly known as the lily-of-the-valley, is a wood plant with small bell-shaped flowers that are sweetly scented. The lily-of-the-valley plants usually flower in late spring and the flowers only last for approximately 10 days. Although the fresh scent of the lily-of-the-valley flowers is popular in perfumery industries, no literature reports were found to assess essential oils from these flowers, nor on-site field sampling of living flower fragrance. The reason for lack of information on this flower might be their short life-time.

The portable cold fiber SPME device was used on-site to extract the volatile components of living lily-of-the-valley flowers. Figure 3.9 illustrates GC/MS chromatogram resulting

from the cold-fiber SPME sampling of lily-of-the-valley fragrance from living flowers during daylight.

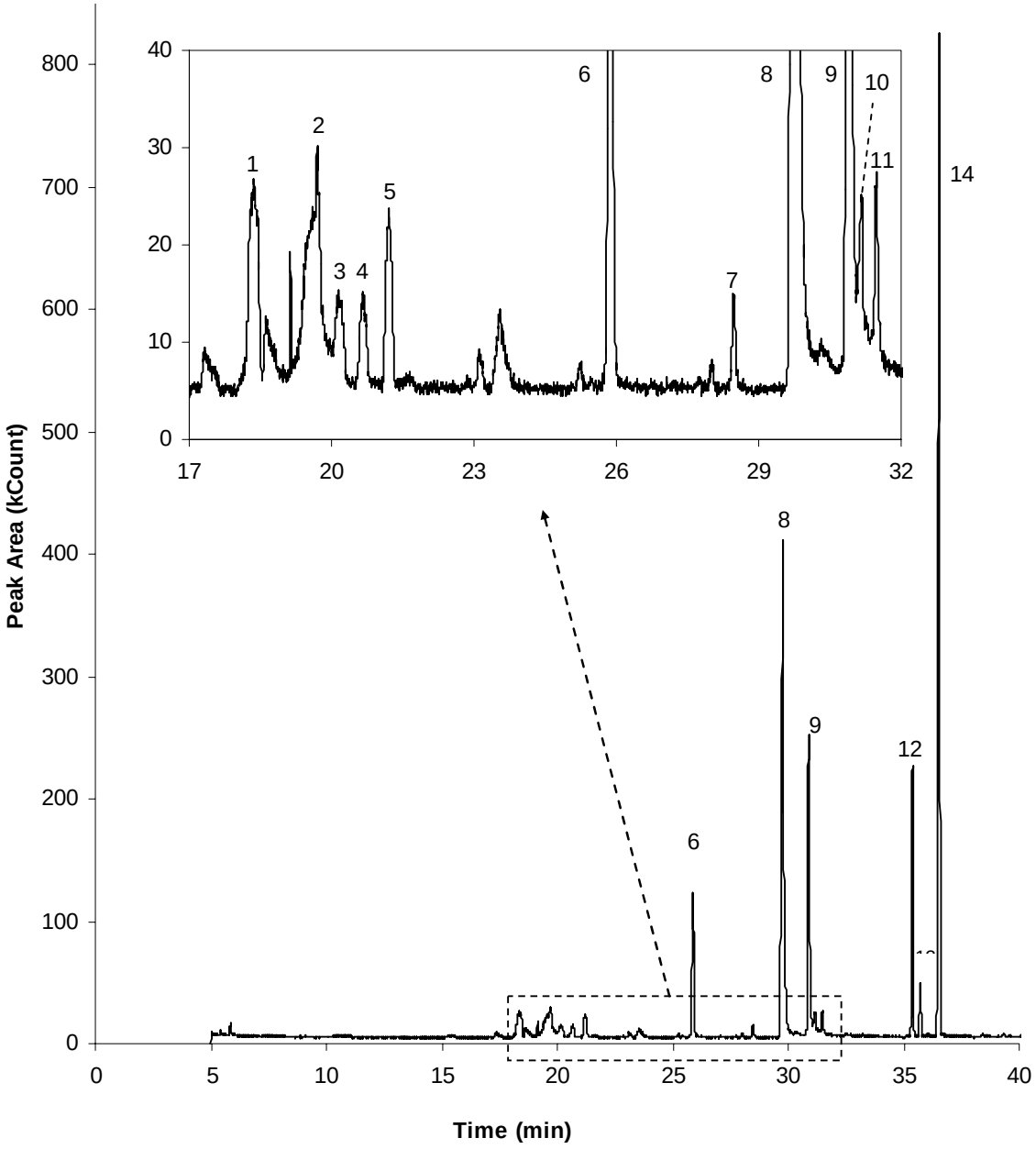

Figure 3.9 *GC/MS chromatogram of field sampled lily-of-the-valley fragrance. (1) beta-pinene, (2) benzyl alcohol, (3) limonene, (4) (E)-ocimene, (5) (Z)-ocimene, (6) benzyl acetate, (7) dodecanal, (8) beta-citronellol, (9) (Z)-geraniol, (10) geranial, (11) indole, (12) citronellyl acetate, (13) neryl acetate, (14) geranyl acetate.*

The volatile components identified by cold fiber extraction are listed in Table 3.4. Limonene, (Z)- and (E)-ocimene, previously identified in Calanthe izu-insularis[2020] (known to have a fresh odour similar to lily-of-the-valley) were detected; however, the abundance of (E)-ocimene was not significant for lily-of-the-valley. The major components were geranyl acetate (34.3%), beta-citronellol (26.2%), cis-geraniol (12.0 %), citronellyl acetate (8.7 %) with rose odour, and benzyl acetate (6.6%) with fresh odour[23]. The structures of the identified compounds are illustrated in Appendix 3.

Table 3.4 Volatile compounds of lily-of-the-valley flowers

Peak number	Name	Reference LTPRI#	LTPRI*	Percentage
1	beta-Pinene	981	985	2.7
2	Benzyl alcohol	1039	1012	3.1
3	Limonene	1033	1020	0.6
4	(E)-Ocimene	1038	1031	0.8
5	(Z)-Ocimene	1043	1041	1.4
6	Benzyl acetate	1162	1132	6.6
7	Dodecanal	1195	1185	0.4
8	beta-Citronellol	1233	1213	26.2
9	(Z)-Geraniol	1276	1237	12.0
10	Geranial	1277	1242	0.5
11	Indole	1292	1250	0.8
12	Citronellyl acetate	1357	1336	8.7
13	Neryl acetate	1362	1343	1.6
14	Geranyl acetate	1382	1362	34.3

* LTPRI: Linear Temperature Program Retention Index
# Reference LTPRI for DB5 column (5% phenyl / 95% dimethylpolysiloxane)[23]

3.4 Conclusion

The effect of heating/cooling system on the extraction recovery of semi volatile organic compounds (two and three ring PAHs) from laboratory contaminated sand samples was investigated. The experimental observations qualitatively followed the theory, i.e. shorter equilibration times and higher extraction recoveries were obtained when cooling was applied. The internal standard calibration curves showed good linearity within the range of 0.005 to

500 ppm, and the average limit of detection of the technique for the extraction of PAHs from laboratory spiked sand was 10 ppb.

Cold fiber SPME with thermoelectric cooling combined with GC/FID was found to be suitable for the determination of off-flavours in the headspace of rice samples. The extraction recoveries obtained with cold fiber SPME were higher than those obtained with commercially available DVB/CAR/PDMS at similar extraction conditions (i.e. temperature and time). The cold fiber SPME method provides recoveries comparable to those obtained by solvent extraction method with the added advantages of being solvent free, more precise and rapid.

The reproducibility and efficiency of extraction with cold fiber SPME was also tested for extraction of n-alkanes from a flow-through system. It was found that the extraction recoveries were significantly higher when the fiber was cooled. Since the precision of the cold fiber SPME device was acceptable in the flow-through system the device was also used for field sampling of volatile compounds of living wisteria and lily-of-the-valley flowers. For extractions from living wisteria flowers, the sensitivity of the cold fiber extraction was 7 times better with respect to without cooling, and the commercial PDMS fiber, and showed 36 times better sensitivity compared to PA fibers based on the peak area of (Z)-ocimene.

Cold fiber SPME with TEC is a portable device, which has the potential to be used with enough sensitivity to omit the chamber-trapping of the volatile components emitted by the living flower, resulting in closer to real analysis of the composition of their fragrances, which is useful in formulation of perfumes. The volatile components of lily-of-the-valley flowers were identified for the first time using on-site field sampling with cold fiber SPME combined with GC/MS. The major identified components and their relative abundance were: geranyl acetate (34.3%), beta-citronellol (26.2%), cis-geraniol (12.0 %), citronellyl acetate (8.7 %), and benzyl acetate (6.6%).

References

1 Miller, J. C.; Miller, J.N.; Statistics for analytical chemistry; 4th edn. Ellis-Horwood, New York, 1994, P-115.

2 Buttery, R.G.; Ling, L.C.; Juliano, B.O.; Turnbaugh, J.G., *J. Agric. Food. Chem.,* **31** (1983) 823-826.

3 Buttery, R.G.; Turnbaugh, J.G.; Ling, L.C., *J. Agric. Food. Chem.*, **36** (1988) 1006-1009.

4 Bennion, M., *The Science of Food*, Harper and Row, San Francisco, USA, 1980.

5 Yasumatsu, K.; Moritaka, S.; Wada, S., *Agric. Biol. Chem*., **30** (1966) 483-486.

6 Shibuya, N.; Iwasaki, T.; Yanase, H.; Chikubu, S., *J. Jpn. Soc. Food Sci. Technol.*, **21** (1974) 597-603.

7 Tsugita, T.; Ohta, T.; Kato, H., *Agric. Biol. Chem*., **47** (1983) 543-549.

8 Gon Shin, M.; Hoo Yoon, S.; Shick Rhee, J.; Kwon, T.-W., *J. Food Sci.*, **51** (1986) 460-463.

9 Champagne, E.T.; Hron, R.J. Sr., *Cereal Chem.*, **70** (1993) 562-567.

10 Grimm, C.; Bergman, C. J.; Delgado, J. T.; Bryant, R., *J. Agric. Food Chem*., **49** (2001) 245-249.

11 Kaykhaii, M.; Rahmani, M., *J. Sep. Sci.,* **30** (2007) 573–578.

12 Bergman, C.J.; Delgado, J.T.; Bryant, R.; Grimm, C.; Cadwallader K.R.; Webb, B. D., *Cereal Chem*., **77** (2000) 454-458.

13 Barták, P.; Bednář, P.; Čáp, L.; Ondráková, L.; Stránský, Z., *J. Sep. Sci.,* **26** (2003) 715-721.

14 Jürgens, A.; Webber, A.C.; Gottsberger, G., *Phytochemistry*, **55** (2000) 551-558.

15 Luyt, R.; Johnson, S.D., *Plant Systematics and Evolution*, **228** (2001) 49-62.

16 Levin, R.A.; Raguso, R.A.; McDade, L.A., *Phytochemistry*, **58** (2001) 429-440.

17 Helsper, J.P.F.G.; Davies, J.A.; Bouwmeester, H.J.; Krol, A.F.; Van Kampen, M.H., *Planta*, **207** (1998) 88-95.

18 Turlings, T.C.J.; Lengwiler, U.B.; Bernasconi, M.L.; Wechsler, D., *Planta*, **207** (1998) 146-152.

19 Yue, Q.; Wang, C.; Gianfagna, T.J.; Meyer, W.A., *Phytochemistry*, **58** (2001) 935-941.

20 Awano, K.; Ichikawa, Y.; Tokuda, K.; Kuraoka, M., *Flavour and Fragrance Journal*, **12** (1997) 327-330.

21 An, M.; Haig, T.; Hatfield, P., *J. Chromatogr. A*, **917** (2001) 245-250.

22 Koziel, J.A.; Martos, P.A.; Pawliszyn, J., *J. Chromatogr. A*, **1025** (2004) 3-9.

23 http://www.flavornet.org/flavornet.html, 2008.

Chapter 4

Study of desorption kinetics of Hydrophobic Organic Chemicals from solid matrices using cold fiber SPME

4.1 Introduction

The organic chemicals used in industries are typically stored in drums and tanks, and in many cases, such as gasoline fuelling stations and trucking companies, they are kept in underground storage tanks (UST). The on-site presence of large amounts of chemicals, gasoline, and diesel fuel is a potential source of ground water and soil contamination.[1] Hydrophobic organic contaminants (HOCs), which appear as persistent contaminants in soils and sediments, are basically introduced to the environment through leaking UST or surface spills.[1,2] HOCs include broad classes of chemicals, most importantly: aromatic compounds in petroleum and fuel residues, tars, and creosotes; chlorinated compounds in commercial

solvents; and persistent organic pollutants (POPs) such as DDT and polychlorinated biphenyls.[2]

Desorption rates of HOCs from suspended soil and sediment particles are important in predicting the transport of these compounds between different environmental media, their bioavailability, and the effect of remediation processes at contaminated sites.[3] Desorption kinetics of hydrophobic organic chemicals (HOCs) in soils and sediments have been proved to occur in two distinct stages: an initial rapid release phase (on the order of minutes to hours) followed by a slower stage (on the order of weeks to years).[3,4,5,6,7] Although the fast desorption can involve a significant fraction of the sorbed mass (especially for volatile HOCs) and is important in prediction of short-term fate of HOCs in the environment, slow desorption has been the focus of most studies since it is proving to make complete remediation difficult.[2]

Adsorption of gaseous organic molecules to polar inorganic surfaces such as snow or ice, small water droplets (<10 μm) as in fog, inorganic aerosols above the sea (i.e. salt) or deserts (i.e. mineral dust), and soil minerals such as quartz and clay at low humidity are also important.[8] Nevertheless, the mass transfer processes between gas phase (i.e. air) and natural surfaces are frequently ignored in the environmental consideration of organic chemicals.[8]

4.1.1 Mechanisms of sorption/desorption of HOCs from geosorbents

The assessment of the organic chemicals in the environment requires understanding of the structure of environmental media (e.g. soils, sediments, aerosols) and the mass transfer mechanisms that can occur in these domains. Soils and sediments (geosorbents) are heterogeneous solids with a variety of sorption sites, resulting in different release rates.[3] A typical geosorbent consists of inorganic; organic; and adherent or entrapped nonaqueous-phase liquid (NAPL) components.[2] Figure 4.1 illustrates the conceptual model of a typical geosorbent, and summarizes the possible sorption mechanisms.

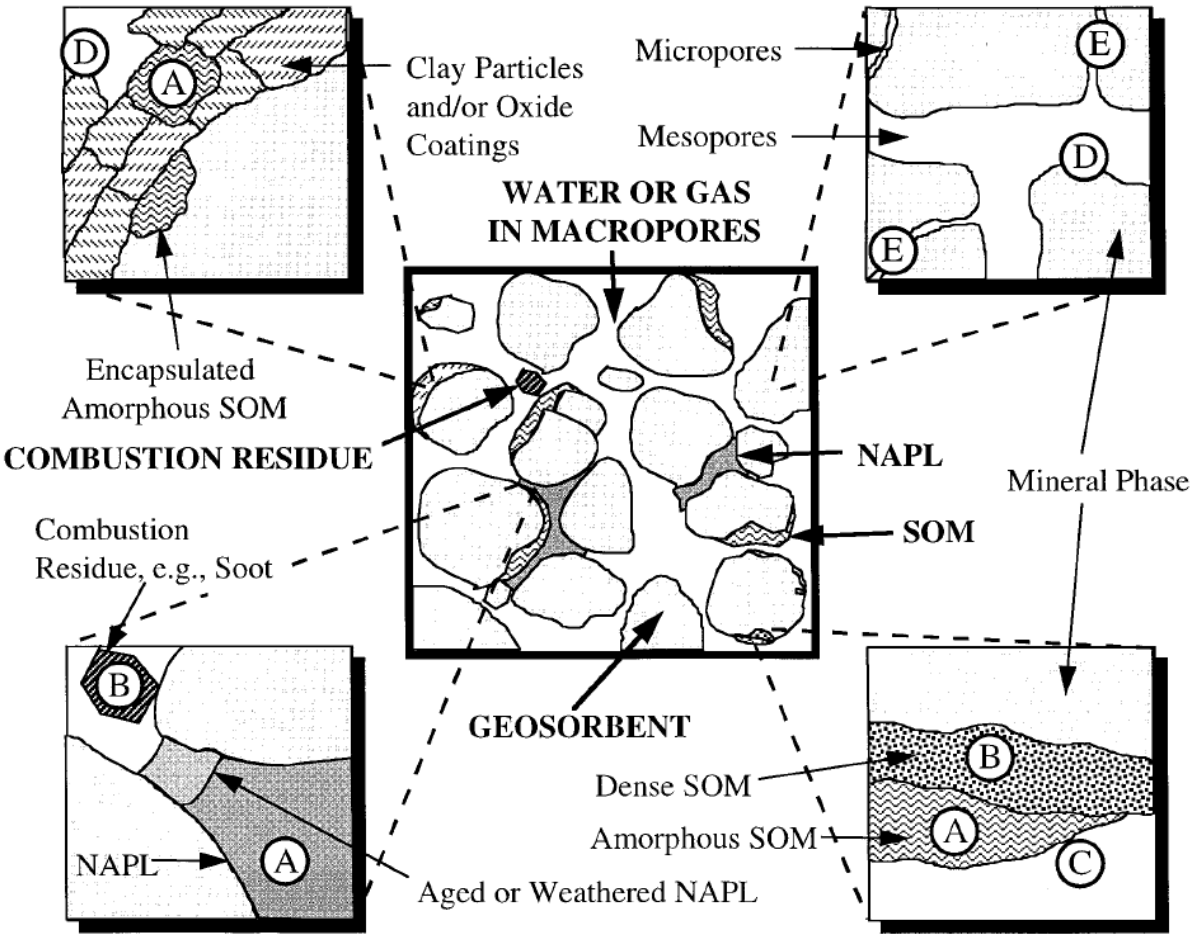

Figure 4.1 *Conceptual models of geosorbent domains. The geosorbent domains include different forms of sorbent organic matter (SOM), combustion residue particulate carbon such as soot, and anthropogenic carbon including nonaqueous-phase liquids (NAPLs). (A) sorption into amorphous or "soft" natural organic matter; (B) sorption into condensed or "hard" organic polymeric matter or combustion residue (e.g., soot); (C) sorption into water-wet organic surfaces (e.g., soot), (D) sorption into water-wet mineral surfaces (e.g., quartz); (E) sorption into microvoids or microporous minerals (e.g., zeolites) with porous surfaces at water saturation <100%.*[2]

The inorganic surfaces of geosorbent mineral components include: external surfaces; swelling clay interlayer surfaces; and internal surfaces.[2] The internal surfaces can be classified as: macropores, mesopores, and micropores.[2] Macropores occupy the space between soil and sediment grains and are larger than 500 Å width.[9] Mesopores are between 20 and 500 Å in

width and build up the majority of pore space within soil and sediment grains.[9] They are usually filled with water due to the capillary effect.[9] Micropores are less than 20 Å wide, are within soil and sediment grains and are suspected to be responsible for slow desorption.[9] The exterior surface of most common minerals consists of hydroxyl groups sticking out of a plane of electron deficient metals (e.g. Si, Al, Fe) and electron rich ligands (e.g. hydroxyl, carbonate).[8] As these surface groups typically include a combination of hydrogen donors and acceptors (e.g. –OH, -OC (O)(OH), and -O-), they can interact with the HOC molecules adjacent to the mineral surface through van der Waals (vdW), H-donor, and H-acceptor forces.[8] It should be noted that because water molecules can make hydrogen bonding with the H-donor and H-acceptor groups, such surfaces strongly prefer to bind water rather than the small nonionic organic compounds.[8]

The organic domain includes different forms of sorbent organic matter (SOM). The natural organic matter that is present in environmental media such as soils, sediments, and atmospheric aerosols consists of two distinct types of organic matter: recognizable biochemicals (e.g. proteins, nucleic acids, lipids, cellulose) and also a menagerie of macromolecular residues formed through diagenesis - the reactions of partial degradation, rearrangement, and recombination of the original molecules formed in biogenesis.[8] Therefore, the structure of the SOM depends on the ingredients available to the particular organisms which live at the vicinity of the environment under study.[8] SOM is somehow polar since it contains several oxygen-containing functional groups; however, the number of such polar groups may vary significantly[8] resulting in hydrophobic and hydrophilic domains.[2] Hence, the affinity of SOM for nonpolar organic compounds depends on the polarity and aromatic carbon content of these sorbents.[2] The rigidity of SOM may also vary from fluid (amorphous, rubbery or soft) to rigid (dense, glassy or hard).[8] The glassy domain may contain nanopores (microvoids of a few nanometer sizes).[8] The nonionic organic compounds are sorbed by absorption into the flexible organic matter and the microvoids of rigid portions, as well as adsorption onto the rigid portions of SOM.[8]

The Nonaqueous Phase Liquids (NAPLs) are organic liquids that are associated with human activities.[9] Some examples of NAPLs are dry fuel oil, gasoline and organic solvents that do not dissolve in water.[9] These liquids are often considered homogeneous with no interfacial resistance to mass transport.[2]

Organic pollutants released to the water may partition between the aqueous solution and the geosorbents, and provided that the contact times are long enough, e.g. at low advective flows (i.e. slow horizontal movement of water) equilibrium may be reached between the two phases. Equilibrium distribution of a chemical between the sorbent and the solution is described by sorption isotherms. Sorption isotherms relate the total sorbate concentration, C_{is} (e.g. mol Kg^{-1}), to the concentration of the chemical in the solution, C_{iw} (e.g. mol L^{-1}). [8] This may be quantitatively described through an empirical relationship known as Freundlich isotherm:

$$C_{is} = K_{iF}.C_{iw}^{n_i} \qquad \text{Equation 4.1}$$

where K_{iF} is the Freundlich constant, and n_i is the Freundlich exponent that represents the linearity of the sorption isotherm.[8] This mathematical relationship is employed to fit experimentally determined sorption data.

The shape of the sorption isotherms depends on the composition of the sorbent and the chemical nature of the sorbate.[8] The simplest case which is called linear isotherm (n_i=1) is that the affinity of the sorbate for the sorbent remains constant over the range of the observed concentration.[8] This is valid when the sorption mainly occurs through partitioning of significantly hydrophobic solutes between homogeneous organic phase such as NAPLs and amorphous SOM (case A in Figure 4.1), and at low concentrations where the adsorption sites on mineral surfaces are far from saturation (case D in Figure 4.1).[2,8] Adsoprtion cases may result in either linear or non-linear sorption isotherm depending on surface properties.[2] Adsoprtion to non-polar heterogeneous organic surfaces (case C in Figure 4.1) should yield

non-linear isotherms (n_i <1) since at higher concentrations of the sorbate, more adsorption sites are occupied and it becomes more and more difficult to occupy the remaining sites.[2,8] There are also rare situations where the sorbent affinity for the sorbate increases after it is loaded with some amounts of the sorbate (n_i >1) (e.g. sorption of anionic or cationic surfactants on geosorbents).[8] In summary, based on the composition of the natural sorbent and on the chemical nature of the sorbate, multiple sorption mechanisms can occur in parallel, resulting in sorption isotherms of various shapes.[2] Although the isotherm type and its degree of linearity depend on the sorption mechanism(s) existing in a given situation, it is not possible to verify what particular sorption mechanism occurs from the shape of the sorption isotherm.[8]

As explained above due to the complex nature of the geosorbents there are a variety of sorption sites available for the organic compound. Partitioning models, based on instant equilibrium between the solution and the solid geosorbent were adequate to describe some transport phenomena (e.g. organic compound exchange between slowly setting suspended solids in lakes and rivers); however, they were not valid in situations where the solid-fluid mass transfers are slow with respect to advective flow.[10] Therefore, over the past two decades scientists have been using kinetic terms rather than equilibrium terms to explain the biphasic nature of desorption of organic compounds from natural sorbents. The kinetic theory considers desorption as a "reaction" (often considered a first order reaction). Similar to chemical reactions the overall rate of desorption "reaction" is controlled by the rate-limiting steps. Therefore, scientists have modeled the biphasic desorption of organic compounds from/through geosorbents by considering various possible rate-limiting steps.

The possible rate-limiting steps are activation energy of sorptive bonds and mass transfer limitations (molecular diffusion).[11] Desorption from a surface is an activated process, with the kinetic energy of desorption (E^*_{des}) being the sum of the thermodynamic energy of adsorption (Q) and the activation energy of adsorption (E^*_{ads})[11](Figure 4.2).

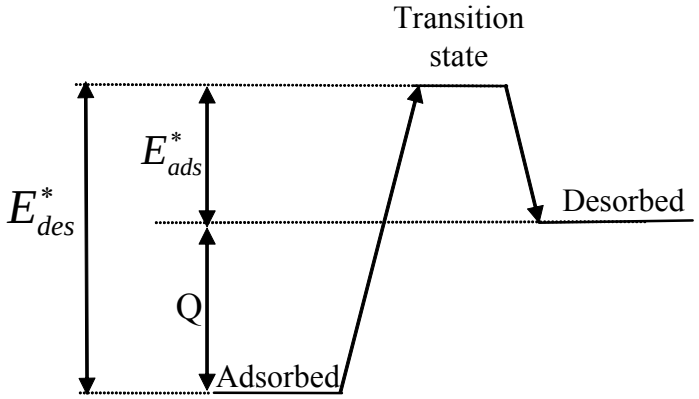

Figure 4.2 *Energy diagram for desorption from the surface.*

Adsorption to flat, unhindered, and rigid surfaces is generally unactivated or slightly activated (i.e. $E^*_{ads} = 0$); and the lifetime of a physisorbed molecule with $Q \geq 40\,\text{kJ mol}^{-1}$, is very short ($\leq 10^{-6}$ s).[11] Therefore, desorption of small molecules from the surfaces are practically instantaneous[11] and are not expected to be the reason for slow desorption of organic compounds from geosorbents. Nevertheless, large or long molecules that can interact simultaneously at multiple points can be more difficult to desorb.[11] Steric hindrance (e.g. in ink bottle shaped pores) may be another reason for activated desorption from porous mineral matrices (case E in Figure 4.1).[11]

Most researchers describe slow kinetics of desorption by diffusion limitations. Diffusion is random movement of molecules due to a concentration gradient.[11] Particles have an aggregated nature and are porous. For the sorbed molecules to leave the particle, they may need to pass through penetrable solid phases (matrix diffusion), pores within the particle (pore diffusion), the relatively immobile liquid "film" extending from the solid surface (film diffusion) and the bulk liquid.[11] Diffusion coefficients of organic molecules are expected to increase with the same order.[11] Currently, the most common model explains the biphasic desorption of organic compounds based on diffusion in SOM.[3] Diffusion through SOM is explained using polymer theory assuming that SOM structure is similar to polymers. While

diffusion through the rubbery (soft) SOM is considered fast, diffusion through the glassy (hard) SOM is known to be slow (the rate- limiting step for desorption).[3]

Diffusion models currently used to fit desorption data are based on Fick's second law of diffusion for spherical particles.[3] The main difference between them is the factors controlling retarded diffusion.[3] These models include the polymer diffusion model[12], radial diffusion model[10], the intraorganic matter diffusion model[13], intraparticle diffusion model[14], and the macro-mesopore and organic matter diffusion model[15].[3]

4.1.2 Two-compartment first-order rate constant (TFRC) model

One of the most universally accepted empirical algorithms used for fitting desorption data is the two-compartment first-order rate constant (TFRC) model.[3] This model is based on the biphasic nature of desorption and the shape of the desorption profiles (i.e. exponential decay curves).[3] It is usually expressed mathematically in the following form:

$$\frac{q_{(t)}}{q_0} = \phi_{Fast}.\exp(-k_{Fast}.t) + (1-\phi_{Fast}).\exp(-k_{Slow}.t) \qquad \text{Equation 4.2}$$

where $q(t)$ and q_0 are the solid-phase chemical concentration at time t and at the start of the experiment (contaminant-mass sorbent-mass^{-1}), respectively; ϕ_{Fast} is the fraction of contaminant present in the fast desorbing compartment; and k_{Fast} and k_{Slow} are the first-order rate constants of the fast and slow desorption, respectively (time^{-1}).[3] This empirical model was originally used by Karickhoff[16] and was modified by other investigators who depending on the applied situation removed the instantaneous equilibration of the fast release compartment[17], or added a third very slow release compartment and rate constant[18,19].[3] The TFRC model is more or less universally approved by researchers as a valid model for interpretation of kinetic data.[20,21,22,23] The first order rate constant values are often experimentally obtained from the slope of the plot of $ln(q_{(t)}/q_0)$ versus time (i.e. desorption plot).

First order rate constants achieved by the TFRC model can be correlated to diffusivity of the organic compounds in the geosorbent to estimate diffusion mechanisms governing the release of these compounds; however, this approach may not necessarily represent the actual process occurring during desorption.[3]

First order rate constants are also used to calculate the apparent activation energy of desorption, which approximately indicates the mechanism of diffusion.[24] For example, activation energies for diffusion through polymer materials are typically above 60 kJ mol^{-1}, whereas they are usually lower (20-40 kJ mol^{-1}) for diffusion through liquids and the interior of micropores.[24] Diffusion is an activated process, therefore, it is positively temperature-dependent in an Arrhenius way.[24] The temperature dependence of the rate of release of the slowly desorbing contaminant fraction can be described in terms of the Arrhenius relationship: [23]

$$k_s(T) = k_0 \exp\left(-\frac{E_{app,d}}{RT}\right) \qquad \text{Equation 4.3}$$

or

$$\ln k_s(T) = \ln k_0 - \frac{E_{app,d}}{RT} \qquad \text{Equation 4.4}$$

where k_0 is the Arrhenius constant, $E_{app,d}$ is the apparent activation energy of the desorption process, R is the universal gas constant, and T is temperature in Kelvin. If the values of the rate constants of a process at different temperatures are known, the apparent activation energy associated with a process can be obtained from the slope of the plot of $lnk_s(T)$ versus $1/T$ (i.e. Arrhenius plot). This approach has been used by investigators to approximately indicate the mechanisms involved in desorption of HOCs from both laboratory spiked samples and naturally contaminated soils and sediments.[23,24] For example, Johnson et al.[23] added phenanthrene to natural sorbents with different properties (e.g. SOM content and pore size) and after adequate equilibration time, which was tested by obtaining sorption isotherms for

each type of sorbent, they determined the apparent activation energies from desorption plots at 75, 100, and 150 ºC. The values of $E_{app,d}$ reported by these scientists ranged from 40 to 80 kJ mol^{-1}, which were consistent with those for diffusion in polymers (approximately of 60 kJ mol^{-1}) and those reported by other scientists.[23]

4.1.3 Techniques for studying desorption kinetics of HOCs from geosorbents

Several techniques including: mild solvent extraction,[25] supercritical CO_2 extraction,[26] gaseous purge system,[27] "vial desorption", and superheated water extraction[28] have been used for studying desorption of hydrophobic pollutants from geosorbents. The advantages and disadvantages of these techniques are discussed in the literature.[23,29] According to these sources, the most acceptable and widely used technique is the so-called "vial desorption", which places the resin in direct contact with the sediment suspension in a closed system (vial/reactor). Since HOCs desorption mainly occurs into aqueous phases, it is most rational to conduct desorption experiments in liquid water rather than non-aqueous sorbents (e.g. organic solvents). However, since this technique limits the measurement of desorption profiles to low temperatures (i.e. below boiling point of water), the characterization of desorption rates of resistant fractions is not possible unless the experiments are continued for long (months or years) periods of time, which is not experimentally practical.[23] John et al. demonstrated that desorption profiles measured at elevated temperature and pressure conditions (using heated or superheated water extractions) matched those at 25 ºC and ambient pressure, while the time scales related to the high temperature measurements were up to three orders of magnitude lower (hours or days compared to months or years).[23] However, this method is experimentally difficult to operate and is still considered time consuming. Therefore, a reliable technique for rapid prediction of the long-term desorption behaviour of HOCs from contaminated soils and sediments would be invaluable for engineers and scientists designing remediation projects and/or assessing risks related to different remediation endpoint decisions.

4.1.4 Objectives

The objective of the present study is to utilize cold fiber SPME for the measurement of desorption profiles at elevated temperatures, with the purpose of developing a relatively fast, automated and reliable method for rapid prediction of desorption behaviour of HOCs from naturally contaminated geosorbents according to the sorbent characteristics.

The main idea is to design a three-phase batch system, in which the contaminated solid sample is placed in a closed (sealed) vial in contact with a gaseous headspace, to which the third phase, the cold fiber, is exposed. Ideally, this batch system would work similar to the "vial desorption" technique, where the highly efficient extraction phase (Tenax resin) is replaced by the cold fiber. The difference is that in the "vial desorption" technique, HOCs are desorbed from the solid sorbent into an aqueous phase and are rapidly extracted by the Tenax resin, whereas in the proposed method, they are released into a gaseous headspace and extracted by cold fiber SPME. Similar to the "vial desorption' technique the sorbent, in this case cold fiber, is removed from the vial after a certain amount of time passed from the start of desorption at a particular temperature, and is immediately transferred to the GC injector, where the extracted compounds are thermally desorbed and subsequently separated in the GC column. A separate sample is used to obtain each data point of the desorption profile.

Polycyclic aromatic hydrocarbons (PAHs) and/or selected BTEX (benzene, toluene, ethylbenzene, and *o*-xylene) were chosen as representative contaminants in this study, since they are widespread pollutants in the environment (distributed in water, soil, and air) and also represent a range of molecular weights and boiling points. Laboratory contaminated sand and silica gel samples were chosen as simple solid models and certified sediments were chosen to represent real environmental samples. Both cold fiber SPME with TEC and cold fiber SPME with CO_2 cooling were used for this study. Since it was not appropriate for applications dealing with elevated temperatures of the matrix, the first device was used in the earlier experiments at low matrix temperatures and the second device was used for later experiments, in which matrix temperatures were higher. To make it more clear, the studies performed with these two devices are explained in two separate sections in this chapter.

4.2 Kinetic model of HS-SPME from solid samples

The TFRC model was modified to study desorption of HOCs from solid samples using HS-SPME. The kinetics of HS-SPME from a solid matrix can be considered a three-stage process: desorption from the solid matrix into the gaseous headspace, mass transfer (diffusion) in the gaseous headspace, and absorption on the polymer coating of the SPME fiber. Since the diffusion coefficients are large in the gas phase, it is assumed that mass transfer in the gaseous headspace occurs relatively fast and the compounds desorbed from the matrix are readily available at the surface of the fiber. Therefore, two stages are considered.

Desorption from the solid into the headspace can be described based on TFRC model (Equation 4.2):

$$\frac{n_{(t)}}{n_0} = \phi_{Fast}.\exp(-k_{Fast}.t) + (1-\phi_{Fast}).\exp(-k_{Slow}.t)$$

where $n_{(t)}$ and n_0 are the mass of the compound in the solid matrix at time t and at the start of the experiment; ϕ_{Fast} is the fraction of contaminant present in the fast desorbing compartment; and k_{Fast} and k_{Slow} are the first-order rate constants of the fast and slow desorption, respectively (time^{-1}).

The model proposed by Ai [30] for non-equilibrium situation in HS-SPME can be applied for extraction of the compounds on the SPME fiber:

$$n_f = n_i\left(1-\exp(-at)\right) \qquad \text{Equation 4.5}$$

where n_f is the amount of analyte absorbed after time t, and n_i is the initial amount of analyte in the headspace. Parameter 'a' is a measure of how fast the equilibrium can be reached between the fiber and the sample and depends on mass transfer coefficients of the analyte in gas and polymer phases as well as the partition coefficient of the analyte between the polymer and head space, and is considered constant with respect to time.

Assuming that the mass transfer in the headspace occurs fast, n_i in Equation 4.5 can be replaced by n_0-$n_{(t)}$, which can be derived from Equation 4.2, resulting in the following equation:

$$n_f = n_0\left(1-\exp(-at)\right).\left[1-\phi_{Fast}.\exp(-k_{Fast}.t)+(1-\phi_{Fast}).\exp(-k_{Slow}.t)\right]$$

Equation 4.6

This equation relates the mass of the compound extracted on the fiber, n_f, to its initial amount in the solid matrix, and can be used for the measurement of important kinetic parameters (i.e. a, k_{fast}, k_{slow}).

Equation 4.6 is a general model and contains kinetic information about both desorption from the matrix and absorption on the fiber (convoluted model of extraction); whereas Equation 4.5 only contains information about absorption of the compounds on the fiber. These equations can be used to fit the extraction data obtained from spiked empty vial (Equation 4.5) and aged spiked model solid matrices or naturally contaminated solid samples (Equation 4.6) to obtain the a- and k-values, respectively. However, rapid and exhaustive extractions (e.g. when using cold fiber SPME with CO_2 cooling[31]), the TFRC model can be directly used to measure the kinetic parameters by calculating $n_{(t)}$ from n_0 and n_f ($n_{(t)} = n_0 - n_f$).

4.3 Study of desorption kinetics of PAHs from laboratory-spiked sand using cold fiber SPME with TEC

Cold fiber SPME with thermoelectric cooling device (see Chapter 2) was employed in the study of the kinetics of desorption of PAHs from a simple model sample (laboratory-spiked sand). The effects of cooling/heating system on the extraction time and extraction recovery of these compounds from solid samples were qualitatively investigated.

4.3.1 Experimental

4.3.1.1 Chemicals and Materials

Naphthalene, acenaphthylene, acenaphthene, fluorene, anthracene, fluoranthene and pyrene were purchased from Supelco (Oakville, ON, Canada). HPLC grade methanol was purchased from BDH (Toronto, ON, Canada). The sand matrix was provided by the Waterloo Center for Groundwater Research. 40 mL vials with assembled screw cap with hole and PTFE/silicone septum were purchased from Supelco (Oakville, ON, Canada). A custom-made heat block together with a heater was used for adjusting the temperature of the vials at the desired experimental temperatures.

4.3.1.2 Preparing samples

A mixture of PAHs in methanol with 100 ppm concentrations of each compound was prepared. Two types of samples were prepared by spiking 3 μL of PAH solution (300 ng of each compound) into 40 mL empty vials and over 2 g sand in 40 mL vials. The samples were incubated at room temperature for 15 min before each experiment.

4.3.1.3 Instruments and supplies

The first prototype of cold fiber SPME with thermoelectric cooling (see Chapter 2) was used for these experiments. Temperature measurements of the fiber were performed prior to the extractions using the same set up as explained in Chapter 2.

Gas chromatography was performed on a Varian 3400 GC system equipped with a flame ionization detector (FID) and an Optic 2 ATAS programmable high volume injector. Separations were performed using a 30 m × 0.25 mm I.D., 0.25 μm CP-Sil & CB Low Bleed/MS fused silica column from Varian (Mississauga, Canada). Helium was chosen as the carrier gas. The injector was used in splitless mode with a constant temperature of 270 °C and splitless time of 10 min. The transfer pressure of carrier gas was set at 40 psi. The initial and final pressures of the carrier gas were set at 35 psi. The split flow rate and the purge flow rate were 100 and 5 mL/min respectively. For direct injections the initial temperature of the injector was set at 50 °C, increasing with the maximum ramp of 16 °C/sec to 270 °C. The column temperature was initially set at -20 °C for 2 min, increased to 150 °C at a rate of 15 °C/min and held for 1 min, then ramped at 10 °C/min to 250 °C and held for 1 min and finally ramped at 30 °C/min to 280 °C and held constant for 5 min. The FID system was used at a temperature of 300 °C with gas flows for hydrogen, high-purity air and nitrogen (make-up gas) set at 30, 300 and 30 mL/min, respectively.

4.3.1.4 Extraction time profiles

Extraction time profiles were obtained at two different temperatures of the sample, while the temperature of the fiber was kept the same. Headspace extractions with cold fiber SPME were performed for different extraction times (2, 5, 15, 30, and 60 min), at two temperatures of 30 and 50 °C. The fiber was not cooled for extractions at 30 °C (no current applied), while it was cooled to 30 °C (applying 1.5 ampere DC current) for the extractions at 50 °C. All experiments were performed in triplicate.

4.3.2 Results and discussion

Figures 4.3a to 4.3g compare the extraction time profiles for PAHs from spiked sand (with matrix) and spiked empty vial (without matrix) at 30 and 50 ºC. Increasing the temperature of the sample while cooling the fiber affects both the recovery of the extraction and the equilibrium time.

For spiked empty vial (without matrix), the extraction recoveries of all compounds increased by increasing the temperature from 30 to 50 ºC, because the partition coefficients of the compounds between the gas phase and the fiber coating increases by increasing the temperature difference between the sample and the fiber (see Equation 1.20). While the equilibrium times were not affected by increasing the temperature for more volatile compounds (naphthalene, acenaphthylene, acenaphthene, and fluorene), they were shortened for less volatile compounds. For example for anthracene, and fluoranthene (Figures 4.3d and f), equilibrium was not reached even after 60 min at 30 ºC, while it was reached in 30 min when the temperature of the sample was increased to 50 ºC. In direct SPME, according to the boundary layer model, equilibrium time is controlled by mass transfer in the sample, the thickness of boundary layer, the thickness of the fiber, and the partition coefficient of the analyte between the sample and the fiber (see Equation 1.8). Increasing the temperature of the sample while cooling the fiber increases the partition coefficient on the fiber, which should result in longer equilibrium times; however, since increasing the temperature of the sample speeds up the mass transfer in the sample and decreases the thickness of the boundary layer, the overall effect of increasing the temperature results in shorter equilibrium times. For volatile compounds, however, the system behaves as a perfectly agitated sample (see Equation 1.7), and the equilibrium time depends on the thickness of the coating and the diffusion coefficient of the analytes in the coating, which are not affected by the heating-cooling condition.

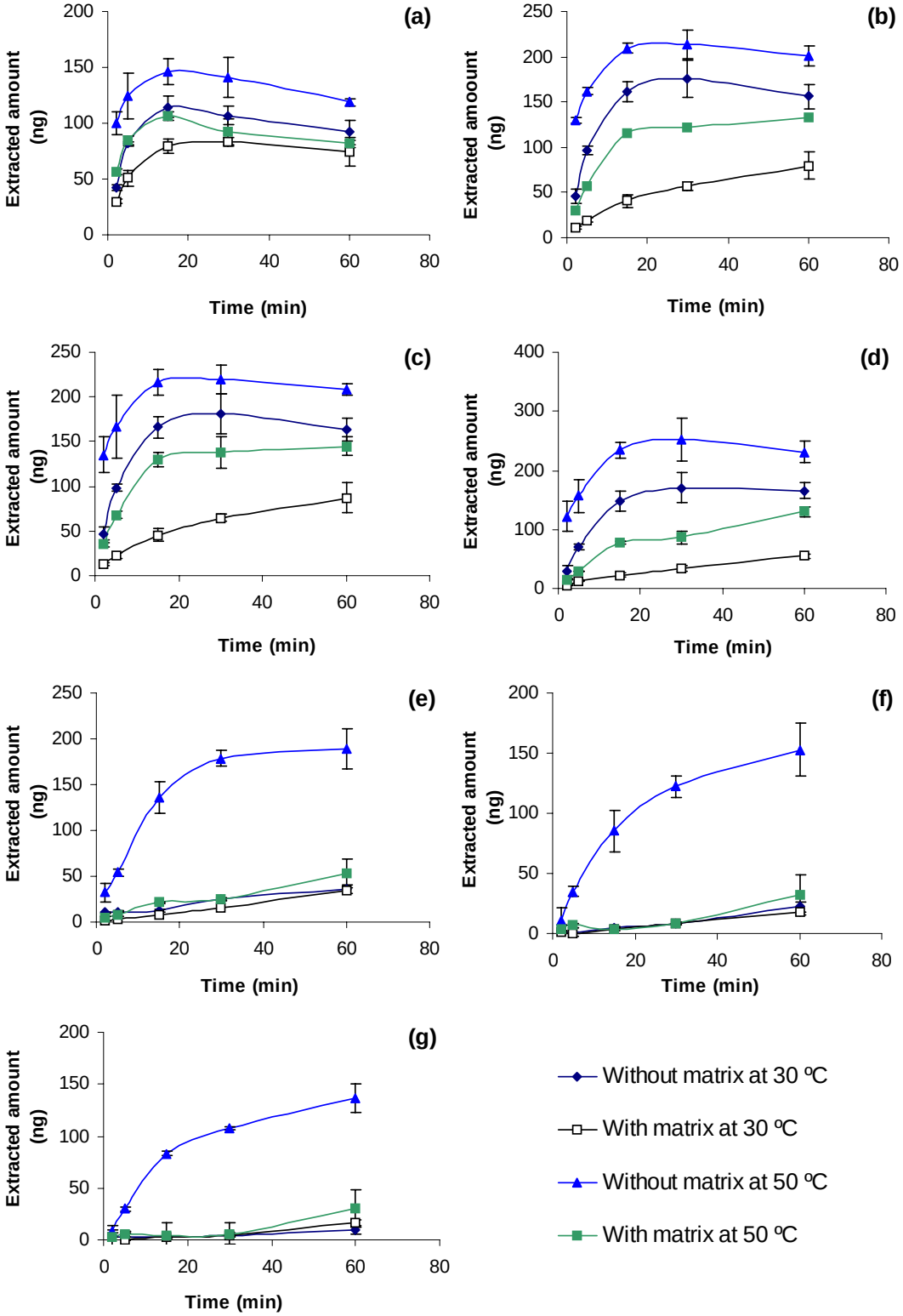

Figure 4.3 *Extraction time profiles for PAHs from sand. (a) naphthalene; (b) acenaphthylene; (c) acenaphthene; (d) fluorene; (e) anthracene; (f) fluoranthene; and (g) pyrene.*

The effect of heating-cooling system on the recovery of extraction in the presence of the matrix can be observed by comparing the profiles obtained with matrix at 30 and 50 ºC. For naphthalene, acenaphthylene, acenaphthene, and fluorene, the recovery of extraction increased with increasing the temperature from 30 to 50 ºC, because heating the sample increases the vapour pressure of these compounds in the headspace. However, for anthracene, fluoranthene and pyrene, the extraction recoveries were not affected, since these compounds have higher boiling points and higher sample temperatures are required to overcome the interactions between these compounds and the matrix. The equilibrium time did not change significantly for naphthalene, but it was shortened for acenaphthylene, acenaphthene, and fluorene from more than 60 min at 30 ºC to approximately 15 min at 50 ºC. The equilibrium time in headspace SPME is controlled by mass transfer in the matrix, mass transfer in the headspace, and the capacity of the fiber (see equation 1.11). Increasing the temperature of the sample while cooling the fiber increases the capacity of the fiber (by increasing the partition coefficient of the analytes between the fiber and the coating) and should result in longer equilibrium times; however, since increasing the temperature speeds up the mass transfer in the matrix and the headspace, the overall effect results in shorter equilibrium time. For anthracene, fluoranthene and pyrene, the equilibrium was not reached even after 60 min at 50 ºC and higher temperatures are required to speed up the mass transfer of these compounds in the matrix and the headspace.

The effect of matrix on extraction recovery can be observed by comparing the extraction time profiles obtained with and without matrix. Although sand is a matrix with low affinity for organic compounds, due to small surface area and low organic material content, the results show that, the equilibrium recoveries decreased at both temperatures in the presence of sand. The ratio of the amount of analyte extracted without matrix to the amount extracted with matrix was larger for less volatile compounds, since the Henry's constant, which controls the vapour pressure of the compound in the headspace, is smaller for these compounds. The Henry's constant increases by increasing the temperature and the vapour pressure of the analytes increases in the headspace, resulting in higher recoveries. For more volatile compounds, with higher Henry's constant, the effect of matrix is not as significant. For

example, for naphthalene (b.p. 217.9 ºC) the ratio of the amount extracted without matrix to the amount extracted at the presence of matrix at equilibrium was 1.5 at both 30 and 50 ºC (Figure 4.3.a), whereas, for fluorene (b.p. 295 ºC) the ratios were 3 and 1.7, at 30 and 50 ºC, respectively (Figure 4.3.d).

In summary, cooling the fiber while heating the sample increases the recovery of extraction, shortens the equilibrium time and lessens the effect of the matrix.

4.4 Study of desorption kinetics of HOCs from laboratory spiked model solids and certified sediments using cold fiber SPME with CO_2 cooling system

The objective of this study was to use cold fiber SPME with CO_2 cooling device for the study of the desorption kinetics of PAHs at elevated temperatures. The possibilities of exhaustive and rapid extraction of PAHs from gaseous samples were first tested. The extraction time profiles for PAHs from spiked empty vials and aged spiked model samples (i.e. sand and silica gel) as well as certified sediments were obtained at different sample temperatures. Since according to the obtained data, it was shown that extractions performed with cold fiber SPME with CO_2 cooling were both fast and exhaustive, the TFRC model (Equation 4.2) was used to measure the rate constants (with $n_{(t)}=n_0-n_f$). On the other hand, considering that the model solid samples (sand and silica gel) only contained low energy sites (i.e. mesopores and inorganic mineral surfaces), the TFRC model was simplified by assuming that desorptions only occurs in the fast stage. On the other hand, since certified sediments are dried and sieved during the certification process, it was assumed that only the slowly desorbing fraction was remained in the samples. To estimate the fast desorption of PAHs from certified sediment samples, deuterated PAHs were spiked to the samples before performing the extractions and the rate constants of desorption were simultaneously measured for these compounds and the native PAHs. Finally, the apparent activation energies of desorption of native PAHs (slow desorption) and spiked (deuterated) PAHs (fast desorption) were measured from Arrhenius plots.

4.4.1 Experimental

4.4.1.1 Chemicals and Materials

Naphthalene, acenaphthylene, acenaphthene, fluorene, anthracene, fluoranthene and pyrene and deuterated PAHs (acenaphthylene-d_{10}, acenaphthene-d_{10}, fluorene-d_{10}, anthracene-d_{10}, fluoranthene-d_{10} and pyrene-d_{10}) were purchased from Supelco (Oakville, ON, Canada). Toluene, ethylbenzene, *o*-xylene were purchased from Sigma-Aldrich. HPLC grade methanol was purchased from BDH (Toronto, ON, Canada). The vacuum pump oil was supplied by BOC Edwards (Wilmington, MA). Flash silica gel of mesh 230-400 (40-60 μm) with the average pore diameter of 60 Å was purchased from SiliCycle. The sand matrix was provided by the Waterloo Center for Groundwater Research. The clay matrix was obtained from the art gallery of the University of Waterloo. Certified sediments HS-6 (sediment A) and CNS300-04-050 (sediment B) were purchased from Environment Canada and Resource Technology Corporation (RTC), respectively.

Spiking solutions of PAHs in methanol with concentrations of 100 ppm (for silica gel and sand experiments) and 500 ppm (for clay-sand mixture experiments) in methanol were prepared. A mixture of toluene, ethylbenzene and *o*-xylene with concentrations of 500 ppm was also prepared as spiking solution for making clay samples. PAH-d_{10} solutions were prepared as spiking solutions for certified sediments. The concentrations of the deuterated PAHs were chosen according to the concentrations of the native PAHs in the certified sediments. The calibration solutions were also prepared within the range of 10 ppb to 500 ppm for PAHs, PAHs-d_{10} and BTEX.

4.4.1.2 Instruments and supplies

For extractions of organic compounds from sand, silica gel, and clay samples, as well as extractions from air samples with cold fiber SPME with CO_2 cooling, gas chromatography was performed on a Varian 3800 GC coupled with flame ionization detection (FID) using Star Chromatography Workstation (ver. 5.51). Automated analysis was performed using a CTC

CombiPAL autosampler (Zwingen, Switzerland) using the associated Cycle composer software (ver. 1.4.0). The PAL was equipped with a SPME fiber/syringe holder and a temperature-controlled six-vial agitator tray. Separations were performed using a 30 m× 0.25 mm i.d., 0.25-μm DB-1 fused silica column (Supelco) installed on Varian GC. Helium was used as the carrier gas at a flow rate of 1 mL/min. The Varian FID was used at a temperature of 250 °C with gas flows for hydrogen, high-purity air, and make up gas (nitrogen) set at 30, 300 and 25 mL/min, respectively. For analysis of PAHs the column temperature was maintained at 45 °C for 2 min, then ramped at 20 °C/min to 280 °C, and held for 5 min. The injector temperature was set to 300 °C. For the analysis of toluene, ethylbenzene, and *o*-xylene, the column temperature was maintained at 35 °C for 1 min and then programmed at 30 °C/min to 230 °C. The injector temperature was set at 250 °C.

For extractions from certified sediment, an Agilent 6890 GC equipped with a Gerstel CIS septum-free injector and Gerstel auto-sampler was used. Separations were performed using 30 m × 0.25 mm I.D., 0.25 μm HR-1 column. The column temperature was initially held at 45 ºC for 2 min, then increased to 280 ºC with a rate of 20 ºC/min and held at that temperature for 5 min. The injector temperature was set to 300 °C. The MSD transfer line heater temperature was set at 290 ºC. The MS Quad and the MS source temperatures were set at 150 and 230 ºC, respectively. The mass range was between 90 to 300 m/z.

The recently modified automated cold fiber SPME with CO_2 cooling [31,32] was used for all experiments.

4.4.1.3 Preparing the samples

Laboratory spiked solid samples were freshly prepared before each extraction by spiking 1 μL of the spiking solution into 10 mL vials loaded with 0.5 g of the solid matrix (sand, silica gel, clay, or clay-sand mixtures. The vials were sealed with the crimp cap right after spiking the solution. It should be mentioned that previously the samples were spiked through the cap septum (i.e. after capping) but the results obtained with this method of spiking (not presented in this text) show very low recoveries even from empty vials (recoveries less than 10%),

because of the leakage from the hole in the septum during aging process. Therefore, although some losses can occur during capping the vials after spiking, the results obtained show that the recoveries were much higher this way. The spiked vials were shaken for 60 min at room temperature at a ramp of 900 rpm. The aged spiked samples were kept in the fridge for 14 days before performing the extractions, while freshly spiked vials were used the same day.

In order to inhibit biodegradation caused by living organisms, clay samples were first sterilized following the procedure recommended by Trevors.[33] Clay batches, 20 g, were weighed in Petri glass dishes (10 cm diameter) and heated in an oven for 30 h at 200 ºC. The dishes were then covered with lids and cooled at room temperature.

For extractions from sediment A, 0.5 g of the sediment was loaded into 10 mL crimp cap vial and capped immediately. Sediment B samples were prepared by spiking 0.5 g of the sediment with 3 μL of the deuterated solution. Both sediments were extracted immediately after preparation.

For studying the kinetics of extraction of PAHs from air samples, the samples were prepared by two methods: spiking the liquid solution of PAHs into 10 mL empty vials using Hamilton syringe (conventional spiking method) and the back equilibration method [34,35,36] (may also be called fiber-spike method). In the latter method, PAHs were loaded onto the fiber by exposure to the headspace of 2.00 g pump oil containing 4.0 mg of each PAH compounds in a 20 mL vial. The loading was performed for 3 min at 50 °C. The fiber was then immediately exposed to the air sealed in a 10 mL vial to allow back equilibration of PAHs at different conditions. The amounts of PAHs spiked with this method were measured by direct injection of the loaded fiber to the GC/FID and the peak areas were compared to those of standard liquid samples (liquid injection). All processes were carried out automatically with the cold fiber SPME with CO_2 cooling using the CTC CombiPAL autosampler.

4.4.2 Results and discussion

4.4.2.1 Exhaustive extraction with cold fiber SPME

For an extraction method to be considered exhaustive, more than 90% of the analyte should be removed from the sample after the extraction is completed.[31] In other words, the ratio of the amount of the compound extracted to its initial amount in the sample should be more than 0.9. In SPME this ratio may be defined by rewriting Equation 1.1:

$$\frac{n}{n_0} = \frac{K_{fs}V_f}{K_{fs}V_f + V_s} \qquad \text{Equation 4.7}$$

where n and n_0 are the extracted amount and the initial amount of the analyte, respectively; K_{fs} is the fiber coating/sample matrix partition coefficient, V_f is the volume of the fiber coating, and V_s is the volume of the sample. In order to achieve exhaustive extraction, i.e., for $n/n_0 \geq 0.9$, K_{fs} should be equal to or larger than 9 (V_s/V_f). As the partition coefficients of volatile and semi volatile organic compounds between the PDMS coating and air, K_{fs}; and the volume of the coating, V_f, are small, exhaustive extractions of organic compounds from air using SPME is only possible for extremely small sample volumes. For example, theoretical calculations estimates that the largest volume of the air sample to achieve an exhaustive extraction of naphthalene (K_{PDMS}= 3000) at room temperature with a PDMS cold fiber coating with the volume of 2.4 μL, is 0.8 mL. However, the volume of the vials most often used in for automation is 10 or 20 mL autosampler vials. Therefore, a significant increase in the partition coefficient is required to achieve exhaustive extractions from these vials. For example, the partition coefficient should have a value equal to or larger than 75,000 for 20 mL vials and 37,000 or larger for 10 mL vials to achieve exhaustive extraction.[31]

As explained in Chapter 1, an efficient way to increase the partition coefficients is to increase the temperature of the sample and simultaneously cool the fiber coating. The partition coefficient in a heating/cooling system can be calculated using Equation 1.20. Table 4.1 presents the calculated partition coefficients for some of the PAHs for the sample

temperatures of 100, 130 and 150 ºC and coating temperature of 5 ºC, using Equation 1.20. According to these calculations, all compounds except for naphthalene have partition coefficients close to or larger than 37,000 at sample temperatures above 150 ºC with cold fiber SPME coating at 5 ºC. Fluorene, anthracene, fluoranthene and pyrene may be exhaustively extracted at temperatures above 130 ºC, and anthracene, fluoranthene and pyrene may even be exhaustively extracted at sample temperature of 100 ºC, in a 10 mL vial, provided that the coating temperature is maintained at 5 ºC or lower. The possibility of exhaustive extraction of seven PAHs with cold fiber SPME, is experimentally demonstrated using automated cold fiber SPME.

Table 4.1 Calculated K_{fs} values for PAHs in heating-cooling system using Equation 1.20. Calculations are based on fiber temperature of 5 ºC (278 K), C_p values were collected from CRC hand books.

Compound	Sample temperature (ºC)		
	100	**130**	**150**
naphthalene	3.96E+03	8.29E+03	1.45E+04
acenaphthylene	9.49E+03	1.99E+04	3.47E+04
acenaphthene	1.61E+04	3.38E+04	5.90E+04
fluorene	1.94E+04	4.06E+04	7.09E+04
anthracene	2.88E+05	7.75E+05	1.64E+06
fluoranthene	3.39E+05	1.02E+06	2.34E+06
pyrene	4.67E+05	1.38E+06	3.13E+06

Experimentally, the possibility of exhaustive extraction of PAHs from air samples was tested by calculating the recovery of extraction of a known amount of these compounds from air samples by cold fiber SPME. Instead of spiking a certain amount of liquid standards into air sample, a newly described fiber-spiked method was used to deliver a certain amount of standards. In this method, the fiber was first loaded with the standards from a standards generator (2 g vacuum pump oil with 0.4 mg of each of PAHs dissolved in it) and then exposed to the air samples contained in a sealed vial in the autosampler six-vessel agitator at a

certain temperature.[33,34,35] The compounds were released from the fiber to the vial and after a certain amount of time, back equilibrium was reached at the fiber. The initial amount of the standards and the amounts of standards remaining on the fiber follow the same distribution law as the extraction process:

$$n_f = \frac{k_{fs} V_f}{K_{fs} V_f + V_s} . n_0 \qquad \text{Equation 4.8}$$

and

$$n_s = n_0 - n_f \qquad \text{Equation 4.9}$$

n_0, was obtained by direct desorption of the fiber in the injector after loading the standards from the standard generator. Since the loading of the standard was reproducible (see Table 2-14), and the determination of n_f and n_0 was fully automated, the recovery could be very accurately estimated without calibration, by assuming that the detector respond was linear with mass, which is true when using FID.[31]

Figure 4.4a presents the results of extraction of PAHs from air samples using the automated cold fiber SPME device. It was found that about 10, 35, 37, and 45% of naphthalene, acenaphthene, and fluorene, respectively, remained on the fiber after 30 min back equilibration at 100 ºC without cooling, whereas, when the temperature of the fiber was cooled to 10-15 ºC during back equilibration for the same time duration, all four compounds completely remained on the fiber. On the other hand, when back equilibration was carried out for 30 min without cooling at 150 ºC, more than 90% of all the PAHs were released from the fiber to the vial, because the partition coefficient between the air and the fiber coating is inversely related to temperature (see Equation 1.13). Therefore by increasing the temperature, the partition coefficient decreases and lower amounts of analytes remain on the fiber coating. However, when cooling is applied during back equilibration for 30 min at 150 ºC, almost all the initial amount of the amounts loaded on the fiber remain in the coating (Figure 4.4b).

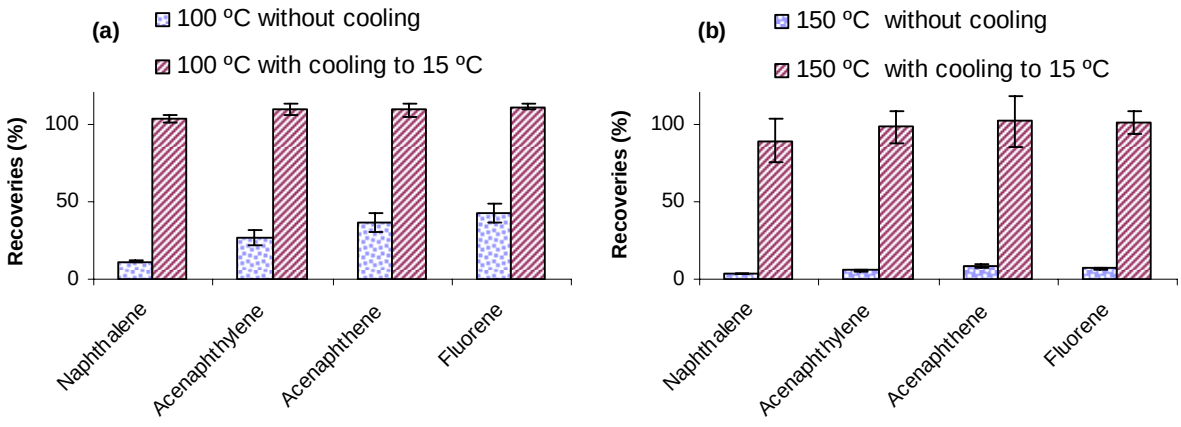

Figure 4.4 *Extraction recoveries of PAHs at (a) 100 °C and (b) 150 °C from air cold fiber SPME based on back equilibration of PAHs preloaded in the fiber coating.*

In summary, exhaustive extraction of naphthalene, acenaphthylene, acenaphthene, and fluorene from air is possible at sample temperatures of 100 and 150 ºC using cold fiber SPME provided that sufficient temperature gap exists between the sample and the fiber (for fiber temperatures of 15-20 ºC or less). The same behavior is expected for less volatile PAHs (e.g. pyrene) since they have higher partition coefficients on PDMS coating compared to more volatile compounds. However, due to their low volatility they were not generated in the headspace of pump oil at 50 ºC and therefore were not tested for exhaustive extraction using back equilibration method.

4.4.2.2 Kinetics of extraction of PAHs from gaseous samples

As explained before, for cold fiber SPME to be an appropriate technique for the study of desorption of HOCs from geosorbents, it should be exhaustive and rapid (relative to desorption from the matrix). The results of the experiments explained in the previous section proved the possibility of exhaustive extraction of PAHs from air samples; however, they do not show how fast the extractions take place. Therefore, extraction time profiles for PAHs from air samples were required to obtain information about the rate of extraction.

The air samples were prepared either by spiking the liquid solution of PAHs into empty vials or by the new back equilibrium (fiber-spike) method.

Extractions from air samples prepared by liquid-spike method: Extraction time profiles were obtained for freshly spiked empty vials for 2, 5, 15, 30, 45, and 60 min at extraction temperature of 150 ºC (vial temperature) and fiber temperature of 25 ºC (Figure 4.5). The extraction recoveries were calculated based on the amount extracted on the fiber (n_f) and the initially spiked amount in the vial (n_0), the latter was measured by direct liquid injection of the spike solution to the GC/FID instrument.

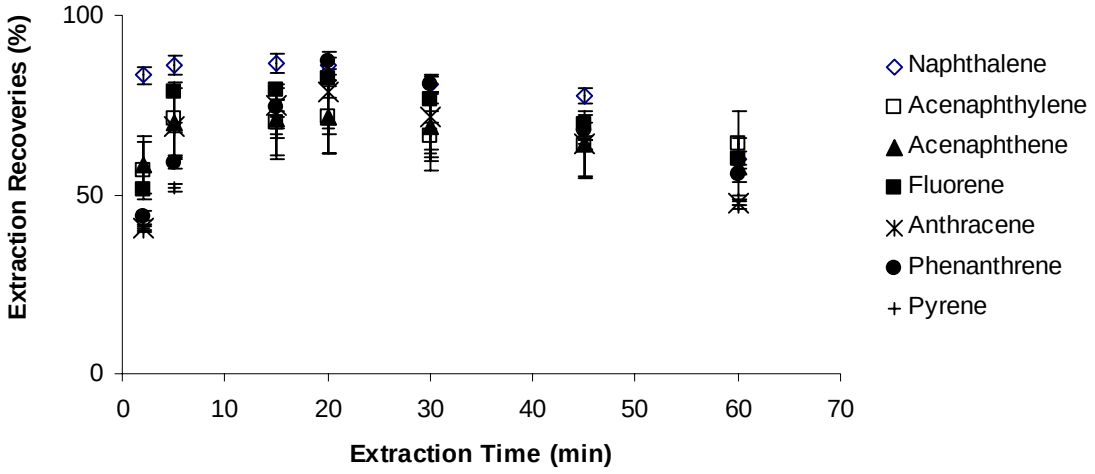

Figure 4.5 *Extraction time profiles for PAHs from freshly- spiked empty vial at 150 ºC.*

The results show that equilibrium time was very short (< 5 min) for most compounds. However, the recoveries were lower than expected from theoretical calculations. The lower recoveries might be due to the losses of the compounds during capping period (after spiking the vial) or leakage from the vial during extractions at a high temperature (150 ºC).

Extractions from air samples prepared by fiber-spike method: In order to eliminate the possibility of loss of the PAHs during spiking with liquid solution, the back-equilibration (fiber-spike) method was used. In these experiments, the PDMS coating of the cold fiber

device was first exposed to the headspace of the pump oil containing the PAHs for 3 min at vial temperature of 50 ºC (without cooling the fiber) and transferred to the empty vial (previously placed in the heater/agitator of CTC CombiPAL autosampler) at 150 ºC. The fiber was exposed to the hot air in the vial for 30 min without cooling the fiber followed by cooling the fiber to 25 ºC for different extraction times (2, 5, and 10 min) to obtain extraction time profiles. The extraction time profiles for naphthalene, acenaphthene and fluorene are presented in Figure 4.6.

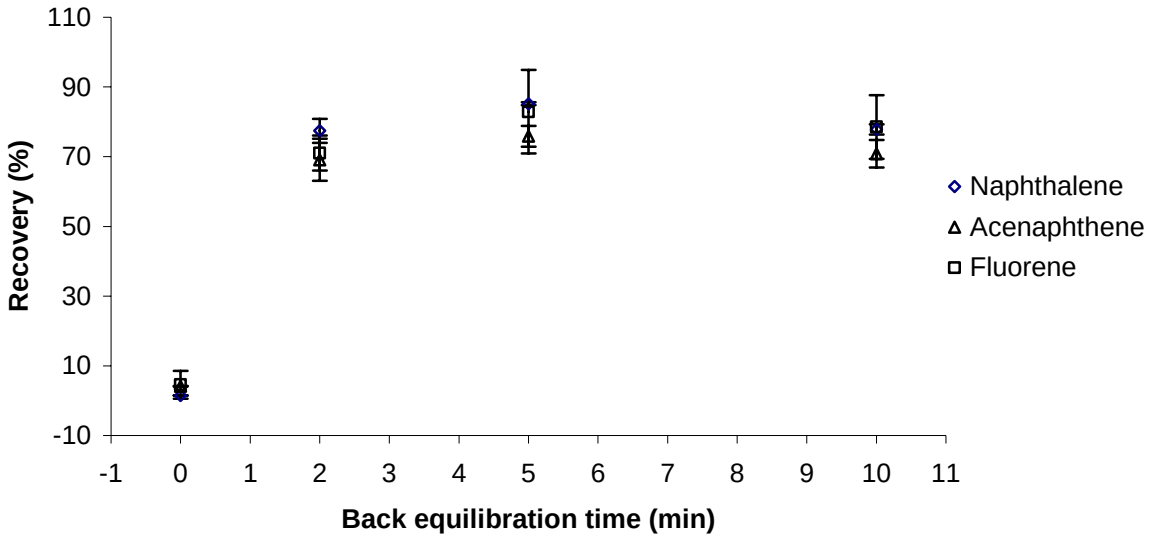

Figure 4.6 *Extraction time profiles for PAHs from fiber-spiked empty vial at 150 ºC.*

The *y*-axis in this profile presents the percentage of the initially loaded compounds that is remained on the fiber after 30 min back equilibration at 150 ºC followed by *t* min (*x*-axis) back equilibration time with cooling (25 ºC). These profiles show that less than 10% of all compounds remains on the fiber after 30 min equilibration time at 150 ºC. At the end of 30 min back equilibration without cooling (at 150 ºC), the fiber is rapidly cooled to 25 ºC using liquid CO_2 and kept at this temperature for different periods of time. It is shown that the back equilibration with cooling reaches its maximum recovery rapidly (2 min or less). The maximum recoveries are higher than those obtained from the liquid-spiked samples, and are more close to exhaustive extraction recoveries.

According to these results cold fiber SPME can be considered a rapid and exhaustive extraction method that can be utilized to study desorption of PAHs from contaminated solid samples based on TFRC model.

4.4.2.3 Temperature dependence of desorption of PAHs from laboratory contaminated sand samples

Comparing extraction time profiles obtained from aged spiked sand to those obtained from the aged spiked empty vial at 150 and 180 ºC show that for more volatile compounds, i.e. naphthalene, acenaphthylene, acenaphthene, and fluorene the graphs approximately superimposed, which means that for these compounds, kinetics of desorption from the matrix are very fast (not activated). Figure 4.7 shows the extraction time profiles for acenaphthylene as an example.

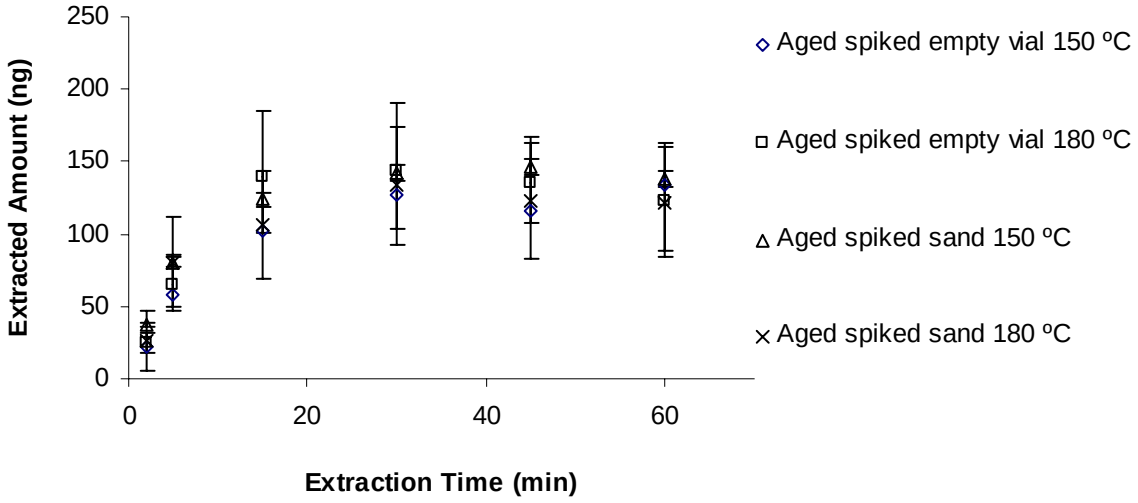

Figure 4.7 *Comparison of extraction time profiles for acenaphthylene from aged spiked empty vial and aged spiked sand samples at 150 and 180 ºC (q_0 = 200 ng).*

The extraction time profiles for phenanthrene and pyrene on the other hand were slightly different with and without matrix and the rates of extraction (or desorption from the matrix) were slightly higher at 180 ºC, compared to 150 ºC. Figure 4.8 shows the extraction time profiles for pyrene as an example.

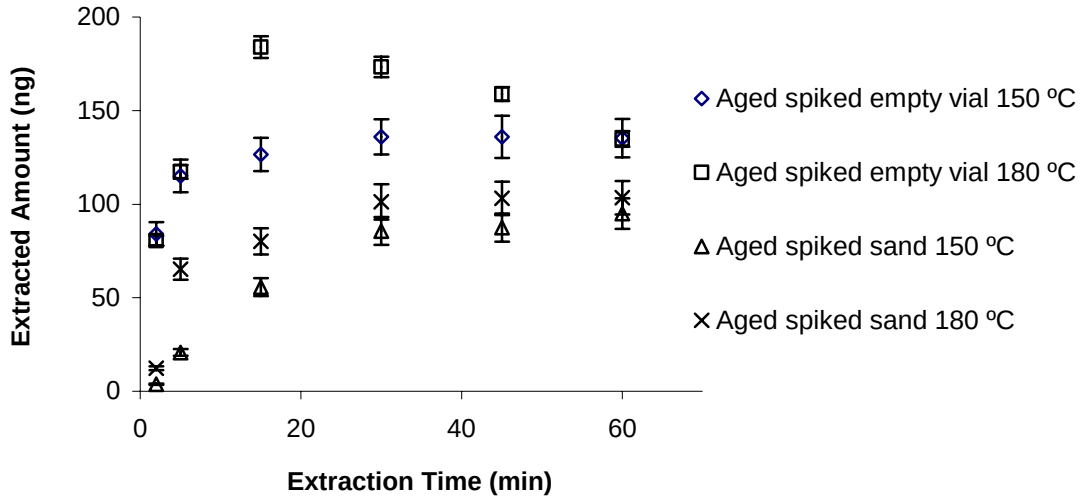

Figure 4.8 *Comparison of extraction time profiles for pyrene from aged spiked empty vial and aged spiked sand samples at 150 and 180 ºC (q_0 = 200 ng).*

Desorption plots ($ln(q_{(t)}/q_0)$ *vs.* time) were established using the data in the kinetic region of the extraction time profiles (i.e. for extraction times before reaching the equilibrium) at two different temperatures (150 and 180 ºC) for pyrene (Figure 4.9). The desorption constants (*k*-values) were obtained from the slope of desroption plots at each temperature. q_0 (the initial amount of the compound in the solid sample) was assumed to be the mass of the compounds initially spiked into the sample (the leakage from the vials during aging time was considered negligible) and $q_{(t)}$ (the amount of the compound remained in the solid sample after time *t*) was calculated by subtracting the extracted mass of the compound for extraction time *t,* n_f, from the initial amount of the compound in the sample (assuming exhaustive extraction from the headspace).

Knowing the *k*-values at two temperatures, T_1 = 423 K (150 ºC) and T_2 = 453 K (180 ºC), the apparent activation energies of desorption ($E_{app,d}$) were calculated using the following equation (rearranged form of the Arrhenius equation):

$$E_{app,d} = \frac{RT_1T_2}{T_2 - T_1} \ln\left(\frac{k(T_2)}{k(T_1)}\right) \qquad \text{Equation 4.10}$$

where R is the standard gas constant (8.3144 J mol^{-1} K^{-1}).

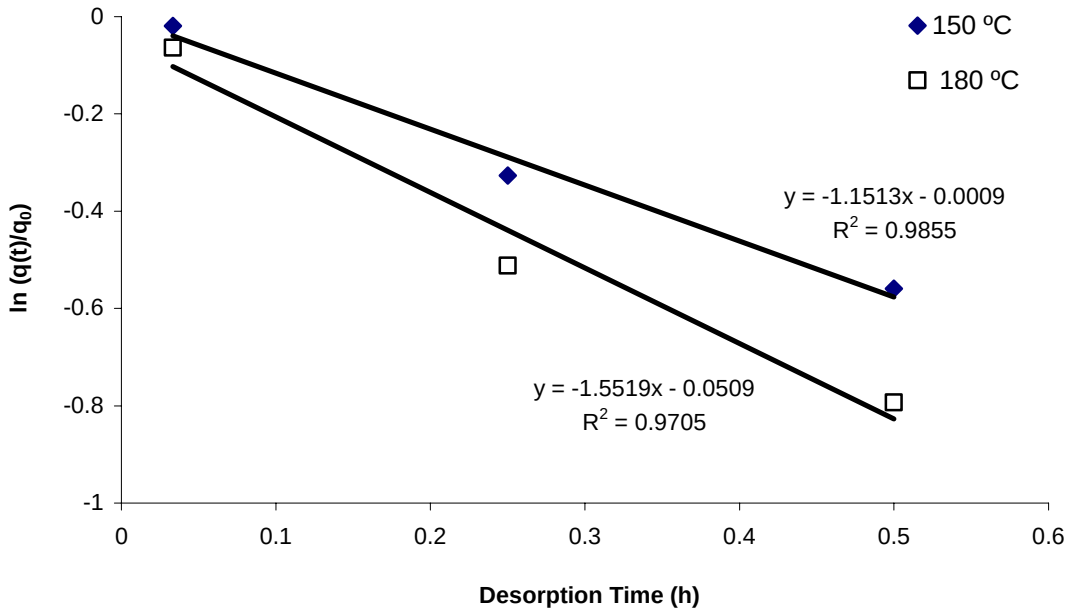

Figure 4.9 *Desorption plots for pyrene from sand samples at 150 and 180 ºC (q_0 = 200 ng, fiber temperature: 5 ºC).*

The *k*-values obtained from the slope of desorption plots for pyrene, at 150 and 180 ºC, were 1.15 and 1.55 h^{-1}, respectively. The apparent activation energy of desorption of pyrene from aged sand sample was 16 kJ mol^{-1}. The low apparent activation energy of desorption can be explained by the non-porous structure of sand particles and the absence of SOM in sand matrix, which means that the two important rate limiting steps in desorption process i.e. retarded diffusion in narrow pores and diffusion through hard SOM are not important when dealing with sand matrices. The interactions between the PAH molecules and the inorganic mineral sorption sites on sand particle surface is of dipole-dipole induced type which are low energy, however the greater the polarizability (see Appendix 3) of the PAH molecules the

stronger are the temporary van der Waals interactions between the molecules and the surface of sand particles.

4.4.2.4 Temperature dependence of desorption of PAHs from lab-contaminated silica gel samples

Silica gel was chosen as a porous solid matrix. Extraction time profiles were obtained for aged spiked silica gel samples at 150 and 180 °C. Extractions were performed for 2, 5, 15, 30, 45, and 60 min. Figure 4.10 shows the extraction time profiles and desorption plots at 150 and 180 °C for naphthalene, fluorene and anthracene as representative examples. Desorption rate constants as well as the apparent activation energies of desorption are presented in table 4.2.

Table 4.2 Rate constants of desorption (k, h^{-1}) at 150 and 180 °C for lab-contaminated silica gel matrices along with the apparent activation energies (kJ mol^{-1}).

Compound	Temperature (ºC)		Ea
	150	180	(kJ mol^{-1})
Naphthalene	1.10	3.38	59
Acenaphthylene	0.11	0.36	56
Acenaphthene	0.1	0.29	58
Fluorene	0.08	0.29	68
Anthracene	0.01	0.07	103

The apparent activation energies of desorption for naphthalene, acenaphthylene and acenaphthene, calculated by this method, were about 60 kJ mol^{-1}, and increased to 70 and 100 kJ mol^{-1} for fluorene and anthracene, respectively. Fluoranthene and pyrene could not be detected at 150 ºC even after 90 min extraction time, and it was not possible to calculate the apparent activation energies for these two compounds. The increase in the activation energies of desorption of PAHs were in the order of the increase in their polarizabilities (see Appendix 3), which was predictable considering that the surface of silica gel consist of inorganic polar sorption sites which can interact with PAHs through dipole-induced dipole interactions.

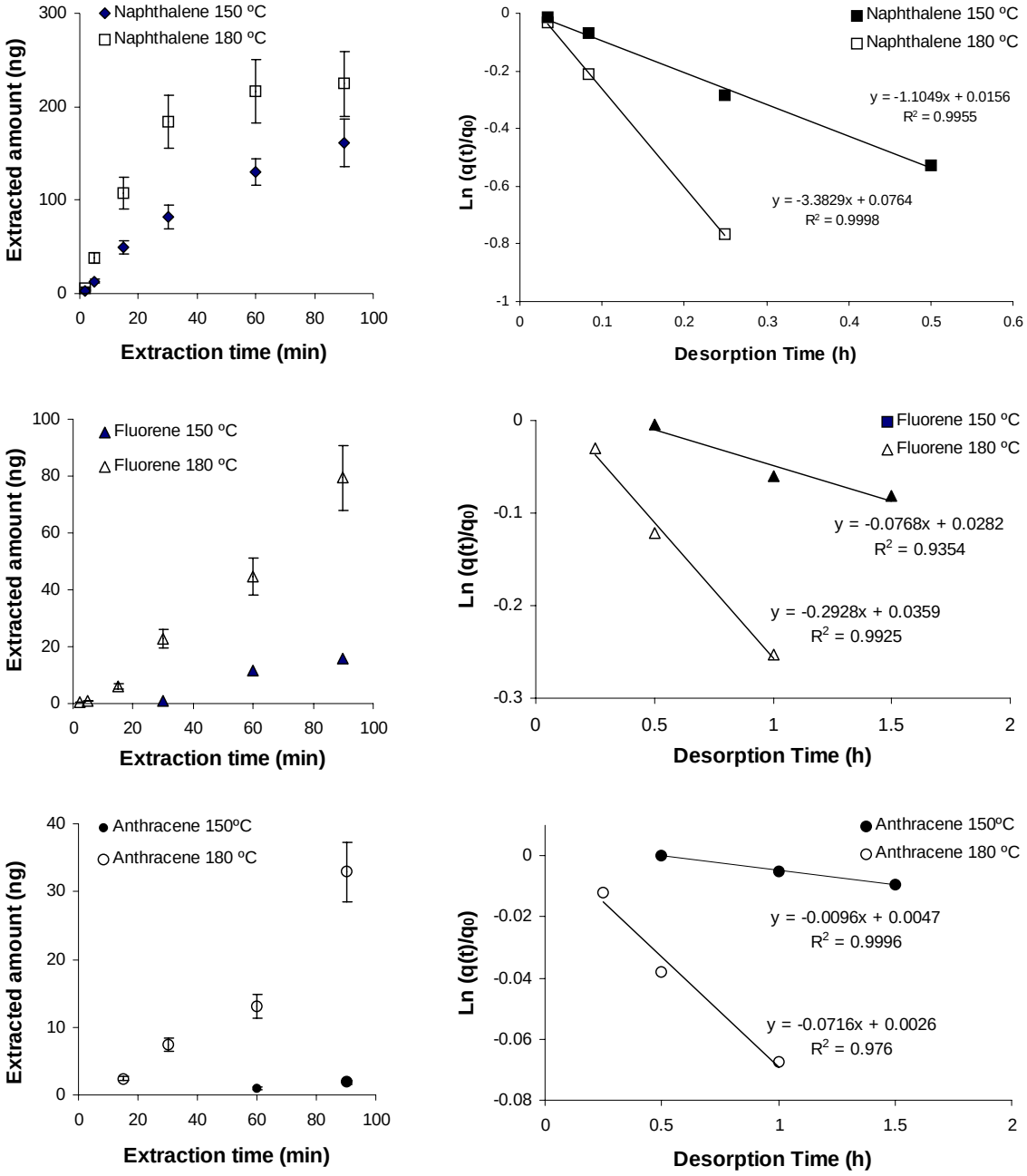

Figure 4.10 *Extraction time profiles (left) and desorption plots (right) for naphthalene, fluorene, and anthracene from silica gel samples at 150 and 180 ºC (q_0 = 200 ng).*

4.4.2.5 Temperature dependence of desorption of PAHs from lab-contaminated clay matrix

The next solid matrix chosen for this study was clay, which is one of the main constituents of natural soils and sediments. It was found that among the PAHs spiked to clay samples only naphthalene could be recovered at a detectable level, which is due to the large surface area of clay, resulting in retardation of the less volatile compounds. Therefore, mixtures of clay and sand were tested. The samples were prepared by mixing different proportions of sand and clay and were then spiked with 1 µL of 500 ppm solution of PAHs and were shaken at 900 rpm over night. Headspace extraction was performed with cold fiber SPME with CO_2 cooling for 5 min at 150 ºC sample temperature. Figure 4.11 shows the extraction recoveries for the PAHs from the sand-clay mixtures.

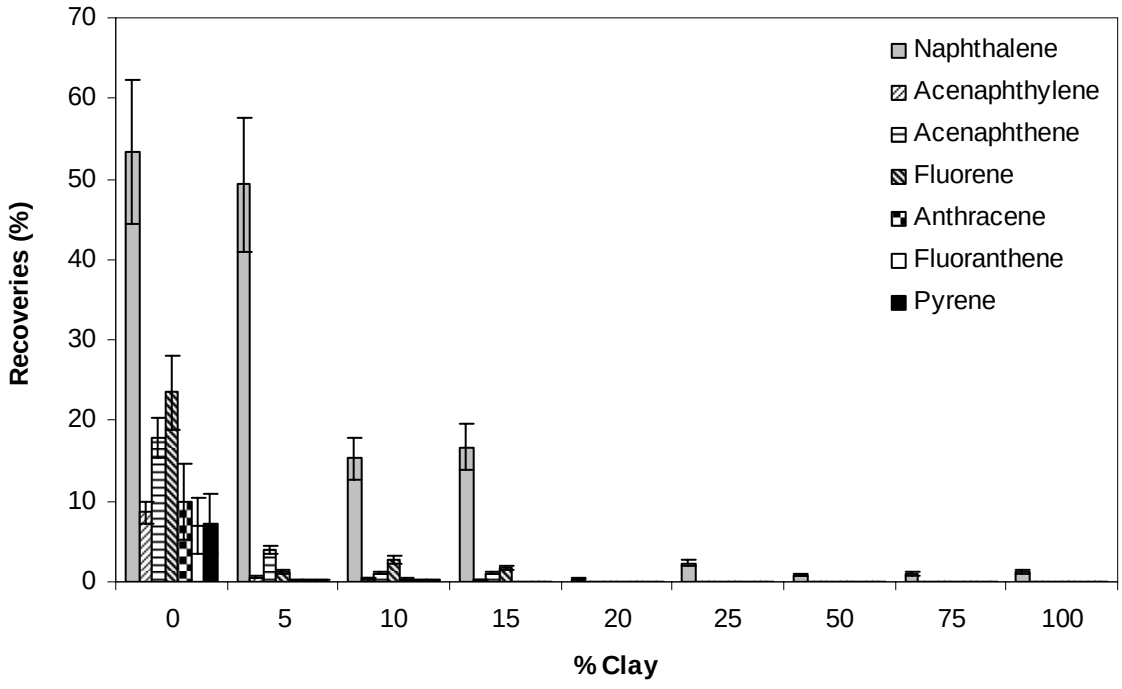

Figure 4.11 *Extraction recoveries of PAHs from sand-clay mixtures. Extraction time: 5 min, extraction temperature: 150 ºC, Fiber temperature: 5 ºC.*

The results show that even when the percentage of clay was as low as 5%, the extraction recoveries for all compounds except naphthalene were lower than 5%. Therefore, it was decided to use a mixture of more volatile organic compounds (toluene, ethylbenzene, and *o*-xylene) instead of PAHs.

4.4.2.6 Temperature dependence of desorption of volatile compounds from clay matrix

4.4.2.6.1 Extraction temperature profiles for toluene, ethylbenzene, and o-xylene from clay matrix

In order to observe the effect of temperature on the recovery of selected BTEX compounds from clay, 0.5 g clay aliquots were weighted into 10 mL crimp cap vials and were spiked with 1 µL of 500 ppm solution of toluene, ethylbenzene and *o*-xylene. The samples were shaken for 1 h and kept in fridge over night. The extraction recoveries were obtained at sample temperatures of 30 to 180 ºC. Extractions were performed for 15 min. The temperature profiles are shown in Figure 4.12.

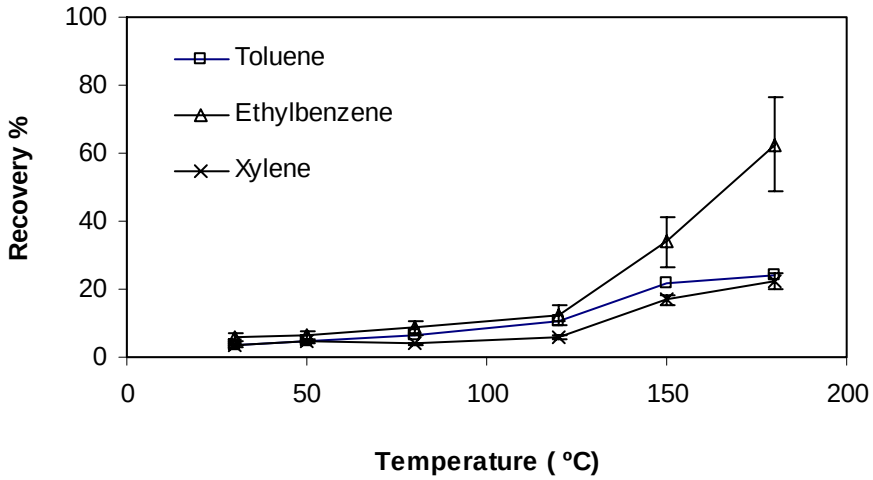

Figure 4.12 *Extraction temperature profiles for toluene, ethylbenzene and o-xylene from clay. Extraction time: 15 min, fiber temperature: 5 ºC.*

The results show that the extraction recoveries were not affected by increasing the temperature up to 120 ºC. At temperatures above 120 ºC, the effect of temperature was more significant for ethylbenzene.

4.4.2.6.2 Temperature dependence of desorption of ethylbenzene from clay matrix

Clay aliquots, 0.5 g, were weighted into 10 mL crimp cap vials and spiked with 1 µL of 500 ppm solution of ethylbenzene (500 ng). The samples were shaken for 1 h and kept in fridge over night before performing the extractions. The extractions were performed for 1, 3, 5, 15, and 30 min at sample temperatures 120 and 180 ºC. Desorption plots for ethylbenzene are shown in Figure 4.13.

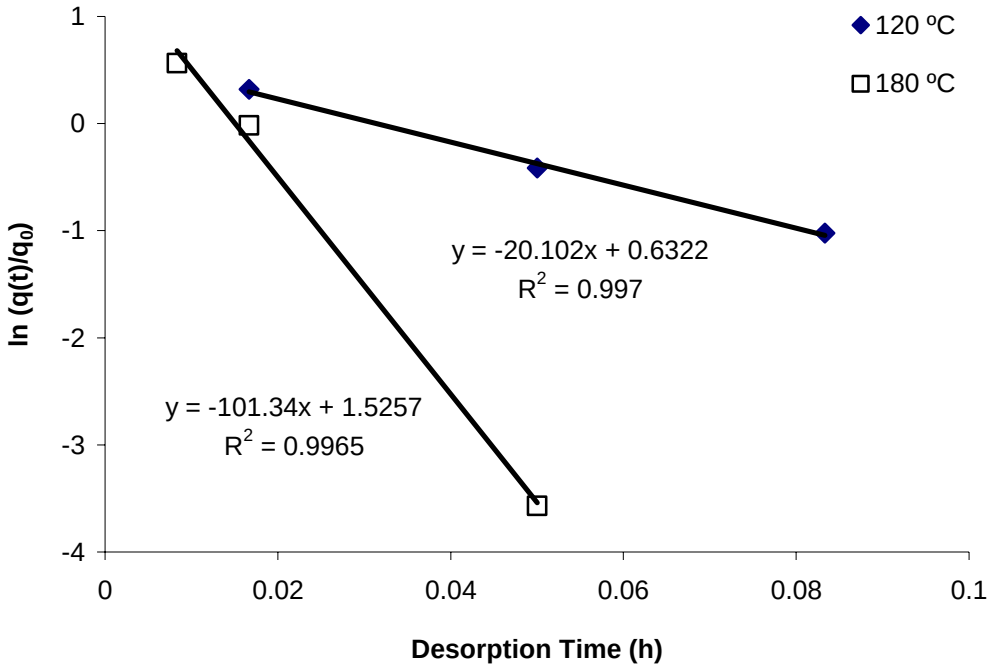

Figure 4.13 *Desorption plots for ethylbenzene at 120 and 180 ºC.*

The k value for ethylbenzene at 120 and 180 ºC were 20 and 101 h^{-1}, respectively; and the apparent activation energy of desorption was 40 kJ mol^{-1}.

4.4.2.7 Temperature dependence of desorption of naphthalene from naturally contaminated certified sediment

Extraction time profiles of naphthalene from certified sediment A were obtained at 120, 140, and 160 ºC. Extraction times of 15, 30, 45, and 60 were performed at each temperature. In all experiments, 0.5 g of the sediment was loaded into 10 mL vials right before extraction was performed. The samples were prepared freshly to avoid the accumulation of the compounds in the headspace of the vial before extraction was started. The vials were subsequently placed in the agitator of the Gerstel auto sampler, which was previously set at the experimental temperature. Desorption plots for naphthalene are illustrated in Figures 4.14.

The apparent activation energy of desorption for naphthalene calculated from the Arrhenius equation was 85 kJ mol^{-1}, which is roughly comparable with the values found in other studies using vial desorption method (60 –70 kJ mol^{-1}). The lower value for $E_{app,d}$ reported in the literature can be explained by the displacement effect of water on desorption of PAHs from sediment.

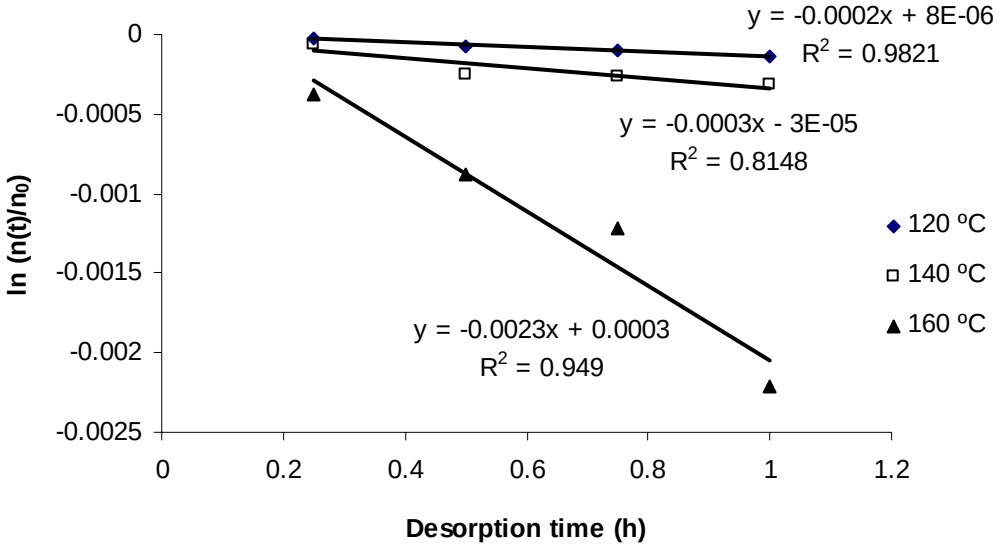

Figure 4.14 *Desorption plots for naphthalene from sediment A at 120, 140 and 160 ºC.*

4.4.2.8 Temperature dependence of fast and slow desorption of PAHs from naturally contaminated certified sediment

In order to study the fast and slow desorption of PAHs from sediment, certified sediment B was spiked with known amounts of PAH-d_{10} compounds and immediately placed in the agitator heat block for extraction with cold fiber SPME with CO_2 cooling. The extraction time profiles were obtained at three different temperatures: 90, 110, and 130 ºC. In all experiments, 0.5 g sediment were loaded into 10 mL crimp cap vial and spiked with 5 µL of PAH-d_{10} solution. Desorption and Arrhenius plots were obtained from these data, resulting in desorption rate constants and the apparent activation energy of desorption, respectively. Table 4.3 summarizes the *k* and $E_{app,d}$ values for these compounds.

Table 4.3 Rate constants of desorption ($k.h^{-1}$) at 90, 110 and 130 °C for certified sediment along with the apparent activation energies for native and spiked (deuterated) PAHs (kJ mol^{-1})

	Rate constants of desorption ($k.h^{-1}$)			
Compounds	**90 ºC**	**110 ºC**	**130 ºC**	**E_a (kJ)**
acenaphthene	0.055	0.088	0.164	33
fluorene	0.014	0.022	0.031	24
fluoranthene	n.d.	0.001	0.004	89
pyrene	n.d.	0.002	0.006	89
acenaphthene-d_{10}	0.210	0.22	0.235	4
fluorene-d_{10}	0.094	0.1	0.125	9
fluoranthene-d_{10}	0.021	0.16	0.2	69
pyrene-d_{10}	0.026	0.07	0.122	70

n.d. = not detected

The results show that desorption rate constant increased by increasing the temperature for all compounds, whether spiked or native, and decreased by decrease in the molecular weight of the compound. The apparent activation energy of desorption was larger for native PAHs

relative to spiked PAH-d_{10} compounds. Native PAHs are sorbed over years on the inner surfaces of the sediment micropores, which can be filled by hard (glassy) SOM, therefore, to reach the headspace of the sample, these compounds need to be released form the high energy compartments of the soil, which requires higher activation energies; whereas spiked PAHs (deuterated compounds) are either adsorbed on the outer surface of the mineral pores or absorbed to the rubbery SOM or entrapped non-aqueous-phase liquid (NAPL) components, which are less activated.

4.5 Conclusion

Cold fiber SPME with CO_2 cooling was used as an exhaustive extraction sorbent phase for extraction of desorbed organic compounds (e.g. PAHs) from both laboratory spiked and naturally contaminated sediments into the gaseous headspace in a batch system. Sand, silica gel and clay matrices were spiked with certain amounts of PAHs or selected BTEX (only for clay samples), and were stored for 14 days for aging. The extraction time profiles were obtained at two or three different elevated temperatures (above 100 ºC). The slow desorption rate constants at each temperature were measured from desorption plots and the apparent activation energies of desorption were obtained from Arrhenius plots. For example, the apparent activation energy of desorption of naphthalene, acenaphthylene and acenaphthene, from spiked silica gel, were approximately 60 kJ mol^{-1}, and increased to 70 and 100 kJ mol^{-1} for fluoranthene and anthracene, respectively.

The value of the apparent activation energy of desorption for native naphthalene from sediment A was 85 kJ mol^{-1}, which is roughly comparable with the values found in other studies (60 –70 kJ mol^{-1}). The lower activation energy reported in the literature is obtained for

desorption of PAHs into water, which is believed to be lower due to the displacement effect of water.

The fast and slow desoption rates of PAHs were obtained by spiking sediment B with deuterated PAHs (PAHs-d_{10}). The native and spiked PAHs were extracted at three different elevated temperatures using cold fiber SPME. The TFRC model was modified and used for the measurement of kinetic parameters. Assuming that native PAHs are desorbed from high energy sorption sites and spiked deuterated PAHs were desorbed from low energy sites, the TFRC model was simplified to describe single stage desorption kinetics. Desorption rate constants and the apparent activation energies of desorptions were obtained from desorption plots and Arrhenius plots, respectively. The activation energies of native PAHs were higher than those of spiked deuterated PAHs, suggesting that the native compounds were more affected by retarded pore diffusion or slow mass transfer into glassy SOM.

The proposed technique in the present study, is more time efficient and versatile compared to the commonly used technique for desorption studies, i.e. vial desorption. The centrifuging step required for separating the resin from the sediment-water suspension as well as solvent extraction of the compounds from the resin in "vial desorption" technique are eliminated and the desorption plots are obtained in a considerably shorter time (a few hours) compared to vial desorption technique (days or weeks).

References

1 Wong, J. H.C.; Lim, C.H.; Nolen G.L., *Design of Remediation Systems*, CRC/Lewis Publishers, Boca Raton, FL, USA, 1997.

2 Luthy, R.G. et al., *Environ. Sci. Technol.*, **31** (1997) 3341-3347.

3 Birdwell, J.; Cook, R.L.; Thibodeaux, L. J., *Environ. Toxicol. Chem.*, **26** (2007) 424-434.

4 Farrell, J.; Reinhard, M., *Environ. Sci. Technol.,* **28** (1994) 63-72.

5 Carroll, K.M.; Harkness, M.R.; Bracco, A.A.; Balcarcel, R.R., *Environ. Sci. Technol.,* **28** (1994) 253-258.

6 Werth, C.J.; Reinhard, M., *Environ. Sci. Technol.,* **31** (1997) 697-703.

7 Cornelissen, G.; Noort, P.C.M.; Govers, H.A., *Environ. Toxicol. Chem.*, **16** (1997) 1351-1357.

8 Schawrzenbach, R.P.; Gschwend, P.M.; Imboden, D.M., *Environmental organic chemistry*, second edition, John Wiley and sons, USA, 2003.

9 Werth, C.J.; Reinhard, M., *Environ. Sci. Technol.,* **31** (1997) 697-703.

10 Wu, S.C.; Gschwend, P.M., *Environ. Sci. Technol.,* **20** (1986) 717-725.

11 Pignatello, J.J.; Xing, B., *Environ. Sci. Technol.,* **30** (1996)1-11.

12 Berens, A.R.; Huvard, G.S.; *J. Dispersion Sci. Technol.,* **2** (1981) 359-378.

13 Brusseau, M.L.; Jessup, R. E.; Rao, P. S.C., *Environ. Sci. Technol.,* **25** (1991) 134-142.

14 Ball, W.P.; Roberts, P.V., *Environ. Sci. Technol.,* **25** (1991) 1237–1249.

15 Shor, L.M.; Rockne, K.J.; Taghon, G.L.; Young, L.Y.; Kosson, D.S., *Environ. Sci. Technol.,* **37** (2003) 1535-1544.

16 Karickhoff, S.W., *Sorption kinetics of hydrophobic pollutants in natural sediments, In* Baker RA (ed) Contaminants and Sediments, 1st ed, Vol 2-Analysis, Chemistry, Biology. Ann Arbor Sciences, Ann Arbor, MI, USA, 1980.

17 Autenrieth, R.L.; DePinto, J.V., *Environ. Toxicol. Chem.,* **10** (1991) 857-872.

18 Cornelissen, G.; Hassell K.A.; van Noort, P.C.M.; Kraaij, R.; van Ekeren, P.J.; Dijkema, C.; de Jager, P.A.; Govers, H.A.J., *Environ. Pollut*., **108** (2000) 69-80.

19 van Noort, P.C.M.; Cornelissen, G.; ten Hulscher, T.E.M.; Vrind, B.A.; Rigterink, H.; Belfroid, A., *Water Res.,* **37** (2003) 2317-2322.

20 Cornelissen, G.; Rigterink, H.; Ferdinandy, M.M.A.; van Noort, P.C.M., *Environ. Sci. Technol.,* **32** (1998) 966-970.

21 Jonker, M.T.O.; Hawthorne, S.B.; Koelmans, A.A., *Environ. Sci. Technol.,* **39** (2005) 7889-7895.

22 Greenberg, M.S.; Burton, G.A.; Landrum, P.F.; Leppanen, M.T.; Kukkonen, J.V.K., *Environ. Toxicol. Chem.*, **24** (2005) 31-39.

23 Johnson, M.D.; Weber, W.J.; *Environ. Sci. Technol.*, **35** (2001) 421-433.

24 Cornelissen, G.; Noort, P.C.M.; Parsons, J.R.; Govers, H.A.; *Environ. Sci. Technol.*, **31** (1997) 454-460.

25 Tang, J.X.; Alexander, M., *Environ. Toxicol. Chem.,* **18** (1999), 2711-2714.

26 Hawthorne, S. B.; Bjorklund, E.; Bowadt, S.; Mathiasson, L., *Environ. Sci. Technol.*, **33** (1999) 3152-3159.

27 Oliver, B.G., *Chemosphere*, **14** (1985) 1087-1185.

28 Johnson, M.D.; Huang, W.L.; Dang, Z.; Weber, W.J., *Environ. Sci. Technol.*, **33** (1999) 1657-1663.

29 Saalfield, S. L.; Wnuk, J.D.; Murray, M.M.; Dunnivant, F.M., *Chemosphere*, **66** (2007) 384-389.

30 Ai, J., *Anal. Chem.*, **69** (1997)1230-1236.

31 Chen, Y.; Pawliszyn, J., *Anal chem*., **78** (2006) 5222-5226.

32 Ghiasvand, A.; Hosseinzadeh, S.; Pawlisyn, J., *J. Chromatogr. A,* **1124** (2006) 35-42.

33 Trevors, J.T., *J. Microbiol. Methods*, **26** (1996) 53-59.

34 Chen, Y.; Wang, Y.; O'Reilly, J.; Pawliszyn, J., *Analyst*, **129** (2004) 702-703.

35 Wang, Y.; O'Reilly, J.; Chen, Y.; Pawliszyn, J., *J. Chromatogr. A,* **1072** (2005) 13-17.

36 Niri, V.H.; Pawliszyn, J., *Analyst,* **132** (2007) 425-430.

Chapter 5

Summary

5.1 Cold Fiber SPME

Solid-phase microextraction (SPME) is based on the removal of a small portion of analytes from a sample matrix by exposing the fiber to the matrix for a certain amount of time, usually until the extraction equilibrium is reached. It is mostly preferred to perform extractions at equilibrium, because at equilibrium the amount of extracted analytes is maximized and the reproducibility of the extraction is improved. However, depending on the volatility of the analyte, the properties of the matrix, and sampling conditions, the equilibrium time can range from seconds to hours. In some cases, the equilibrium cannot be reached within the practical time frames and there is a need for speeding up the mass transfer processes involved in partitioning of analytes on the fiber. In the case of headspace SPME, the rate-limiting step of the whole mass transfer process is often the transfer of analytes within the sample matrix or from the sample matrix into its headspace. Increase of temperature is an efficient way to

desorb analytes from solid particles and accelerate mass transfer, but it decreases distribution coefficients of the analytes between the extraction phase and the sample matrix, potentially resulting in a lower extracted amount under equilibrium. Internally cooled SPME or cold fiber SPME was developed to overcome this drawback by cooling the fiber while heating the sample. This sampling approach accelerates the mass transfer, and creates a temperature gap between the internally cooled coated fiber and the hot headspace, which significantly increases the distribution coefficient.

The first approach of cold fiber SPME was based on using liquid CO_2 for cooling the fiber. This approach was further modified, miniaturized and automated and was applied in different areas of analytical chemistry. However, due to the heavy parts and complexity of operation there was still a need for a more versatile and portable approach for cold fiber SPME.

5.2 Contributions of this thesis

A new approach for cold fiber SPME was developed based on using thermoelectric coolers (Chapter 2). The new cold fiber SPME was applied in the laboratory analysis of off-flavors in rice and the results were compared to a classic solvent extraction method (Chapter 3). The portable cold fiber device was applied for field sampling of volatile components from living flowers (Chapter 3). The effect of cooling on the sensitivity of SPME extraction of volatile components from living wisteria flowers was demonstrated and the volatile components of living lily-of-the-valley flowers were identified for the first time (Chapter 3). It was shown that the new cold fiber SPME approach could be used as an alternative to the previous approach in laboratory applications and as the only available cold fiber SPME choice for field sampling (Chapter 3).

One of the important issues in environmental chemistry is the measurement of desorption constant rates for desorption of hydrophobic organic chemicals (HOCs) from naturally contaminated geosorbents (soil and sediments). As a part of this study, the cold fiber SPME with CO_2 cooling approach was utilized for the first time for the purpose of the measurement of desorption rate constants of selected organic compounds from geosorbents. In this

approach, cold fiber SPME with CO_2 cooling worked as an exhaustive extraction method to extract the organic compounds released from contaminated solid samples at different elevated temperatures within a range of extraction times. The extraction data were used to calculate desorption data from which desorption plots and Arrhenius plots were obtained. The rate constants of desorption and activation energies of desorption were measured using these plots for laboratory contaminated model solid samples as well as naturally contaminated samples. The results were comparable to those reported in literature.

5.3 Prospective

The results of the work done so far clearly demonstrate that cold fiber SPME with TEC device has the potential to be applied both in laboratory and field applications of SPME where better sensitivity is required. The device can be further improved by using thermoelectric coolers that have higher efficiency, especially for laboratory applications where high powers can be used and portability is not an issue. The low weight device can be redesigned to be mounted on autosampler arms and be fully automated.

The proposed method for applying cold fiber SPME with CO_2 cooling to environmental studies can be extended to the study of desorption of organic chemicals from different solid matrices (i.e. with different composition, texture, organic content, etc.). This method is fast and requires low amounts of sample and has the potential to be fully automated and therefore is a powerful method for the study of the parameter dependence of desorption of organic chemicals from solid samples which is important in remediation studies.

Appendix 1- List of collaborations

1. Collaboration with Dr. Ali Ghiasvand in application of cold fiber SPME with CO_2 cooling for quantification of polycyclic aromatic hydrocarbons in sediments. The results of this work are published in Journal of Chromatography A, 1124 (2006) 35-42 (NOT presented in this thesis). Also Dr. Ghiasvand's work on screening the aroma of rice using cold fiber SPME with CO_2 cooling device was a motivation for me to quantify off-flavours in rice using cold fiber SPME with thermoelectric cooling.

2. Collaboration with Dr. Yong Chen in early applications of automated cold fiber CO_2 cooling (the results published in Analytical Chemistry 78 (2006) 5222-5226), through which I learnt to use the system later for my research work in kinetic studies. Dr. Chen developed the automated internally cooled coated fiber with CO_2 cooling and I further modified and used it for the investigations reported in Chapter 4 of this dissertation.

3. Collaboration of student technical services (STS) in making the devices used in this study. In more detail, STS collaborated in both cold fiber systems. In case of CO_2 cooling system, STS provided us with the temperature controller and some syringe parts and in case of TEC system, they provided us with the prototypes based on our requirements.

4. Dr. Vadoud Niri discussed and provided some input regarding the kinetic experiments and interpretation of the results. Moreover, he read my thesis carefully and gave me constructive advice.

Appendix 2- Raw data of graphs

Table 1 Raw data for Figure 2.6

Distance from the cooling source (mm)	Temperature of the fiber (ºC) for different diameters of copper wire (micrometer)		
	250	**380**	**800**
10	-1.5	-5	-7.9
20	4.8	-1.1	-3.7
30	12.6	8.9	-2
40	19	12.7	3.5

Table 2 Raw data for Figure 2.11

Time (min)	Temperature of the fiber at different sample temperatures (ºC)		
	25	**100**	**150**
0	25.8	50.2	61.3
5	10.9	26.8	42.4
30	11.6	27.2	42.3
60	12	27.4	42

Table 3 Raw data for Figure 2.12

Temperature of the coating (ºC) versus the temperature of the cooler (ºC) at different sample temperature (ºC)							
40		**60**		**80**		**100**	
T_{Cooler}	$T_{Coating}$	T_{Cooler}	$T_{Coating}$	T_{Cooler}	$T_{Coating}$	T_{Cooler}	$T_{Coating}$
29.8	31.5	31.2	36.2	33	41.9	39.2	51.5
3.7	15.3	3.5	19.4	2.4	22.7	5.1	29.4
-7.4	8.6	-7.3	12.6	-9.3	19	-5	24.3
-17.7	3	-17.8	8.5	-15.8	15.8	-17.3	18.7
-25.1	-1.4	-24.5	5.1	-25.2	12.2	-24.5	18.4

Table 4 Raw data for Figure 2.13

Sample temperature (ºC)	Water content (w/w%)				
	<1	**1**	**3**	**5**	**10**
40	-1.5	3.4	8.3	10	8.3
60	5.1	12	17.5	22	22.3
80	12.2	22	30	35	36
100	24	38	52	58	60

Table 5 Raw data for Figure 3.1

Sample temperature (ºC)	Extraction recovery (%) for PAHs from spiked sand versus extraction temperature.						
	Naphthalene	Acenaphthylene	Acenaphthene	Fluorene	Anthracene	Fluoranthene	Pyrene
40	8.96	56.4	61.7	63.8	19.0	9.43	10.4
60	16.1	62.3	72.8	82.1	35.2	8.18	8.56
80	15.4	68.9	79.9	99.7	72.3	27.4	28.5
100	24.7	68.8	89.3	104	100	46.1	47.1

Table 6 Raw data for Figure 3.2

Extraction time (min)	Extracted amount (ng) of PAHs from spiked sand at 100ºC versus extraction time (min)						
	Naphthalene	Acenaphthylene	Acenaphthene	Fluorene	Anthracene	Fluoranthene	Pyrene
5	155.1	247.5	333.0	300.4	167.2	102.6	107.8
30	74.08	328.0	383.5	521.4	481.5	263.1	266.3
60	83.62	445.4	587.2	755.1	742.9	542.7	537.7
90	69.99	434.0	590.6	696.1	787.2	712.8	747.9

Table 7 Raw data for Figure 3.3

Extraction temperature (ºC)	Extracted amount (ng)					
	Internally cooled PDMS hollow fiber			Commercial DVB/CAR/PDMS fiber		
	hexanal	**nonanal**	**undecanal**	**hexanal**	**nonanal**	**undecanal**
50	62.29	20.14	n.d.	13.81	2.64	n.d.
70	196.49	74.18	6.37	31.13	34.94	1.61
90	288.70	116.30	8.92	15.76	28.88	7.43
110	299.03	167.72	12.53	13.08	9.32	4.80

n.d.= not detected

Table 8 Raw data for Figure 3.4

Extraction time (min)	Extracted amount (ng)					
	110 ºC			70 ºC		
	hexanal	nonanal	undecanal	hexanal	nonanal	undecanal
5	63.50	38.25	3.46	22.36	15.56	0.99
15	62.46	41.64	4.87	32.97	22.19	1.08
30	60.79	38.47	5.37	51.04	26.70	2.32
45	63.57	37.77	3.98	52.77	29.21	2.62
60	60.28	34.41	3.25	54.00	28.41	4.16

Table 9 Raw data for Figure 3.6

Peak areas obtained by extractions with and without cooling from n-alkanes in a flow through system (n=3)				
without cooling				
n	n-octane	n-nonane	n-decane	n-undecane
1	6657681	8380378	9710513	13366143
2	6108291	6670509	6787903	10311156
3	7319855	9231159	9059561	14331839
Ave	6695276	8094015	8519326	12669713
SD	606656.3	1304122	1534374	2098865
RSD%	9	16	18	16
with cooling				
n	n-octane	n-nonane	n-decane	n-undecane
1	36983939	35705699	30579295	44711707
2	29211477	34389084	32118600	75162399
3	27606410	32535945	32865448	58559102
Ave	31267275	34210243	31854448	59477736
SD	5015401	1592427	1165743	15246117
RSD%	16	5	4	25

Table 10 Raw data for Figure 3.8

SPME mode/coating	Peak area			
	(E)-beta-ocimene	(Z)-ocimene	linalool	indole
Cold fiber device-with cooling	5839711	253151174	54242386	1764711
Cold fiber device-without cooling	1151500	37464907	11869592	n.d.
PDMS commercial fiber	n.d.	35393017	1822429	n.d.
PA commercial fiber	n.d.	6858789	5811369	n.d.

n.d. = not detected

Table 11 a-g Raw data for Figure 4.3

(a) Naphthalene				
	30 ºC		**50 ºC**	
Time (min)	**Without matrix**	**With matrix**	**Without matrix**	**With matrix**
2	42.4	30.0	100.2	56.4
5	81.5	50.7	124.4	84.7
15	114.4	80.1	146.1	106.7
30	106.9	83.5	141.3	92.2
60	91.7	74.8	118.6	82.0
Standard deviations				
2	2.3	1.9	10.2	3.1
5	2.0	6.8	20.5	3.5
15	9.5	6.4	11.3	4.0
30	8.4	3.5	18.0	11.3
60	11.2	12.7	3.8	3.2
(b) Acenaphthylene				
	30 ºC		**50 ºC**	
Time (min)	**Without matrix**	**With matrix**	**Without matrix**	**With matrix**
2	45.3	11.5	130.4	30.0
5	96.6	19.7	161.9	57.7
15	161.3	40.6	209.6	115.5
30	175.2	57.5	213.5	122.3
60	156.4	79.7	200.8	132.2
SD				
2	8.1	1.8	20.3	3.0
5	4.7	2.6	32.8	3.6
15	10.9	6.9	12.6	6.3
30	20.6	4.5	18.0	16.1
60	13.5	14.8	5.4	11.3
(c) Acenaphthene				
	30 ºC		**50 ºC**	
Time (min)	**Without matrix**	**With matrix**	**Without matrix**	**With matrix**
2	46.1	12.9	135.3	35.8
5	98.4	22.4	166.3	67.6
15	166.0	45.3	216.4	129.3
30	181.1	64.8	219.9	138.4
60	163.5	87.3	208.2	144.8
SD				
2	9.1	2.0	20.4	4.4
5	4.4	3.0	35.4	3.9
15	12.0	7.0	13.8	7.8
30	22.3	3.9	15.6	17.9

60	13.4	16.8	6.1	10.4
(d) Flourene				
	30 ºC		**50 ºC**	
Time (min)	**Without matrix**	**With matrix**	**Without matrix**	**With matrix**
2	29.9	6.0	122.4	15.5
5	69.9	12.8	156.4	29.0
15	147.9	22.8	234.3	76.8
30	170.5	33.6	252.1	86.3
60	165.7	55.4	231.4	129.9
Standard deviations				
2	8.5	2.3	25.2	1.0
5	4.3	1.9	28.9	0.3
15	17.1	2.9	12.6	2.8
30	25.3	4.2	36.3	11.1
60	14.1	3.4	19.0	8.0
(e) Anthracene				
	30 ºC		**50 ºC**	
Time (min)	**Without matrix**	**With matrix**	**Without matrix**	**With matrix**
2	10.3	1.3	32.5	4.1
5	11.3	2.6	54.3	8.2
15	12.3	8.0	135.8	21.1
30	24.5	15.8	178.3	24.9
60	36.4	34.2	188.9	53.1
Standard deviations				
2	3.0	0.3	15.2	1.9
5	0.9	0.3	6.7	2.4
15	1.2	0.8	29.2	5.0
30	3.1	1.1	16.4	2.6
60	10.1	2.8	19.8	6.7
(f) Fluoranthene				
	30 ºC		**50 ºC**	
Time (min)	**Without matrix**	**With matrix**	**Without matrix**	**With matrix**
2	2.5	1.5	10.7	4.1
5	1.3	0.4	34.8	6.6
15	5.3	3.1	85.3	3.8
30	8.4	8.1	122.1	8.4
60	22.1	17.6	152.6	32.1
Standard deviations				
2	0.3	1.2	10.2	2.6
5	0.9	0.1	4.0	2.3
15	1.1	1.1	17.5	1.4
30	1.0	2.4	8.8	1.0
60	4.5	5.5	22.1	16.2
(g) Pyrene				

Time (min)	30 ºC		50 ºC	
	Without matrix	**With matrix**	**Without matrix**	**With matrix**
2	3.1	0.0	8.2	3.3
5	3.4	0.4	30.2	5.8
15	2.9	2.1	83.4	4.6
30	4.5	4.7	107.6	6.1
60	9.6	16.1	136.6	30.7
Standard deviations				
2	0.5	0.0	10.2	1.2
5	3.7	0.1	2.80	2.0
15	0.5	0.6	11.7	2.5
30	0.1	2.2	10.21	0.8
60	4.4	3.60	17.70	14.0

Table 12 Raw data for Figure 4.4

	Naphthalene	**Acenaphthylene**	**Acenaphthene**	**Fluorene**
150 ºC without cooling	4.04	5.54	8.37	6.83
150 ºC with cooling to 15 ºC	88.7	97.7	101	100
100 ºC without cooling	11.4	26.9	36.0	42.5
100 ºC with cooling to 15 ºC	103	109	109	111
Standard deviations				
150 ºC without cooling	0.18	0.51	0.95	0.94
150 ºC with cooling to 15 ºC	13.9	10.0	16.3	7.51
100 ºC without cooling	0.66	5.03	6.00	6.55
100 ºC with cooling to 15 ºC	2.37	3.96	4.29	1.63

Table 13 Raw data for Figure 4.5

Recoveries (%)							
Extraction Time (min)	**Naphthalene**	**Acenaphthylene**	**Acenaphthene**	**Fluorene**	**Anthracene**	**Phenanthrene**	**Pyrene**
2	53.1	41.0	40.0	36.5	35.3	42.4	40.5
5	45.5	50.5	48.7	46.3	41.0	44.2	41.4
15	77.5	64.8	64.1	61.0	53.1	52.0	52.0
20	29.0	50.2	47.7	48.1	43.7	46.4	46.9
30	33.6	45.7	45.1	50.3	45.2	57.8	55.5
45	48.0	51.7	52.9	61.8	60.6	65.3	63.8
60	59.9	50.4	54.9	52.3	48.5	49.6	56.0
RSD(%) (for 5 min)	50	21	18	14	13	5	1

Table 14 Raw data for Figure 4.6

Peak areas			
Initial loading	**Naphthalene**	**Acenaphthene**	**Fluorene**
1	10149418	388429	159065
2	8294032	430306	192357
3	8326131	421036	183242
Ave	8923194	413257	178221
SD	1062063	21995.6	17204.5
RSD (%)	12	5	10
30 min at 150 ºC			
1	117352	16904	n.d.
2	123152	17445	14387
3	122339	17766	11363
30 min at 150 ºC followed by 2 min at 25ºC			
1	5986783	260953	110245
2	6572751	318590	143096
3	6624288	298795	134698
30 min at 150 ºC +5 min at 25ºC			
1	6979914	331910	163377
2	7037389	317835	144233
3	7084560	313306	141111
30 min at 150 ºC + 10 min at 25 ºC			
1	6473867	313958	150357
2	6358315	302791	143181
3	6432485	282804	132273

Table 15 Raw data for Figure 4.7

Acenaphthylene				
Extracted amount (ng)				
Extraction time (min)	Empty vial		Sand	
	150 ºC	180 ºC	150 ºC	180 ºC
2	3.90	6.79	1.39	20.5
5	9.84	18.2	2.99	31.1
15	17.5	39.0	4.59	37.3
30	21.7	40.1	5.28	41.0
45	20.0	27.8	5.44	40.3
60	22.9	34.5	5.12	38.0

Table 16 Raw data for Figures 4.8 and 4.9

Pyrene				
Extracted amount (ng)				
Extraction time (min)	Empty vial		Sand	
	150 ºC	180 ºC	150 ºC	180 ºC
5	8.70	3.70	1.79	5.67
15	8.85	5.80	4.81	6.97
30	9.37	5.47	7.40	9.52
45	11.3	3.72	7.56	8.96
60	10.2	4.25	8.20	8.99

Table 17 Raw data for Figure 4.10

Amount extracted (ng)						
Extraction time (min)	150 ºC			180 ºC		
	Naphthalene	Fluorene	Anthracene	Naphthalene	Fluorene	Anthracene
2	3.07	n.d.	n.d.	6.19	0.51	n.d.
5	13.3	n.d.	n.d.	38.2	0.95	n.d.
15	49.5	n.d.	n.d.	107	5.90	2.39
30	81.9	0.87	n.d.	184	22.9	7.47
60	88.2	11.7	0.99	217	44.7	13.0
90	161	15.6	1.91	225	79.5	32.9
Standard deviations						
2	0.48	-	-	0.96	0.07	-
5	2.07	-	-	5.92	0.14	-
15	7.67	-	-	16.6	0.85	0.32
30	12.7	0.13	-	28.5	3.29	0.98
45	13.7	1.68	0.13	33.6	6.43	1.72
60	25.0	2.24	0.25	34.9	11.4	4.34

n.d. = not detected

Table 18 Raw data for Figure 4.11

Extraction recoveries (%)							
Clay %	**Naphthalene**	**Acenaphthylene**	**Acenaphthene**	**Fluorene**	**Anthracene**	**Fluoranthene**	**Pyrene**
0	53	8.6	18	23	10	6.9	7.3
5	49	0.5	3.9	1.2	0.1	0.1	0.2
10	15	0.4	1.0	2.8	0.3	0.2	0.2
15	17	0.3	1.1	1.8	n.d.	n.d.	n.d.
20	0.3	0.0	0.1	0.1	n.d.	n.d.	n.d.
25	2.3	n.d.	n.d.	n.d.	n.d.	n.d.	n.d.
50	0.8	n.d.	n.d.	n.d.	n.d.	n.d.	n.d.
75	1.0	n.d.	n.d.	n.d.	n.d.	n.d.	n.d.
100	1.3	n.d.	n.d.	n.d.	n.d.	n.d.	n.d.
RSD (%)	17	16	14	19	47	49	52

Table 19 Raw data for Figure 4.12

Extraction recoveries (%)			
Extraction temperature (ºC)	**Toluene**	**Ethylbenzene**	**o-Xylene**
30	3.78	5.91	3.31
50	4.56	6.25	4.78
80	6.61	8.57	3.91
120	10.8	12.4	5.87
150	21.6	33.9	16.8
180	24.1	62.6	22.3
RSD%	22	10	17

Table 20 Raw data for Figure 4.13

ln(n(t)/n(0))			
Time (h)	**120 ºC**	**Time (h)**	**180 ºC**
0.02	3.18E-01	**0.01**	5.65E-01
0.05	-4.16E-01	**0.02**	-1.85E-02
0.08	-1.02E+00	**0.05**	-3.57E+00

Table 21 Raw data for Figure 4.14

ln(n(t)/n(0))			
Time (h)	**120 ºC**	**140 ºC**	**160 ºC**
0.25	-2.31E-05	-6.20E-05	-3.75E-04
0.5	-7.59E-05	-2.52E-04	-8.78E-04
0.75	-1.05E-04	-2.60E-04	-1.22E-03
1	-1.39E-04	-3.20E-04	-2.21E-03

Appendix 3 Structures of organic compounds

Table 1 Structures and physical properties of compounds used in kinetic studies (Chapter 4)				
Name	**Structure**	**Molecular Weight**	**B.P. (°C) at 760 mmHg**	**Polarizability**
Toluene	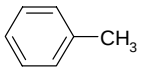	92.14	110.6	11.8
Ethylbenzene	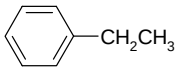	106.17	136.25	14.2
o-xylene	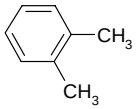	106.17	144	14.9
Naphthalene	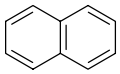	128.17	217.9	17.5
Acenaphthylene	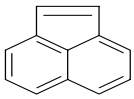	152.20	280	-
Acenaphthene	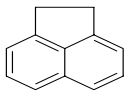	154.21	279	20.6
Fluorene	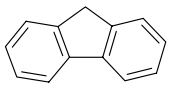	166.22	295	21.7
Anthracene	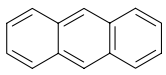	178.23	342	25.9
Fluoranthene	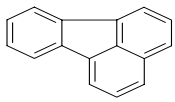	202.26	384	28.3
Pyrene	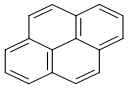	202.26	404	29.3

Source: CRC Handbook of Chemistry and Physics

Table 2 Volatile compounds of lily-of-the-valley (Chapter 3-Table 3.3)

Name	**Structure**
beta-Pinene	
Benzyl alcohol	
Limonene	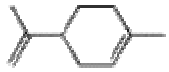
(E)-Ocimene	
(Z)-Ocimene	
Benzyl acetate	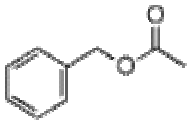
Dodecanal	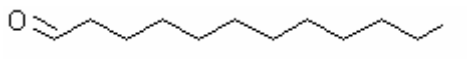
beta-Citronellol	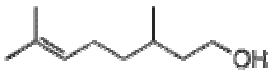
(Z)-Geraniol	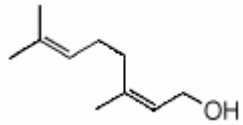
Geranial	
Indole	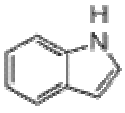
Citronellyl acetate	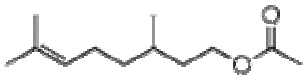
Neryl acetate	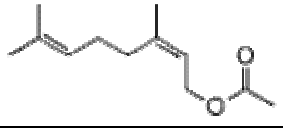
Geranyl acetate	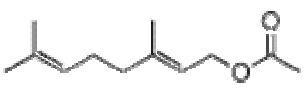

Table 3 Volatile compounds of wisteria (Chapter 3-Table 3.3)

Name	**Structure**
(E)-beta-Ocimene	
(Z)-Ocimene	
Linalool	
Indole